TECHNISCHE UNIVERSITÄT MÜNCHEN

Lehrstuhl für Entwicklungsgenetik

Characterization of Semaphorin 4C and Semaphorin 4G as candidate ligands of Plexin-B2

Viola Maier

Vollständiger Abdruck der von der Fakultät Wissenschaftszentrum Weihenstephan für Ernährung, Landnutzung und Umwelt der Technischen Universität München zur Erlangung des akademischen Grades eines

Doktors der Naturwissenschaften

genehmigten Dissertation.

Vorsitzender: Univ.-Prof. Dr. S. Scherer

Prüfer der Dissertation:

1. Univ.-Prof. Dr. W. Wurst
2. Univ.-Prof. Dr. M. Götz
   (Ludwig-Maximillians-Universität München)

Die Dissertation wurde am 28.02.2011 bei der Technischen Universität München eingereicht und durch die Fakultät Wissenschaftszentrum Weihenstephan für Ernährung, Landnutzung und Umwelt am 27.06.2011 angenommen.

Contents

1. SUMMARY

Semaphorins and Plexins are cognate ligand-receptor families that regulate a wide range of biological processes, including axon guidance and cell migration during development of the nervous system. Several studies have addressed the function of Semaphorin 3s and their Plexin-A/Neuropilin receptors as regulators of axon guidance, but relatively little is known about the *in vivo* function of Plexin-Bs and their respective ligands.

The Plexin-B2 receptor is critically involved in neural tube closure and cerebellar granule cell development, but its relevant *in vivo* ligands are not yet determined. It was therefore the goal of my thesis work to identify candidate ligands for Plexin-B2, and to examine the *in vivo* function of these molecules in neural development.

In this study, it was shown by *in situ* hybridization and binding assays that two members of the Semaphorin 4 family, Sema4C and Sema4G, are expressed in the developing cerebellum and that both bind to Plexin-B2 expressing cells *in vitro* and *in vivo*. Phenotypic analyses and genetic interactions studies support the model that Sema4C and Sema4G are functional ligands of Plexin-B2. Like *Plxnb2-/-* mutants, *Sema4c-/-* mutants develop exencephaly with partial penetrance. *Sema4c-/-* mutants that bypass exencephaly are viable and fertile, but display distinctive cerebellar defects, including gaps in the internal granule cell layer (IGL) of rostral lobules, fusions of the IGL between caudal lobules, and ectopic granule cells in the molecular layer. In addition to the neural defects in *Sema4c-/-* mutants, also ventral pigmentation defects were observed that are similar to those found in Plexin-B2 homozygous mutants, pointing to a functional ligand-receptor relationship in melanocyte development. The Sema4G gene deletion causes no overt phenotype by itself, but combined deletion of Sema4C and Sema4G revealed an enhanced cerebellar phenotype. However, the overall severity of the cerebellar phenotypes of Sema4C or Sema4C/Sema4G mutants is less severe than that of Plexin-B2 mutants, indicating that further ligands of Plexin-B2 exist during cerebellar development. In explant cultures of the developing cerebellar cortex, Sema4C promoted migration of cerebellar granule cell precursors in a Plexin-B2-dependent manner, supporting the model that a reduced migration rate of granule cell precursors is the mechanistic basis of the cerebellar phenotypes of the Sema4C/Sema4G mutants.

In summary, these results give the first genetic *in vivo* evidence that Sema4C and Sema4G are ligands for Plexin-B2, and indicate that Sema4C and Sema4G control cerebellar development through regulation of the migratory properties of granule cell precursors by binding to the Plexin-B2 receptor.

ZUSAMMENFASSUNG

Semaphorine und Plexine sind zugehörige Liganden-Rezeptor Familien, die eine Vielzahl von biologischen Prozessen regulieren, wie zum Beispiel axonale Wegfindung und Zellwanderung während der Entwicklung des Nervensystems. Mehrere Studien haben die Funktion der Semaphorin 3 Familie und ihrer Plexin-A/Neuropilin Rezeptoren als Regulatoren axonaler Wegfindung untersucht, jedoch ist relativ wenig über die *in vivo* Funktion der Plexin-B Rezeptoren und ihrer potentiellen Liganden bekannt.

Der Plexin-B2 Rezeptor ist entscheidend an der Schließung des Neuralrohrs und an der Körnerzell Entwicklung im Kleinhirn beteiligt, aber die relevanten *in vivo* Liganden sind nicht bekannt. Deshalb war es das Ziel meiner Doktorarbeit, mögliche Liganden von Plexin-B2 zu ermitteln und die *in vivo* Funktion dieser Moleküle in der neuronalen Entwicklung zu untersuchen.

Mit Hilfe von *in situ* Hybridisierungen und Bindeasssays wurde in dieser Arbeit gezeigt, dass zwei Mitglieder der Semaphorin 4 Familie, Sema4C und Sema4G, im sich entwickelnden Kleinhirn exprimiert werden und dass beide *in vitro* und *in vivo* an Zellen binden, die Plexin-B2 exprimieren. Phänotypische Analysen und genetische Interaktionsstudien unterstützen das Modell, dass Sema4C and Sema4G funktionale Liganden von Plexin-B2 sind. Ebenso wie *Plxnb2*-/- Mutanten entwickeln auch *Sema4c*-/- Mutanten Exencephalie mit partieller Penetranz. *Sema4c*-/- Mutanten, die keine Exencephalie ausbilden, sind lebensfähig und fruchtbar, zeigen aber bestimmte Defekte im Kleinhirn, wie zum Beispiel Lücken in der inneren Körnerzellschicht (IGL) der rostralen Lobuli, Fusionen des IGLs zwischen caudalen Lobuli und ektope Gruppen von Körnerzellen in der Molekularschicht. In Sema4C homozygoten Mutanten wurden zusätzlich zu den neuralen Defekten auch ventrale Pigmentierungsdefekte beobachtet, die ähnlich den Pigmentierungsdefekten der Plexin-B2-/- Mutanten sind. Dieser Befund deutet auf eine funktionale Liganden-Rezeptoren Beziehung dieser Moleküle in der Melanozyten Entwicklung hin.

Die alleinige Gendeletion von Sema4G zeigte keinen offensichtlichen Phänotyp, die kombinierte Deletion von Sema4C and Sema4G zusammen zeigte jedoch einen verstärkten Phänotyp im Cerebellum. Da der Phänotyp von Sema4C oder Sema4C/Sema4G Mutanten aber insgesamt schwächer ist als der von Plexin-B2 Mutanten, ist zu vermuten, dass es neben Sema4C und Sema4G noch andere Liganden für Plexin-B2 während der Entwicklung des Kleinhirns gibt. In Explantaten von Körnerzellen der äußeren Körnerzellschicht des Cerebellums wurde gezeigt, dass Sema4C die Wanderung von

Körnerzellvorläufern in Abhängigkeit von Plexin-B2 fördert. Dieser Befund führt zu dem Modell, dass die Phänotypen von Sema4C/Sema4G Mutanten auf einer reduzierten Wanderungsrate der Körnerzellvorläufer zurückzuführen sind.

Zusammenfassend sind diese Ergebnisse die erste genetische *in vivo* Evidenz dafür, dass Sema4C and Sema4G Liganden von Plexin-B2 sind. Die Befunde deuten darauf hin, dass Sema4C and Sema4G die Entwicklung des Kleinhirns durch die Regulation der Wanderungseigenschaften von Körnerzellvorläufern mittels Bindung an den Plexin-B2 Rezeptor kontrollieren.

2. INTRODUCTION

2.1 Cerebellum

The cerebellum is a component of the vertebrate hindbrain that is primarily involved in integration of somatosensory perception and planned motor movement (Schmahmann et al., 2004). Cerebellar injury results in movements that are slow and uncoordinated. Human individuals with cerebellar lesions tend to sway and stagger when walking. Its highly repetitive structure makes it a preferred model system for studying nervous system development and determining cellular and molecular mechanisms of neuronal migration (Hatten and Mason, 1990; Rakic et al., 1994).

The mature cerebellum has a stereotypical morphology of cellular architecture and lobular foliation, which is consistent between individuals and highly conserved across vertebrates. The established terminology partitions the cerebellum on each side of the midline into three longitudinal regions along the rostral to caudal plane: the vermis (medial cerebellum), the paravermis, and the hemispheres (Apps and Garwicz, 2005). Each of these regions is folded into lobules and each lobule is further subdivided into folia. The mouse cerebellum is organized at the vermis in ten distinct lobuli, numbered I-X from rostral to caudal (Figure 2.1).

2.1.1 Cerebellar development

The cells of the cerebellar cortex originate in two different progenitor zones (see (Millen and Gleeson, 2008) for review). The ventricular progenitor zone gives rise to Purkinje neurons, local interneurons, and Bergmann glia. In contrast, granule cell precursors are initially born in the upper rhombic lip and then migrate rostrally over the cerebellar anlage from approximately embryonic day E13 on to form the external granule layer (EGL) (Figure 2.2). The EGL is a heavily proliferating progenitor zone that gives rise to the entire population of cerebellar granule cells.

In newborn mice, the EGL is divided in the upper and lower EGL. In the early postnatal cerebellum, granule cell precursors actively proliferate in the upper layer of the EGL

(Komuro et al., 2001). After their final mitosis, the cerebellar granule cells first migrate tangentially in the lower EGL. After a short stationary period in this layer, the granule cells initiate a shift from tangential to radial migration across the molecular layer (ML) along Bergmann glial fibers ((Komuro and Yacubova, 2003); Figure 2.3). The extraordinary migratory dimensions of granule cells were already noticed by S. Ramon y Cajal, who was the first to describe the different phases of their migration (Cajal, 1911). The main phase of cerebellar granule cell proliferation occurs during postnatal days, with a peak around postnatal day P10. Cerebellar development of the mouse ends at about P21, when the architectures at the cellular, neural circuit, and lobular levels show almost no difference to those of the adult.

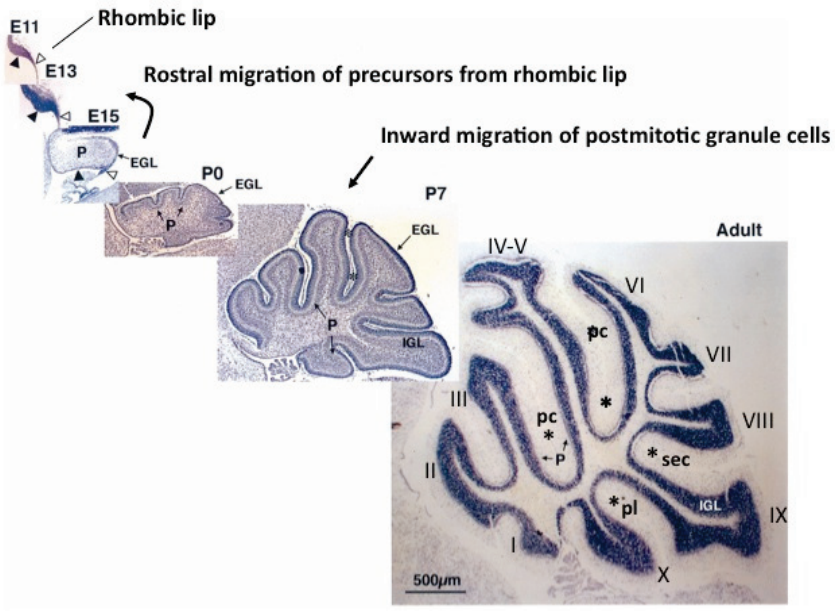

Figure 2.1 Development of the cerebellum
Sagittal sections of mouse cerebella from embryonic days E11, E13 and E15, as well as from postnatal days P0 and P7, and adulthood are shown from left to right.
Asterisks indicate fissures, P labels the Purkinje cell layer, IGL labels the internal granule cell layer, and EGL labels the external granular layer. In the three embryonic pictures, the filled arrowheads point to the ventricular neuroepithelium, and the unfilled arrowheads point to the germinal trigone.
pc, preculminate; pr, primary; sec, secondary; pl, postolateral fissure
Scale bar for all photomicrographs 500µm
Figure modified after (Goldowitz and Hamre, 1998).

During the postnatal growth period, the surface of the cerebellum changes from a smooth surface to a species-specific lobular architecture. The process of foliation is a series of remodeling steps beginning with the formation of four principal fissures (preculminate,

primary, secondary, and postolateral) (Figure 2.1) that result in a final architecture with ten lobules (Sillitoe and Joyner, 2007).

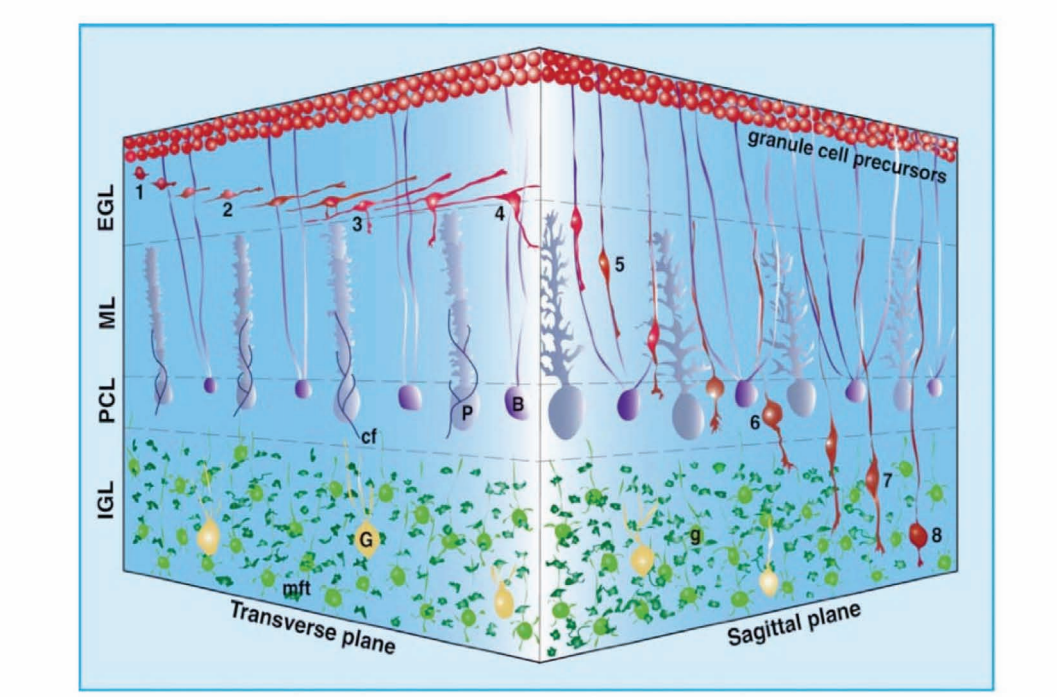

Figure 2.2 Three-dimensional representation of granule cell migration in the early postnatal mouse cerebellum
Phases of granule cell migration from the external granule layer (EGL) to the internal granule layer (IGL): 1, extension of the granule cell precursor migration near the top of the EGL; 2, tangential migration in the middle of the EGL; 3, development of vertical process near the border between the EGL and the molecular layer (ML); 4, initiation of radial migration at the EGL-ML border; 5, radial migration in the molecular layer (ML) along the Bergmann glia cells; 6, stationary state in the Purkinje cell layer (PCL); 7, Bergmann glia-independent radial migration in the IGL; 8, finalization of migration in the middle or the bottom of the IGL. P, Purkinje cell; B, Bergmann glia; G, Golgi cell; g, postmigratory granule cell; cf, climbing fiber; mft, mossy fiber terminal.
Figure from (Komuro and Yacubova, 2003)

2.1.2 Cellular organization of the cerebellar cortex

Neurons in the cerebellum are arranged within inner and outer parts, constituting the deep cerebellar nuclei and cerebellar cortex, respectively. The main constituents of the cerebellar cortex are excitatory granule cells and their post-synaptic targets, the GABA-ergic Purkinje cells. Smaller numbers of local inhibitory interneurons are distributed throughout all layers of the cerebellar cortex. Bergmann glia cells, which are cerebellar radial glia cells, provide a lattice-like scaffold to the cortex. The mature cerebellar cortex

can be divided into three layers: the molecular layer (ML), Purkinje cell layer (PCL), and the granule cell layer (GCL) (Figure 2.3).

There are two main types of extracerebellar axons projecting to the cerebellar cortex: the mossy fibers that contact the granule cells and have several origins in the hindbrain and spinal cord, and the climbing fibers that project to Purkinje cells and originate from the inferior olivary nucleus in the brainstem (Kahle et al., 1993).

Molecular layer

The main constituents of the molecular layer (ML) are axonal projections of granule cells, the so-called parallel fibers, and the dendritic trees of Purkinje cells. The parallel fibers of granule cells form excitatory synapses on Purkinje cells dendrites. The molecular layer also contains two types of local interneurons, the basket and stellate cells.

Purkinje cell layer

The Purkinje cell layer contains the cell bodies of the Purkinje cells, which send dendritic aborizations into the molecular layer. Purkinje cells are generated during the early embryonic phase, between E10 and E13 from the ventricular zone (VZ) (Hoshino et al., 2005), and they migrate outward to form a monolayer (Purkinje cell layer) during the early postnatal days (Hatten and Heintz, 1995). They are the earliest neurons to migrate into the cerebellar cortex and arrange the development of the synaptic connections in the cerebellar cortex.

Purkinje cells form the exclusive output of the cerebellar cortex and project to the deep nuclei of the cerebellum, where they form GABA-ergic synapses. The parallel fibers of granule cells and the climbing fibers of neurons of the inferior olive form the afferent input of Purkinje cells. The Purkinje cell layer also contains the cell bodies of the Bergmann glia cells. Bergmann glia cells locate their cell bodies around the Purkinje cells, and extend radial fibers surrounding synapses of Purkinje cell dendrites (Yamada and Watanabe, 2002). During development, Bergmann glia fibers guide the migration of granule cells (see 2.1.1).

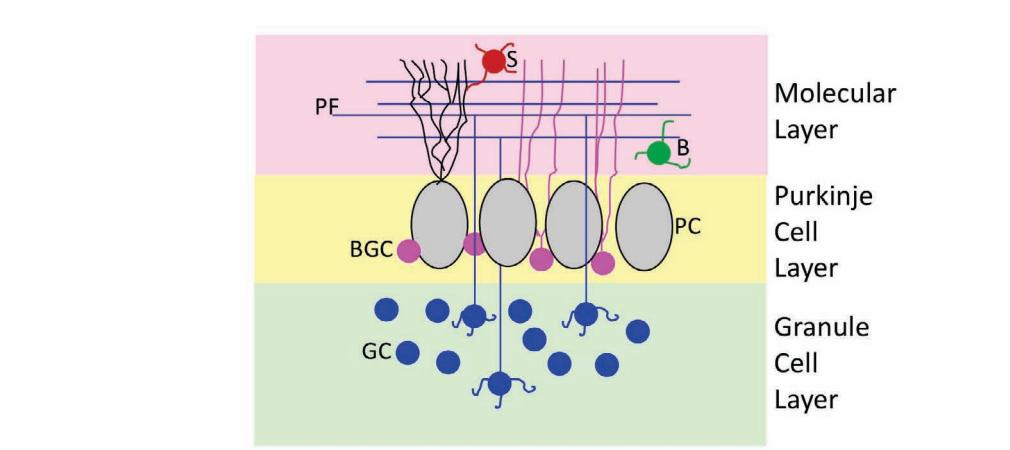

Figure 2.3 Cellular organization of the cerebellar cortex.
The cerebellar cortex has three layers. The outermost layer is the molecular layer that contains two main types of interneurons, the basket (B) and the stellate (S) cells. The Purkinje cell layer contains the cell bodies of Purkinje cells (PC) and the cell bodies of the Bergmann glia cells. The deepest layer, the granule cell layer, contains the cell bodies of granule cells (GC) and other interneurons such as Golgi cells and Lugaro cells (not depicted here).

Granule cell layer

The deepest layer, the granule cell layer, contains the cell bodies of granule cells and other interneurons such as Golgi cells, Lugaro cells, and unipolar brush cells. It also contains glial cells, such as oligodendrocytes and astrocytes. Granule cells are the most numerous neuronal types in the whole brain, and are thought to make up as many as half of the neurons in the brain. Granule cells are glutamatergic interneurons and have axons, which rise up and then branch out into parallel fibers. These fibers form in the ML synaptic contacts with Purkinje cell dendrites (Huang et al., 2006). Mossy fibers, which come from the brainstem and spinal nuclei, form the afferent input projection of granule cells.

2.2 Semaphorin and Plexin families

The Semaphorin gene family consists of more than 30 members (Neufeld et al., 2005) and is divided into 7 classes. Invertebrate Semaphorins are grouped into classes 1 and 2, whereas classes 3-7 are expressed in vertebrates (Semaphorin Nomenclature Committee, 1999). In addition, some DNA viruses encode functional Semaphorins that are assigned to class V (Suzuki et al., 2008).

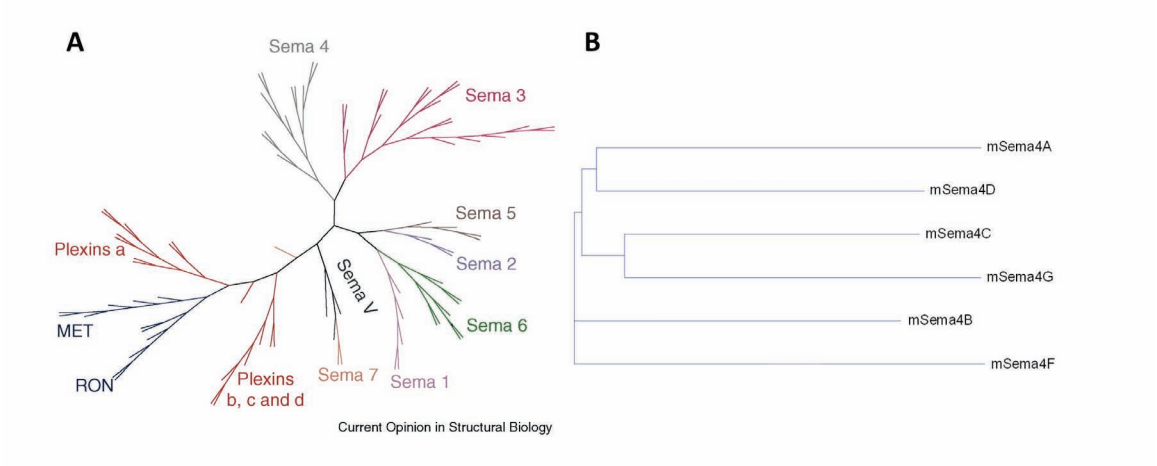

Figure 2.4 Phylogenetic tree of Semaphorins and Plexins
(A) Phylogenetic tree of the Semaphorins and Plexins based on the sequence similarity of their sema domain. (B) Evolutionary tree of mouse class 4 Semaphorins, calculated by comparison of the Semaphorin amino acid sequences. Sema4C and Sema4G are the closest related Sema4s.
Figure (A) modified after (Gherardi et al., 2004)

The main signaling receptors for Semaphorins are the Plexins, which have nine members in mammals, classes A through D (Tamagnone et al., 1999).

The phylogenetic tree based on the sema domain sequences shows that the Semaphorins and Plexins are evolutionary related (Figure 2.4 A). The Semaphorin family underwent early development and divergence in vertebrates (Gherardi et al., 2004). The Plexins clusters in two main branches, Plexin-A, and Plexin-B, Plexin-C, and Plexin-D. In the Semaphorin 4 family, Sema4A and Sema4D, and Sema4C and Sema4G are closely related family members (Figure 2.4 B).

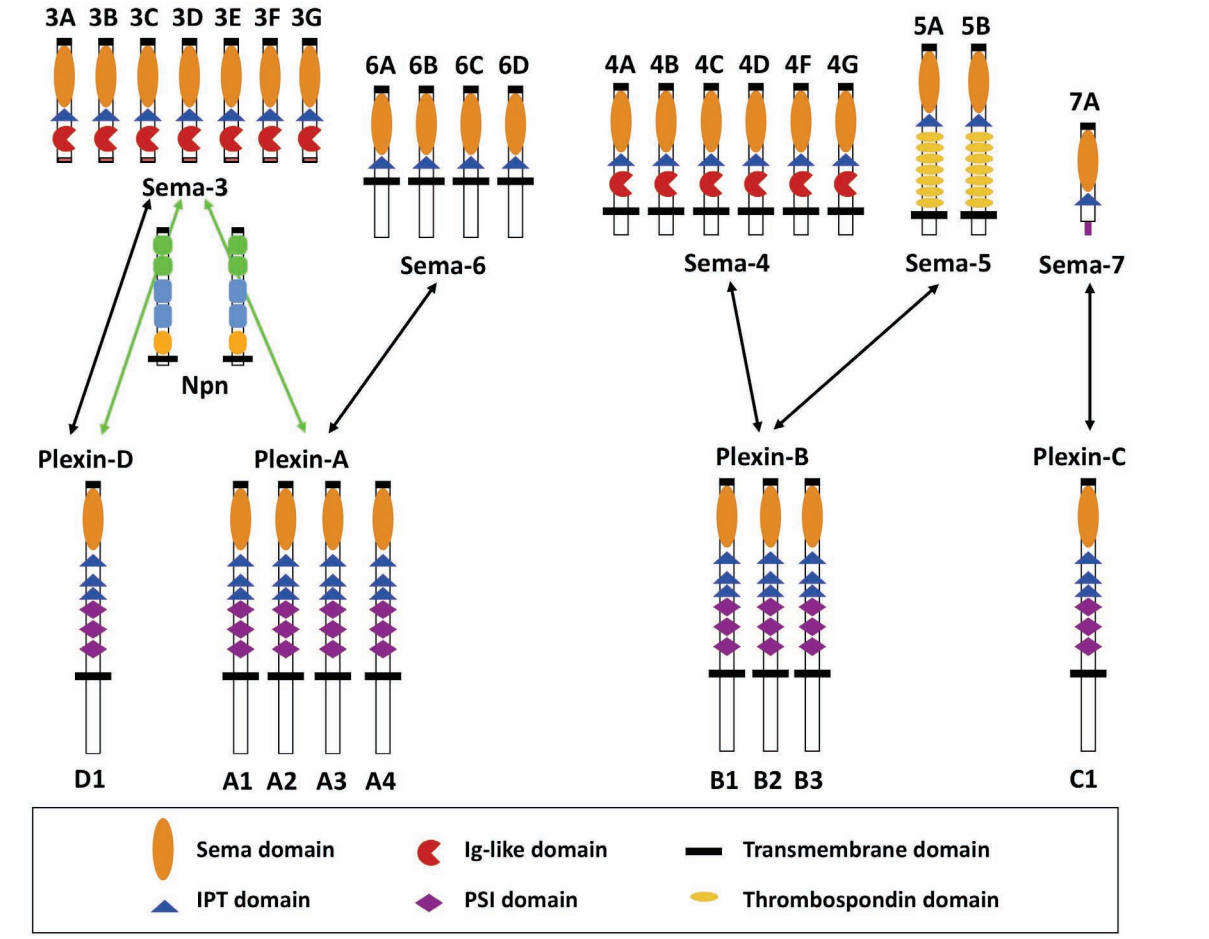

Figure 2.5 Semaphorins and Plexins in mammals
Semaphorin class 3 proteins are secreted, whereas the other members of other classes are synthesized as transmembrane proteins. There are four A-type Plexins, three B-type, one C-type and one D-type. Both Semaphorins and Plexins are characterized by sema domains. Additional domains that are present in Semaphorins include PSI (Plexin, Semaphorin and integrin) domains, immunoglobulin (Ig)-like domains, thrombospondin domains, and PDZ-domain-binding sites. Additional domains present in Plexins include PSI domains, IPT (Ig-like, Plexins and transcription factors) domains, a GTPase-binding domain, and a segmented GAP (GTPase-activating protein) domain. Semaphorins of class 4, 5, 6 and 7 directly interact with Plexins, whereas class 3 Semaphorins need Neuropilin-1 or Neuropilin-2 as co-receptors.

2.2.1 Structure of Semaphorins and Plexins

Semaphorins are either secreted or membrane-bound glycoproteins containing a ~500-amino acid extracellular domain, the Semaphorin (sema) domain, one or more small cystein-rich domains, present in Plexins, Semaphorins and integrins (PSI domain), followed by class specific motifs (Semaphorin Nomenclature Committee, 1999). Sema3 and Sema4 family members contain a single copy of an immunoglobulin (Ig) domain on the extracellular side. Class 5 is unique in containing seven copies of a thrombospondin repeat (Figure 2.5).

Class 3 Semaphorins are soluble proteins, whereas class 7 Semaphorins are linked through a glycosylphosphatidylinositol (GPI) -anchor to the cell membrane. As membrane-bound proteins, Sema4, Sema5, and Sema6 possess a type I transmembrane domain and a prolin-rich intracellular domain (Gherardi et al., 2004). Sema4D exists as membrane-bound, as well as in secreted forms, which result from protease cleavage of the extracellular domain (Wong et al., 2007).

Plexins are like Semaphorins, characterized by a common large extracellular sema domain (Gherardi et al., 2004; Kolodkin et al., 1993). The sema domain consists of a highly conserved variant form of the seven-blade β-propeller fold (Figure 2.6; (Gherardi et al., 2004)).

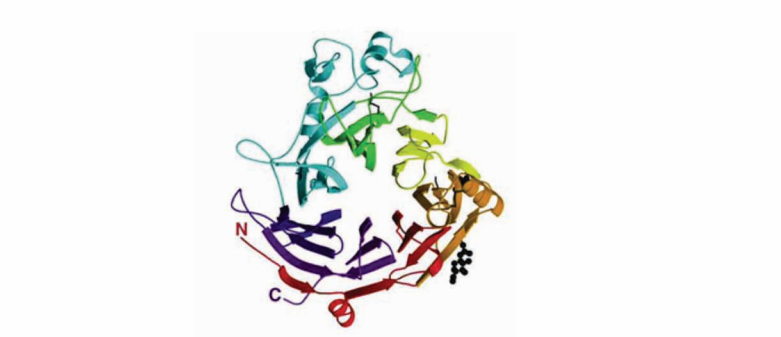

Figure 2.6 The sema domain of Semaphorins and Plexins
The sema domain displays a seven-bladed β-propeller fold
Figure from (Gherardi et al., 2004)

Following the sema domain, Plexins contain in their extracellular region also three PSI domains and three IPT (Ig-like, Plexins and transcription factors) domains. The intracellular domain is highly conserved between different Plexins and contains a segmented Ras-GAP domain.

2.2.2 Semaphorin-Plexin interactions

Plexins can function both as ligand-binding receptors and as signaling receptors for Semaphorins. The interactions between Plexins and Semaphorins are mainly mediated through direct binding of the sema domains of both proteins. The exception are class 3 Semaphorins, which require Semaphorin binding co-receptors, the Neuropilins, for signaling through Plexin-A family members ((Kolodkin and Ginty, 1997); Figure 2.5).

Neuropilins are transmembrane proteins of about 900 amino acids with a short intracellular domain. They also function as the ligand-binding partner in co-receptor complexes with vascular endothelial growth factor receptors (VEGFRs).

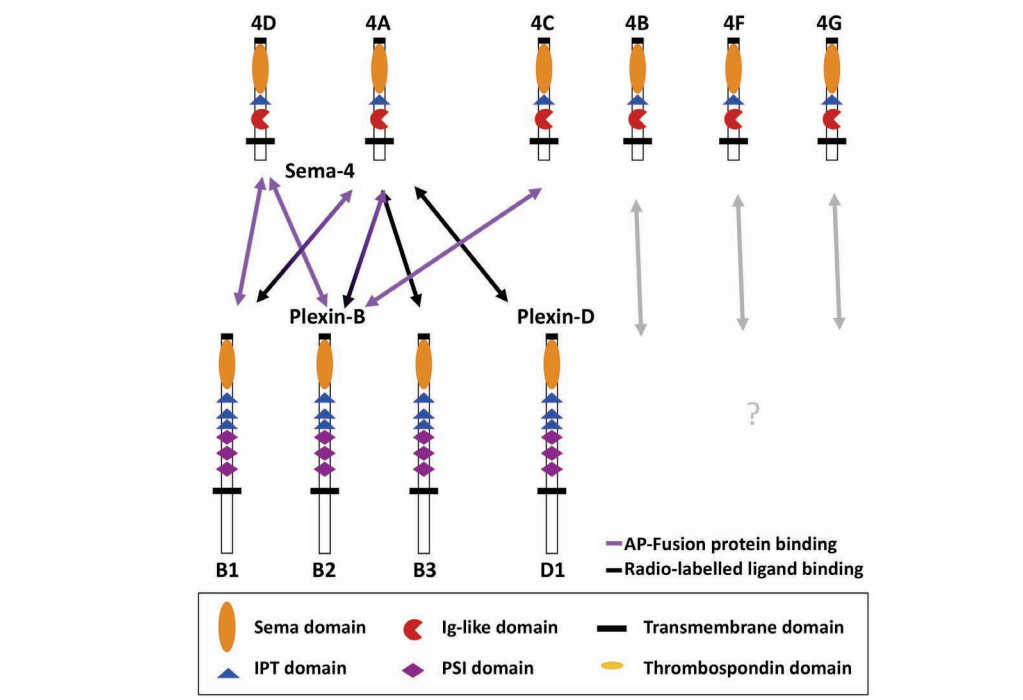

Figure 2.7 Semaphorin 4 family interactions with Plexins
In vitro studies showed that Sema4D binds to Plexin-B1 and Plexin-B2. Sema4D can interact to all three Plexin-Bs and also to Plexin-D1. Also Sema4C shows binding to Plexin-B2. For Sema4B, Sema4F, and Sema4G, the interaction partners remain still unknown.

In vitro experiments have suggested that B-Plexins can be activated by class 4 Semaphorins (Kruger et al., 2005). Plexin-B1 binds Sema4D (Tamagnone et al., 1999), while Plexin-B2 was identified as a receptor for Sema4C and Sema4D (Deng et al., 2007; Masuda et al., 2004). In general, class 4 Semaphorins (Sema4s) can bind to Plexin-B receptors. However, specific ligand-receptor pairings between the six mammalian Sema4s (Sema4A-D, F, G) and the three Plexin-Bs (Plexin-B1-B3) remain poorly defined (Figure 2.7).

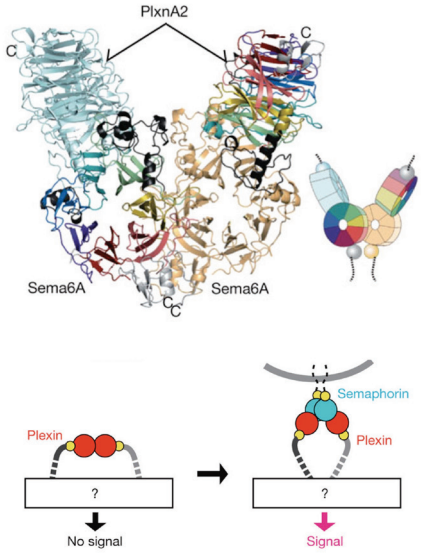

Figure 2.8 Crystal structure of a Semaphorin homodimer bound to two Plexin receptors and possible structural mechanism of Semaphorin-induced Plexin signaling.
A Semaphorin dimer binds two Plexin molecules, and the resulting conformational change activates Plexin signaling.
Figure from (Nogi et al., 2010)

Crystal structures and cellular assays of wild type and mutant proteins showed that Semaphorin dimers bind two Plexin molecules (Figure 2.8). The signaling is critically dependent on the avidity of the resulting bivalent complex of two Semaphorins and two Plexins (Janssen et al., 2010). It seems that binding of a Semaphorin dimer changes the relative orientation of the Plexin molecular axis, possibly altering the conformation of the cytoplasmic GAP domain, resulting in activation of the Plexin signaling (Janssen et al., 2010; Nogi et al., 2010). By crystal structures, similar ligand-receptor complexes have been identified in the crystal structures for binding of Sema6A to Plexin-A2, of Sema4D to Plexin-B1, and of Sema7A to Plexin-C1 (Jannsen et al., 2010). Nevertheless, the association states of the transmembrane and cytoplasmic regions remain unknown.

2.2.3 Semaphorin signaling

The activation of Plexins by Semaphorins triggers several intracellular signaling pathways that involve small GTPases of the Ras and Rho families (Zhou et al., 2008). The intracellular domain of a Plexin contains two highly conserved regions that are similar to a R-Ras-GAP domain, which is divided in two by a linker region. Other Ras family members

stimulate the ERK/MAPK pathway, while R-Ras has only a limited effect on ERK/MAPK but primarily functions to regulate integrin activity.
When Semaphorins bind Plexins, the Plexin GTPase activating protein (GAP) activity promotes the catalysis of R-Ras-GTP to R-Ras-GDP. R-Ras that is bound to GDP is inactivate, which in consequence reduces integrin adhesion and function ((Oinuma et al., 2006); Figure 2.9). The Ras-GAP activity of Plexins requires also binding of the protein Rnd1 to the Plexin cytoplasmic domain.

Whereas all Plexin family members possess a R-Ras GTPase activating protein (GAP) domain, only Plexin-B family members mediate the activation of RhoA through interaction with Rho guanine nucleotide exchange factor (RhoGEF) proteins. The Rho GTPases are a group of small G proteins that control cell motility through actin and microtubule dynamics, and integrin adhesion (Zhou et al., 2008). PDZ-RhoGEF activity is stimulated upon Sema4 binding, leading to an increase in Rho-GTP (Hirotani et al., 2002). This association of Rho GTPases with Plexins leads to increased cell migration through regulation of actin dynamics.

Upon Semaphorin stimulation, Plexins become phosphorylated in their cytoplasmic domain (Tamagnone et al., 1999). Plexin-Bs seem to associate either with the receptor tyrosine kinases Met and ErbB2, which can determine the outcome of Plexin-B activation (Giordano et al., 2002; Swiercz et al., 2008). After Sema4D binding, Plexin-B1 activates RhoA in the presence of ErbB-2, and in presence of Met RhoA is inhibited (Giordano et al., 2002; Swiercz et al., 2008).

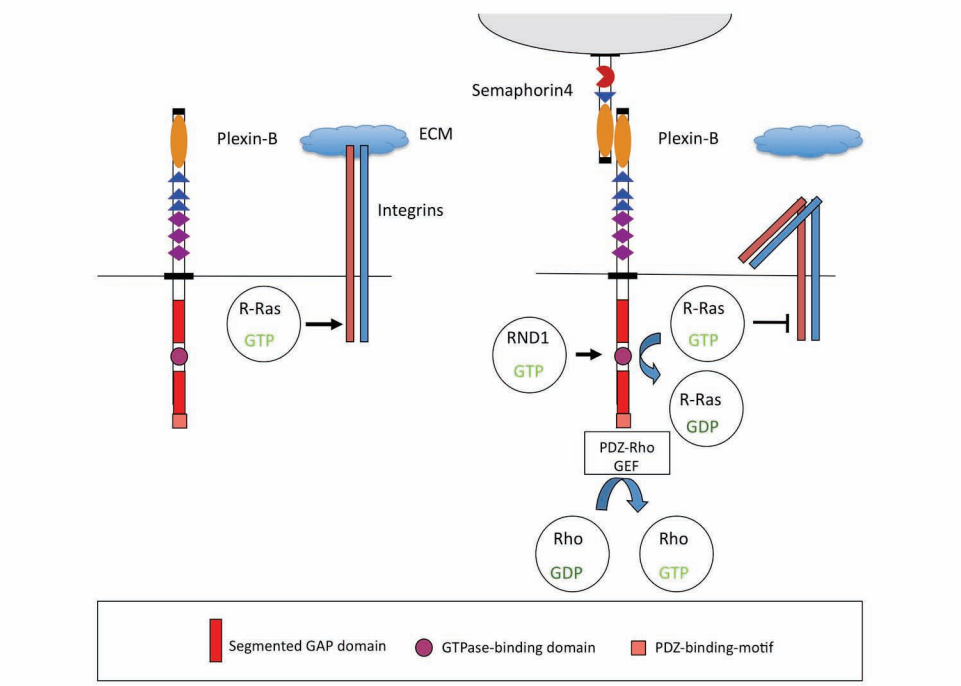

Figure 2.9 Plexin signaling
Components of Plexin downstream signaling are depicted for Plexin-Bs.
Binding of Sema4 to Plexin-B directly activates the receptor. The Plexin GAP activity, which requires RND1 binding, promotes R-Ras-GTP catalysis to R-Ras-GDP. PDZ-RhoGEF activity is stimulated upon Sema4 binding, leading to an increase in Rho-GTP.

2.2.4 Biological functions of the Sema3 family

Function in the nervous system

During development of neuronal network, neurons form connections by projecting long axons tipped with a specialized sensing device called the growth cone (Plachez and Richards, 2005). When the individual axons are guided to their targets, they interact directly with molecules within the environment. To find their targets, axonal growth cones utilize guidance molecules that can either attract or repel them (Song and Poo, 2001). Most Semaphorins are chemorepulsive, but they also can act as chemoattractans. The balanced expression, temporally and spatially, of multiple Semaphorins is required for the precise control of neural development.

Sema3A, the first identified vertebrate Semaphorin, induces retraction and collapse of growth cones (Luo et al., 1993). Through exerting repulsive effects on developing axons, Sema3A helps to guide the axons of sympathetic, motor and sensory neurons to their target

areas (Adams et al., 1997; Bagnard et al., 1998). Multiple class 3 Semaphorins are involved in fine-tuning the axonal growth during development. During cortical development, Sema3E can attract cortical axons, whereas Sema3D inhibits axonal branching (Bagnard et al., 1998).

The balance of attractive and repulsive Semaphorins is also responsible for mediating axonal fasciculation. Mice with mutations in Neuropilin-1, the co-receptor of Sema3A, display a defasciculation phenotype of sensory fibers that parallels the defects observed in mice lacking the ligand Sema3A (Kitsukawa et al., 1997; Taniguchi et al., 1997). Sema3A knock-out mice demonstrate also a highly defasciculated phenotype in motor and sensory axon outgrowth (Huber et al., 2005). This indicates that Sema3A-Npn-1 signaling regulates the fasciculation, timing, and fidelity of motor axon growth.

Function in angiogenesis

Class 3 Semaphorins are also involved in the development of the cardiovascular system. Sema3A knock-out mice display cardiac defects (Behar et al., 1996), and deletion of Sema3A disrupts the vascular patterning of the developing kidney (Reidy et al., 2009). Mice deficient for Sema3C exhibit strong dysfunctions of vasculature (Feiner et al., 2001). These severe cardiovascular system defects cause death within several hours after birth. In the mouse, Sema3E secreted by developing somites controls the patterning of the growing vasculature through repelling Plexin-D1 expressing endothelial cells (Gu et al., 2005).

Function as tumor suppressors

Members of the Semaphorin 3 family are also involved in cancer and tumorigenesis. Sema3B and Sema3F have been revealed as potential tumor suppressors, as they are located on chromosome 3p21, where homozygous deletion is a frequent event in lung and ovarian cancers (Tse et al., 2002; Xiang et al., 1996; Zabarovsky et al., 2002). Sema3B expression increases apoptosis in lung and breast cancer cells (Castro-Rivera et al., 2004; Tomizawa et al., 2001) and Sema3F blocked metastasis of melanoma cells (Bielenberg et al., 2004). The diminished motility of metastasizing cells could be linked to a decrease in ß1-Integrin-mediated attachment. Other members of class 3 Semaphorins, such as

Sema3A, Sema3D, Sema3E and Sema3G have also been characterized as tumor suppressors and inhibitors of tumor angiogenesis (Kigel et al., 2008). All of these four Semaphorins possess anti-tumorigenic properties.

2.2.5 Biological functions of the Sema4 family

Function in the nervous system

Class 4 Semaphorins have stimulatory as well as inhibitory effects on cell migration *in vitro* (Kruger et al., 2005), and bind specifically to B-type Plexins. Of the class B Plexins, Plexin-B1 and Plexin-B2 are widely expressed both inside and outside the developing nervous system, while Plexin-B3 is restricted to postnatal oligodendrocytes (Perälä et al., 2005; Worzfeld et al., 2004).

The sema domain of Plexin-B3 is essential for homophilic interaction independent of Semaphorin signaling mechanisms, possibly influencing neuronal morphogenesis or function. In the murine cerebellum, Plexin-B3 is a strong stimulator of neurite outgrowth of primary neurons (Hartwig et al., 2005). Targeted deletion of the Plexin-B3 genes in mice show no obvious histological and behavioral abnormalities. These findings indicate that Plexin-B3 is not fundamental for normal development and function of the central nervous system (Deng et al., 2007; Fazzari et al., 2007; Worzfeld et al., 2009).

Plexin-B1 and Plexin-B2 are both strongly expressed in the neuroepithelium and in developing neurons, but *in vivo* only Plexin-B2 seems to be required in the developing nervous system for proliferation, migration and pattern formation in the murine forebrain and cerebellum (Deng et al., 2007). Plexin-B1 mutants show defects in migration of Gonadotropin Releasing-Hormone 1 (GnRH-1) expressing neurons during development of the nervous system (Giacobini et al., 2008).

The Plexin-B2 mutation results in two different phenotypes, depending on the genetic background (Friedel et al., 2007). The knock-out of Plexin-B2 leads to exencephaly and neonatal lethality in the C57BL/6 inbred strain (Deng et al., 2007; Friedel et al., 2007). In the CD-1 outbred strain, many *Plxnb2-/-* mutants survive and displayed a severe disruption of the cerebellar cortex. Foliation defects were detected as fusions of lobules I-III and VI-VII. The other fissures were less pronounced and had an irregular shape. The mutants show also gaps in the rostral granule cell layer and many caudal ectopic cerebellar granule cells

(CGCs) (Figure 2.10 E). This severe phenotype was caused by a disturbed migration of cerebellar granule cell precursors (Friedel et al., 2007). In contrast, their proliferation and apoptosis rates were largely unchanged.

The detailed model of Plexin-B2 function in the developing cerebellum proposes that in newborn *Plxnb2-/-* mutants, granule cells that migrate in the molecular layer (ML) and inside the Purkinje cell layer (PCL) are aberrantly proliferating. In contrast, in newborn wild type mice, granule cell progenitors proliferate exclusively in the upper EGL and postmitotic granule cells start differentiating and migrate in the lower EGL (Figure 2.10 A, B, see 2.1.1). In adult *Plxnb2-/-* mutants, some ectopic granule cells are found at the surface of the molecular layer and islands of Purkinje cells are embedded between differentiated granule cells. Normally, Purkinje cells are positioned in a monolayer, above differentiated granule cell bodies, which are all localized in the IGL (Figure 2.10 C, D, E).

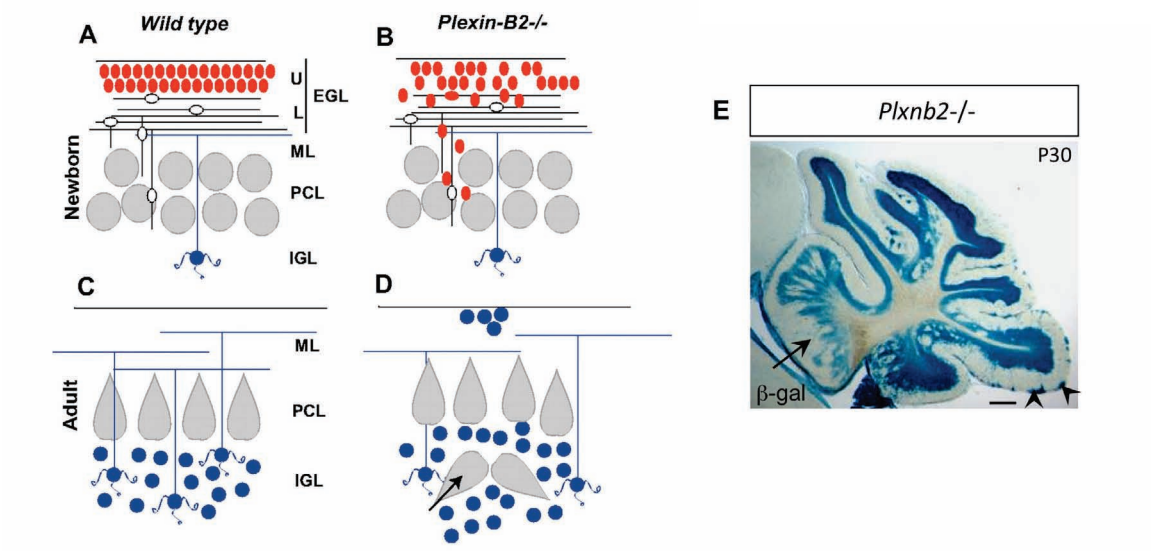

Figure 2.10 Model of Plexin-B2 function in the developing cerebellum
(A) In newborn wild type mice, granule cell progenitors (in red) proliferate exclusively in the upper EGL (U). Postmitotic granule cells start differentiating and migrate in the lower EGL (L) before migrating radially through the molecular layer (ML) and the Purkinje cell layer (PCL) to the IGL. At this stage, Purkinje cells (in gray) are still distributed in multiple layers. (B) In newborn *Plxnb2* mutants, granule cells keep proliferating during their migration in the ML. (C) In adult mice, Purkinje cells are aligned in a monolayer, above differentiated granule cell bodies (in blue). (D) In adult *Plxnb2* mutants, some ectopic granule cells are found at the surface of the ML and the cerebellar cortex is fragmented. Islands of Purkinje cells (arrow) are embedded between differentiated granule cells.
(E) The defect timing of proliferation and migration results in *Plxnb2-/-* mutants in profound disorganization of the cerebellum. Lobules II and III are fused and lobules VI and VII distorted. The mutants also showed gaps in rostral granule layer (arrow) and caudal ectopic CGCs (arrowhead).
Scale bar in (E): 300µm

Sema4C was proposed to play a role in myogenesis (Ko et al., 2005; Wu et al., 2007). However, it is predominantly expressed in tissues of the nervous system, and it was therefore further investigated regarding its function in the developing and adult CNS (Inagaki et al., 2001; Ohoka et al., 2001; Shifman and Selzer, 2006). Sema4C interacts with its C-terminus with the post-synaptic density protein PSD-95, and may function in cortical neurons as a bi-directional transmembrane ligand (Inagaki et al., 2001).

Even though Sema4G is expressed in the brain and spinal cord as well as in several sensory organs and specific projection neurons during early development (Li et al., 1999), its function in the nervous system has not been investigated yet.

When the ligand Sema4D activates its receptor, Plexin-B1 it leads to an acute collapse of axonal growth cones in hippocampal and retinal neurons during early stages of neurite outgrowth (Vodrazka et al., 2009). However, secreted Sema4D can also act as an enhancer of neurite outgrowth, as has been shown for embryonic dorsal root ganglion neurons and PC12 cells *in vitro* (Fujioka et al., 2003; Masuda et al., 2004).

Function in the immune system

Several Semaphorin family members are involved in diverse immune cell interactions. The immune function of Semaphorins was first described in B-cells through functional analysis of Sema4D (also known as CD100 in the field of immunology). Sema4D is in the immune system constitutively expressed on T-cells and has a low basal expression on B-cells (Bougeret et al., 1992; Delaire et al., 1998). The transmembrane form of Sema4D induces aggregation and improves survival of B-lymphocytes and may also function as lymphocyte receptor (Tamagnone et al., 2000). Interestingly, the extracellular domain of Sema4D can be proteolytically cleaved and shed by immune cells (Delaire et al., 2001), and the secreted form has been shown to promote immune responses as well as proliferation and viability of lymphocytes (Hall et al., 1996).

In contrast to the nervous system, in the immune system the receptor for Sema4D has been shown to be the non-Plexin receptor CD72 (Kumanogoh et al., 2000). Analysis of Sema4D-deficient mice has shown that Sema4D is important in T-cell-mediated immunity (Suzuki et al., 2008).

Sema4A is expressed by dendritic cells and enhances activation and differentiation of cultured T-cells through the receptor TIM-2 (Kumanogoh et al., 2002). But unlike Sema4D, Sema4A acts directly on T-cells.

Function as tumor promoters and tumor suppressors

Members of the Semaphorin 4 family can function both as promoters and/or suppressors of tumors. Sema4D induces invasive growth and angiogenesis of endothelial cells through binding of the Met receptor to Plexin-B1 (Conrotto et al., 2005; Giordano et al., 2002). Moreover, overexpression of Sema4D occurs in several carcinomas including breast, colon, lung and prostate cancers (Wong et al., 2007).

Sema4D and its receptor Plexin-B1 can also act as tumor suppressors. Both block tumorigenesis in primary melanoma and suppress migration in late-stage cells (Argast et al., 2009). Interestingly, Plexin-B1 has repeatedly been linked to cancer progression (Gómez Román et al., 2008; Rody et al., 2007; Tong and Buck, 2005; Wong et al., 2007; Ye et al., 2010).

Sema4C has been shown to possibly play an important role in oncogenesis of human breast cancer (Wu et al., 2009b).

Function in kidney development

Plexin-B1 deficient mice exhibit abnormalities in epithelial branching and morphogenesis during development of the kidney (Korostylev et al., 2008). Sema4D represses ureteric duct branching by signaling through Plexin-B1, mediated by the Rho-ROCK pathway (Korostylev et al., 2008). It has also been recently suggested that Sema4C-Plexin-B2 signaling may positively modulate ureteric branching in developing kidney (Perälä et al., 2010).

Sema4G is expressed both in the embryonic and adult kidney (Li et al., 1999). Interestingly, Sema4G expression was discovered to be elevated in the kidney during malaria infection with Plasmodium yoelii (Lau et al., 2001).

2.2.6 Biological functions in the Sema5, Sema6, and Sema7 family

Sema5 family

Class 5 Semaphorins comprise only two family members (Sema5A, B). Their protein structures are characterized by seven copies of a thrombospondin repeat (Adams et al., 1996). It was found by *in vitro* studies that Plexin-B3 can act as a receptor of Sema5A (Artigiani et al., 2004). However, other receptor-ligand combinations of Plexin-Bs and Sema5s are not known. Sema5A can function as a bifunctional guidance cue for developing axons, by exerting both attractive and inhibitory effects on axons. The thrombospondin repeat domains mediate regulatory interactions with sulfated proteolgycans that regulate how Sema5A affects neuronal growth cones (Kantor et al., 2004).

Sema6 family

The class 6 Semaphorins are transmembrane Semaphorins composed of four members (Sema6A-D).

In the cerebellum of Sema6A-deficient mice, many granule cells stay at ectopic positions in the molecular layer. The analysis of ectopic granule cell morphology, granule cell migration, and neurite outgrowth in cerebellar explants suggested that Sema6A controls the switch from a tangential to a radial migration of granule cells (Kerjan et al., 2005).

In Plexin-A2–deficient mice, an almost identical phenotype was observed. Plexin-A2 is likely to be the receptor that controls Sema6A function in migrating granule cells by controlling centrosome positioning (Renaud et al., 2008).

In addition, Sema6D, plays an important role in cardiac morphogenesis through its receptor Plexin-A1. Overexpression of Sema6D enhances cardiac tube looping and expansion of the ventricle (Toyofuku et al., 2004a; Toyofuku et al., 2004b).

Sema7 family

Sema7A is a GPI-anchored member of the Semaphorin family of guidance proteins. It has been first described for its immunomodulatory effects. Sema7A is expressed on activated T-cells and stimulates macrophages through α1β1-integrin to promote inflammatory responses (Suzuki et al., 2007). Sema7A is closely related to viral Semaphorins, which activate Plexin-C1 on dendritic immune cells (Liu et al., 2010). In analogy, it is likely that Sema7A is an *in vivo* ligand of Plexin-C1 for immune functions. This model is also supported by the recent crystal structure analysis of a Sema7A-Plexin-C1 ligand-receptor complex (Janssen et al., 2010; Nogi et al., 2010)

The function of Sema7A in nervous system is mediated independently of Plexins through β1-integrin receptors. Sema7A enhances central and peripheral axon growth and is essential for proper axon tract formation during embryonic development (Pasterkamp et al., 2003).

2.3 Aims of the thesis

Semaphorins and Plexins are cognate ligand-receptor families that regulate important steps during nervous system development. In vertebrates, the Semaphorin gene family is divided into five classes, and the main signaling receptors, the Plexins, have nine members (classes A through D).
One member of the Plexin-B family, Plexin-B2 is critically involved in neural tube closure and cerebellar granule cell development (Deng et al., 2007; Friedel et al., 2007). However, the *in vivo* ligands of Plexin-B2 are not known. To further elucidate the function of Plexin-B2 in cerebellar development, the main goal of this thesis project was to identify functional *in vivo* ligands of Plexin-B2.

My studies comprised the following aims:

- To identify candidates for ligands of Plexin-B2 in the cerebellum, mRNA *in situ* hybridizations (ISH) in the developing mouse brain were performed. Since *in vitro* studies had shown that Plexin-Bs can be activated by Semaphorin 4s, my studies focused on the expression patterns of all Semaphorin 4 family members.

- To investigate the binding properties of Semaphorin 4 candidate ligands to Plexin-B receptors, ligand binding assays on transfected cells and on cerebellar sections were performed.

- To examine the *in vivo* function of putative Plexin-B2 ligands. Therefore, phenotypic analyses of mouse mutants of candidate ligands were carried out. In this study, I analyzed mutants of Sema4C and Sema4G. By genetic interaction studies, I also investigated the possibility that both act in parallel as ligands for Plexin-B2.

- Finally, to study the cellular effects of Semaphorin 4 on the migratory behavior of Plexin-B2 expressing granule cells, transwell migration assays and EGL microexplant cultures with wild type, *Sema4c*-/-, or *Plxnb2*-/- granule cell precursors (GCP) were performed.

3. RESULTS

3.1 Expression studies on Semaphorin 4 and Plexin-B genes

Only little data were available about the expression patterns of Semaphorin 4 (Sema4) and Plexin-B genes in the mouse cerebellum. To obtain detailed and comprehensive information about the expression patterns and time points of the expression of Sema4 family members and Plexin-Bs in the developing mouse brain, non-radioactive mRNA *in situ* hybridizations (ISH) were performed.

3.1.1 Construction of ISH probes

For the first series of ISH experiments on brain sections, a set of Sema4 and Plexin-B probes with an approximate length of about 700 bp was used. These probes, however, revealed only weak signals with the non-radioactive ISH technique. To obtain ISH probes that yield a more sensitive signal, a set of plasmids with Sema4 and Plexin-B probe fragments of about 2kb length was cloned. The identity of the nucleotide sequences between the different probes was in the range of 43% to 54%, thus providing sufficient specificity for the detection of individual gene family members.

The ISH probe fragments were amplified with corresponding primer pairs from a cDNA preparation from RNA of E11.5 mouse embryos and cloned into a TOPO-TA cloning vector (pCRII-TOPO). For ISH, the vectors were linearized with different restriction enzymes at the end of the cDNA insert, and the riboprobes were synthesized with T7 or Sp6 RNA polymerase (for details, see Material and Methods).

Figure 3.1 Position of the ISH probes
Position of the 2 kb ISH probes (red line) on the Sema4 and Plexin-B mRNAs (coding sequence marked by a thickened box)

3.1.2 Expression of Sema4 genes at E8.5

The gene knock-out of Plexin-B2 leads to exencephaly in the C57BL/6 inbred strain (Friedel et al., 2007). Because the onset of the exencephaly phenotype occurs around embryonic day E9.0, a screening for the mRNA expression of Sema4 genes in the E8.5 embryo was performed. This time point is shortly before the neural tube starts to close along the dorsal midline, which is completed by E9.5. Only expression of Sema4C and Sema4G was observed, but not of other Sema4 family members (Figure 3.2).

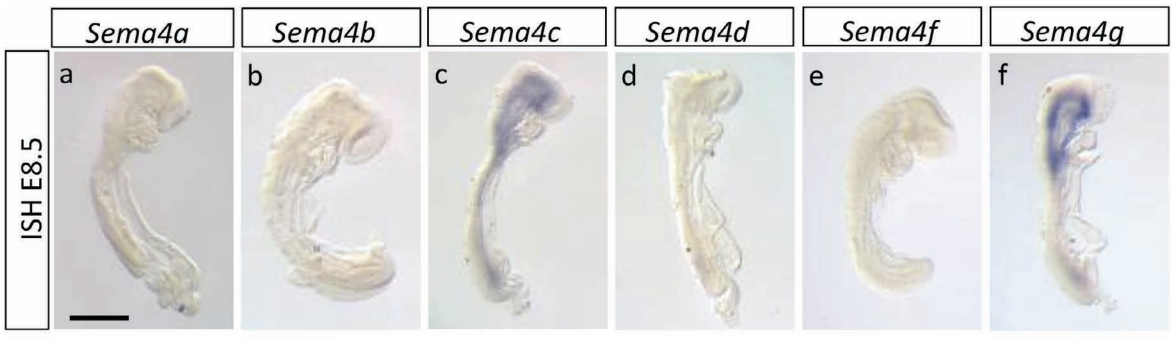

Figure 3.2 Expression of Sema4 genes at E8.5 in whole mount embryo preparations
Sema4c and *Sema4g* expression was detected in the developing nervous system by whole mount *in situ* hybridization of E8.5 embryos with DIG-labeled riboprobes (c and f). No expression could be observed for *Sema4a*, *Sema4b*, *Sema4d*, and *Sema4f* (a, b, d, e).
Scale bar: 1mm

3.1.3 Expression of Sema4 and Plexin-B genes in the developing cerebellum at P10

To investigate the expression of Sema4 and Plexin-B genes in the developing cerebellum, mRNA *in situ* hybridization at postnatal day P10 was performed (Figure 3.3). This time point corresponds to the main phase of cerebellar granule cell neurogenesis. Expression patterns were correlated to specific cell types by co-labeling with cell type specific immunohistochemical markers (see below).

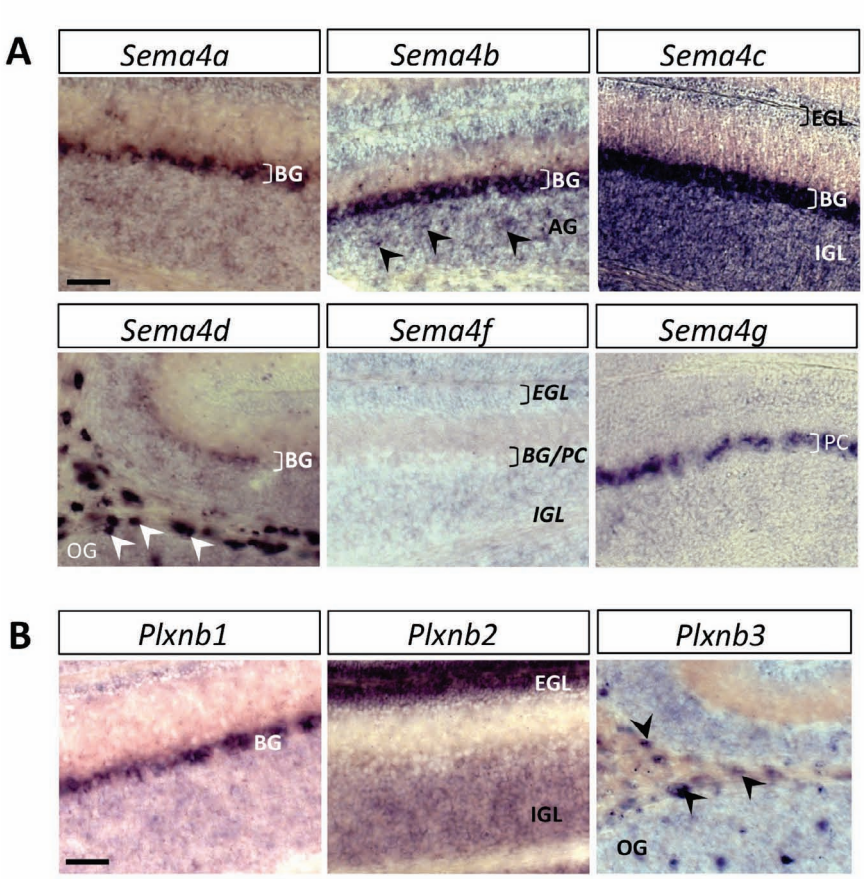

Figure 3.3 Expression of Sema4 and Plexin-B genes at P10 in the cerebellar cortex
(A) *Sema4a* corresponded in its expression pattern to Bergmann glia cells, *Sema4b* to Bergmann glia and astroglia, *Sema4c* to granule cells and Bergmann glia, *Sema4d* to oligodendroglia, and *Sema4g* to Purkinje cells. *Sema4f* mRNA was not detectable in the developing cerebellum.
(B) The *Plxnb1* expression pattern corresponded to Bergmann glia cells, the *Plxnb2* pattern to granule cells, and the *Plxnb3* pattern to oligodendroglia.
BG, Bergmann glia; AG, astroglia; EGL, external granule cell layer; IGL, Internal granule cell layer; PC, Purkinje cells; OG, oligodendroglia.
Scale bar in (A, B): 25µm.

Of the six murine Sema4 genes, *Sema4a*, *Sema4b*, and *Sema4d* revealed patterns that correlated with glial cell types. *Sema4a* transcript was detected in Bergmann glia, *Sema4b* transcript was detected in Bergmann glia and in astroglia, and *Sema4d* transcript was detected in oligodendroglia (Figure 3.3 A). Only *Sema4c* and *Sema4g* revealed patterns correlating with neuronal expression. *Sema4c* was detected in cerebellar granule cells of the external granule cell layer (EGL) and internal granule cell layer (IGL), and also in Bergmann glia. *Sema4g* expression was detected in Purkinje cells and *Sema4f* expression was not detectable in the P10 cerebellum.
Also the expressions of the putative Sema4 receptors of the Plexin-B family in the cerebellar cortex were investigated (Figure 3.3 B). *Plxnb1* expression was restricted to Bergmann glia. *Plxnb2* appeared to be specifically expressed in cerebellar granule cell precursors of the EGL, and at reduced levels also in the IGL, consistent with previous reports (Friedel et al., 2007). *Plxnb3* expression was found in oligodendroglia.

To correlate expression patterns with specific cell types, co-labeling with specific immunohistochemical markers was performed (Figure 3.4). *In situ* hybridizations of P10 cerebellar sections (purple stain) were co-labeled for immunohistochemical markers with DAB staining (brown stain). As a marker for glia cells, antibodies against the beta-subunit of S100 protein (S100β) and glial fibrillary astrocytic protein (GFAP) were used (Liesi et al., 1983; Van Eldik et al., 1984). The glial-derived protein S100β labels astroglia cells, and GFAP is an intermediate filament protein that labels Bergmann glia cells. Pax6, a nuclear transcription factor essential for the development of the CNS, is a marker for granule cells (Walther et al., 1991). Calbindin, a member of a large family of intracellular calcium binding proteins, is used as a marker for cerebellar Purkinje cells (Kawasaki et al., 1998). As a marker for oligodendrocytes, Olig2, a transcription factor that controls development and differentiation of oligodendrocytes was used (Marie et al., 2001).

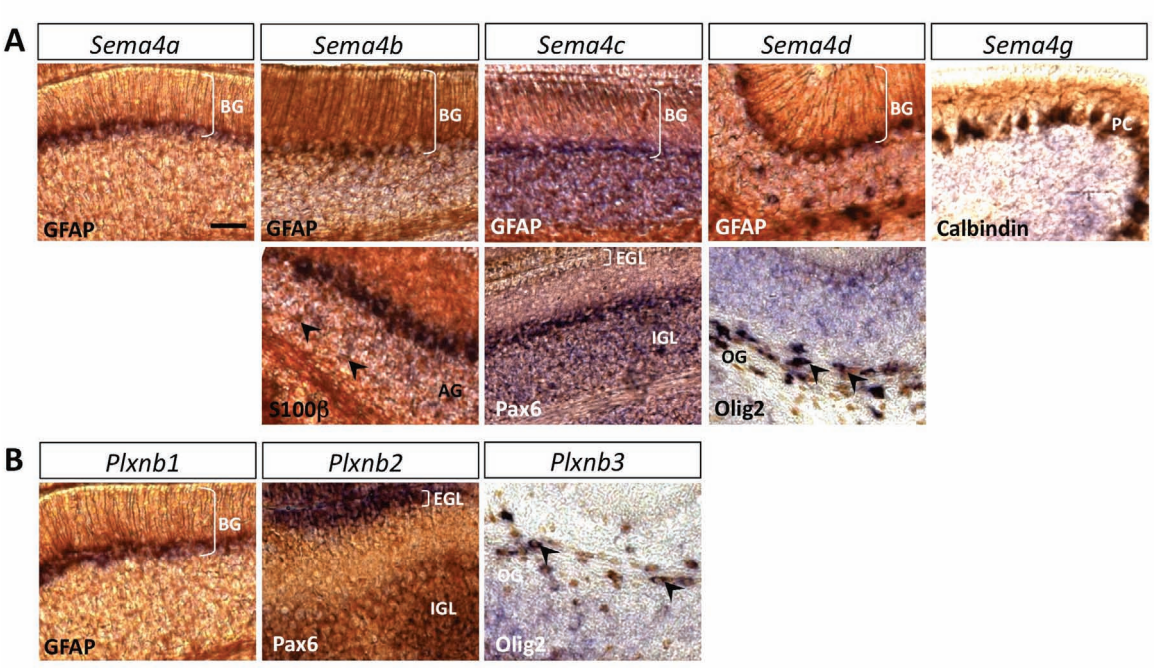

Figure 3.4 Expression of Sema4 and Plexin-B genes in specific cerebellar cell types
(A) *Sema4a in situ* signal overlapped with GFAP in cell bodies of Bergmann glia cells, *Sema4b* with GFAP and S100β in Bergmann glia and astroglia cells, *Sema4c* with GFAP in Bergmann glia and Pax6 in granule cells, *Sema4d* with Olig2 in oligodendroglia, and *Sema4g* with calbindin in Purkinje cells.
(B) *Plxnb1 in situ* signal overlapped with GFAP in cell bodies of Bergmann glia cells, *Plxnb2* with Pax6 in granule cells, and *Plxnb3* with Olig2 in oligodendroglia.
BG, Bergmann glia; AG, astroglia; EGL, external granule cell layer; IGL, Internal granule cell layer; PC, Purkinje cells; OG, oligodendroglia
Scale bar in (A, B): 25µm.

In summary, all Sema4 members except *Sema4f* reveal expression patterns that would be consistent with a ligand function for Plexin-B2. *Sema4a*, *Sema4b*, *Sema4c*, and *Sema4d* are expressed in radial Bergmann glia, which are in contact with migrating granule cells.

Table 3.1 Summary of detected expression patterns in the developing cerebellar cortex.

	Sema4a	*Sema4b*	*Sema4c*	*Sema4d*	*Sema4f*	*Sema4g*	*Plxnb1*	*Plxnb2*	*Plxnb3*
Granule cells			+					+	
Purkinje cells						+			
Bergmann glia	+	+	+	+			+		
Astroglia		+							
Oligodendroglia				+					+

Sema4g is present on Purkinje cells, while *Sema4c* is the only Sema4 that is also co-expressed with *Plxnb2* in granule cells (Figure 3.4).

3.1.4 Expression of Sema4C and Sema4G in the early developing cerebellum

Since no cerebellar phenotypes have been identified in mice deficient of Sema4A, Sema4B, or Sema4D (data not shown and (Friedel et al., 2007), and since the expression patterns of Sema4C and Sema4G are consistent with a role as ligands for Plexin-B2, the focus was set on further analysis of Sema4C and Sema4G.

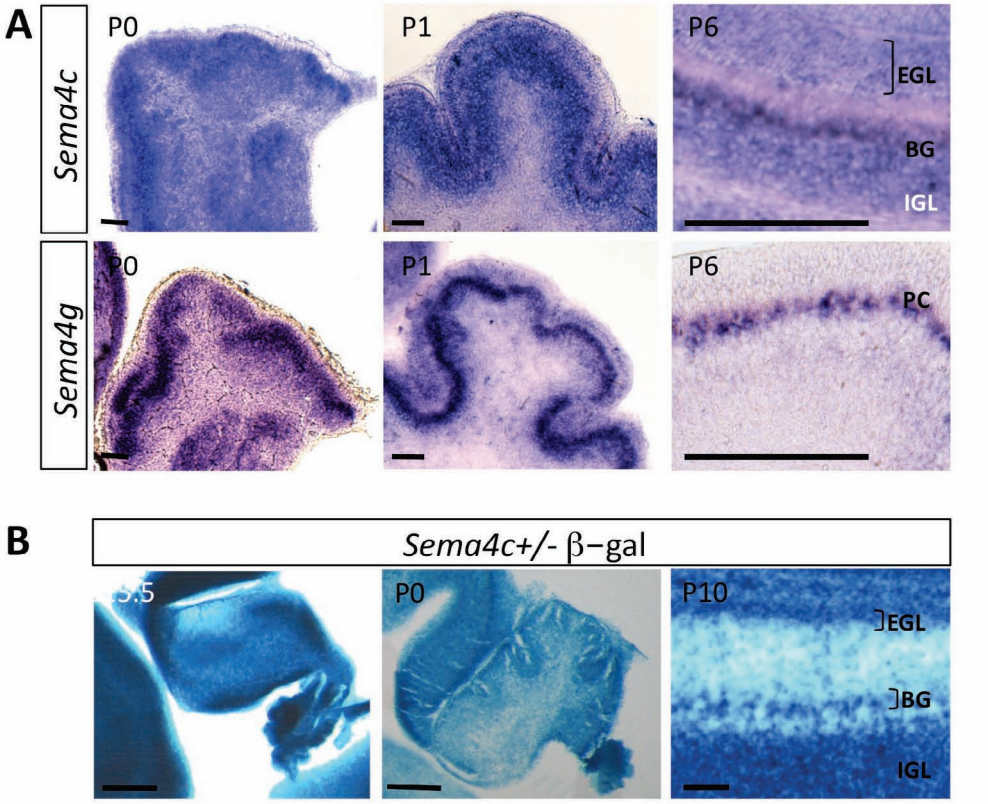

Figure 3.5 Expression of Sema4c and Sema4g in the early developing cerebellum
(A) *In situ* hybridization for *Sema4c* and *Sema4g* expression at postnatal days P0, P1, and P6. *Sema4c* gene expression was found in the granule cell and Bergmann glia layers, and Sema4g gene expression was found in the Purkinje cell layer. (B) X-gal stainings for the β-galactosidase reporter of *Sema4c*+/- animals on cerebellar sections at E15.5, P0, and P10.
BG, Bergmann glia; AG, astroglia; EGL, external granule cell layer; IGL, Internal granule cell layer; PC, Purkinje cells; OG, oligodendroglia.
Scale bars in (D): for P0 and P1 100 µm, for P6 25 µm; (E): for E15.5 and P0 250µm, for P10 25 µm.

Therefore, the *Sema4c* and *Sema4g* gene expression was analyzed at earlier time points of cerebellar development. Both genes were robustly expressed in the developing cerebellar cortex between P0 and P6, with patterns that indicate the expression of *Sema4c* in granule cells and Bergmann glia, and of *Sema4g* in Purkinje cells (Figure 3.5 A). To additionally confirm the expression of *Sema4c*, the β-galactosidase (β-gal) reporter that is present in the Sema4c targeted trap allele was utilized (described in detail further below). Heterozygous Sema4c+/- mice were analyzed for β-gal reporter expression at different developmental time points (E15.5, P0 and P10), supporting the observation of *Sema4c* expression in granule cells and Bergmann glia (Figure 3.5 B).

3.2 Generation of Sema4 and Plexin-B expression plasmids

For the different *in vitro* assays that were used in this study (binding assay, transwell migration assay, and EGL explants), expression plasmids for VSV-tagged Plexin-B1, Plexin-B2 and Plexin-B3, and for ectodomains of Sema4C, Sema4G, and Sema4D fused to an alkaline phosphatase (AP) reporter were utilized.

The plasmids ph-PB1-VSV and pm-PB2-VSV, encoding human Plexin-B1 and mouse Plexin-B2 with an N-terminal VSV-peptide tag, respectively, and pcDNA1-S4C-hPLAP-Str and pS4D-AP, encoding ectodomains of Sema4C and Sema4D fused with AP, respectively, were obtained from Dr. Luca Tamagnone, University of Torino, Dr. Steven Strittmatter (Yale University), and Dr. Roland Friedel (Helmholtz Center Munich). In addition, new plasmids for Plexin-B3-VSV expression and for Sema4G-AP expression were generated for this study.

3.2.1 Plexin-B3 Expression Plasmid

A cDNA fragment comprising the mouse Plexin-B3 coding sequence downstream of its signal sequence was PCR amplified from an E10.5 embryonic cDNA, and ligated into the pCRII-TOPO plasmid. Absence of mutations was confirmed by sequencing of the fragment. The existing pmPB2-VSV construct was used to obtain a vector backbone of an expression vector with a signal sequence followed by a VSV peptide tag. The Plexin-B2

sequence was removed and replaced by the Plexin-B3 cDNA fragment, resulting in the pmPlexin-B3-VSV construct.

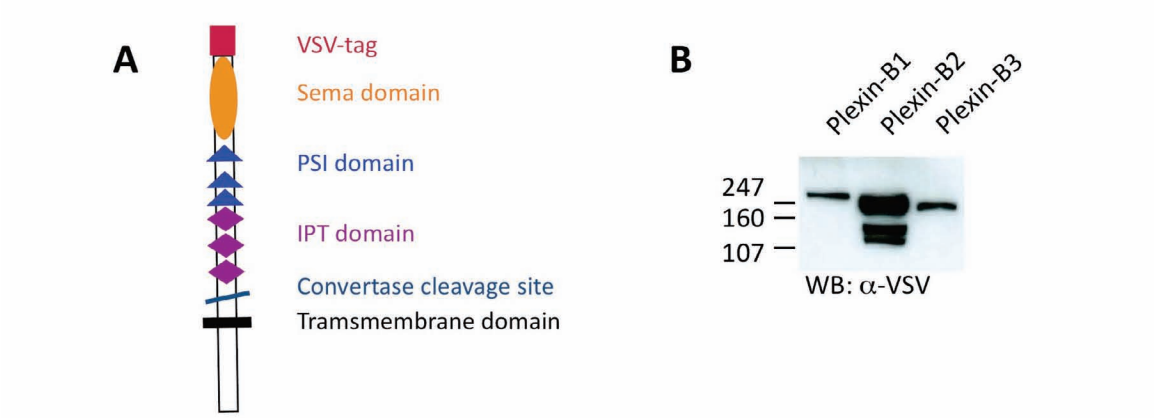

Figure 3.6 Schematic illustration and Western blot analysis of VSV tagged Plexin-Bs
(A) Schematic illustration of the VSV-Plexin-B protein with the VSV tag at the N-terminus of the plexin. (B) Expression of transfected Plexin-B plasmids was confirmed by Western blot analysis of cell lysates with an antibody directed against the VSV-tag. Predicted sizes: VSV-Plexin-B1, 235kDa; VSV-Plexin-B2, 207 kDa; VSV-Plexin-B3, 213 kDa.

The correct full-length expression of the VSV-Plexin-B proteins was confirmed by Western blot analysis of protein lysates of transfected fibroblast cells. An antibody directed against the VSV peptide tag revealed full-length expression of hPlexin-B1-VSV, mPlexin-B2-VSV, and Plexin-B3-VSV (Figure 3.6). *In vivo*, Plexin-B proteins also occur in a processed form that is generated by protease cleavage of the ectodomains near the transmembrane region. Possibly due to insufficient protein processing in the fibroblast cell line, smaller protein bands corresponding to cleaved ectodomains were only observed for VSV-Plexin-B2 expression.

3.2.2 Sema4G-AP expression plasmid

A cDNA fragment encoding the extracellular part of Sema4G was amplified by PCR from cDNA of murine E10.5 embryos and ligated into a pCRII-TOPO vector. After confirmation of sequence integrity, it was subcloned into the backbone of the existing pcDNA1-S4C-hPLAP-Str vector to generate an expression plasmid for the production of Sema4G-AP. In this construct, the Sema4G ectodomain cDNA is directly followed by the human placental alkaline phospatase (hPLAP) sequence, resulting in a fusion protein detectable by AP staining.

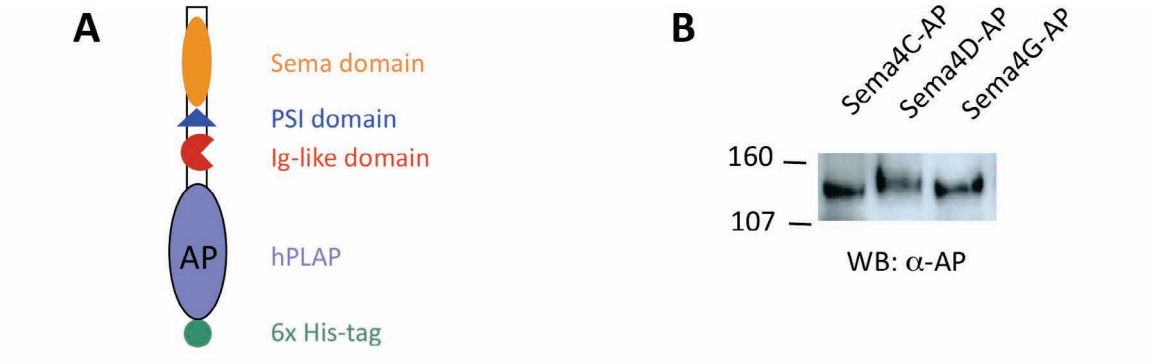

Figure 3.7 Schematic illustration and Western blot analysis of Sema4-AP constructs
(A) Schematic illustration of the Sema4-hPLAP fusion protein with the His-tag at its C-terminus.
(B) Size of recombinant Sema4-AP constructs was confirmed by Western blot analysis with an antibody directed against the AP polypeptide. Predicted sizes: Sema4C-AP, 128 kDa; Sema4D-AP, 125 kDa; Sema4G-AP, 127 kDa.

COS cells were transfected with the plasmids for Sema4C-AP, Sema4D-AP, and Sema4G-AP, causing the cells to secrete soluble Sema4-AP fusion proteins into the cell culture media supernatant. The correct full-length expression of the tested proteins was confirmed by Western blot analysis of supernatants with an antibody against the AP polypeptide, and bands of predicted sizes were observed (Sema4C-AP, 128 kDa; Sema4D-AP, 125 kDa; Sema4G-AP, 127 kDa).

3.3 Binding Assays with alkaline phosphatase fusion proteins

3.3.1 Sema4C and Sema4G bind to Plexin-B2 in cell culture

In vitro binding assays were performed to determine the ligand-receptor relations of the class 4 Semaphorins Sema4C, Sema4D, and Sema4G with the B-type Plexins. For the binding studies, COS cells were transfected with expression plasmids for Plexin-B1, Plexin-B2, and Plexin-B3. Transfection with EGFP served as a negative control for unspecific binding, and also as a positive control for transfection efficiency.
The transfected cells were incubated with the cell culture supernatants containing secreted Sema4C-AP, Sema4G-AP, or Sema4D-AP fusion proteins. After an incubation time of 2 h, cells were washed and stained for AP activity with the NBT/BCIP color substrate (Figure

3.8). Staining time was typically over night, but was extended in some cases for up to 2 days.

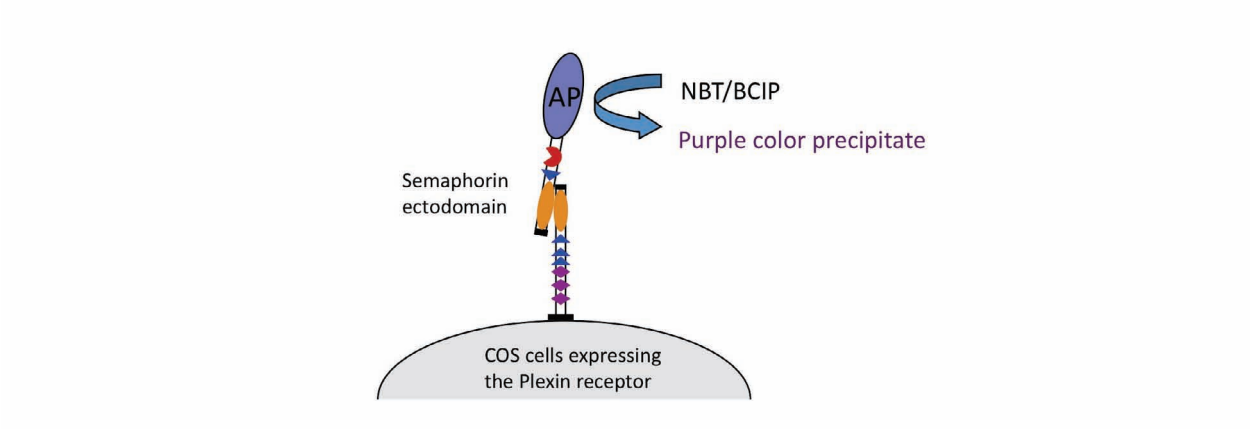

Figure 3.8 Principle of alkaline phosphatase ligand-receptor detection
The AP is fused to the soluble ectodomain of the Semaphorin. The Semaphorin-AP binds to its Plexin receptor, expressed on the surface of transfected cells. The bound Semaphorin is visualized by adding NBT/BCIP substrate, which is catalyzed by AP into an insoluble black-purple precipitate.

The experiments were done twice with Semaphorin-AP that was produced by COS cells, and once with Semaphorin-AP that was produced by HEK293 cells. Binding results were essentially identical with both types of probes. Specific binding resulted in well-defined dark purple staining of cell bodies. Unspecific binding, as seen in the EGFP negative control, was characterized by a light background with few purple spots of a much paler color than the specific binding.

All experiments showed preferential binding of Sema4C to Plexin-B2, and only weak binding to Plexin-B1. However, no binding of Sema4C to Plexin-B3 was observed. In the Plexin-B2 wells treated with Sema4G-AP, the staining was less intense than in Plexin-B2 transfected wells treated with Sema4C-AP, but still very likely represented specific binding characteristics. Sema4G did not bind to Plexin-B1 or Plexin-B3.

Sema4D revealed robust binding to both Plexin-B1 and Plexin-B2, as has been reported previously (Masuda et al., 2004; Tamagnone et al., 1999), and also weaker binding to Plexin-B3 (Figure 3.9).

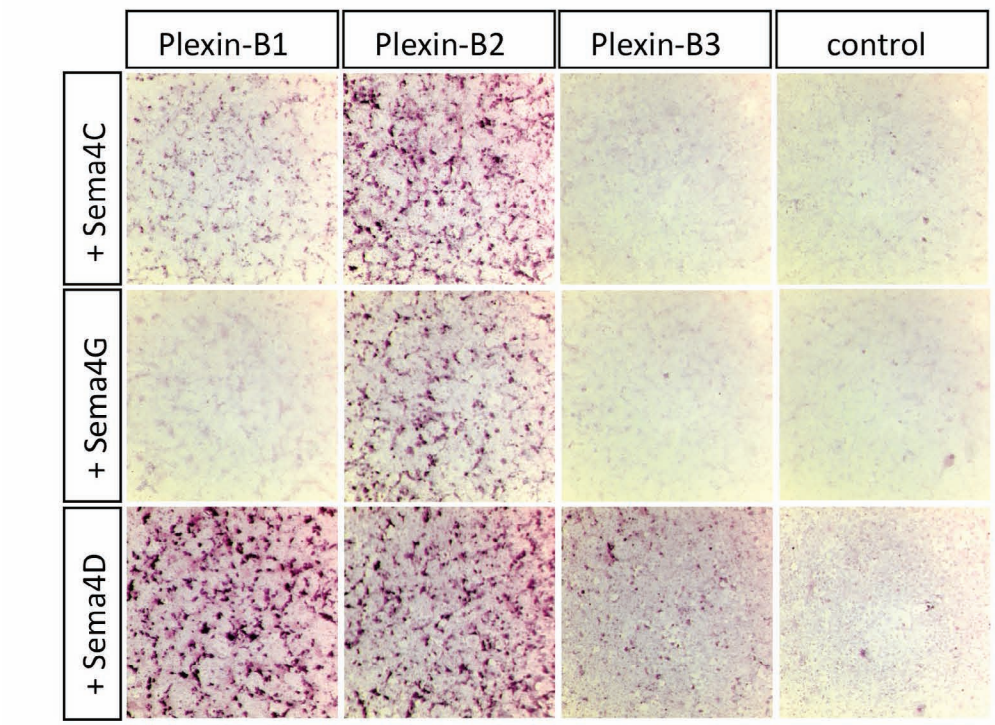

Figure 3.9 Binding of Sema4 to Plexin-Bs
Binding of Sema4 ectodomains fused to an alkaline phosphatase (AP) reporter to COS fibroblasts that were transiently transfected with expression plasmids for Plexin-B1, -B2, -B3 or GFP (control). Sema4C bound robustly to Plexin-B2 and weaker to Plexin-B1 expressing cells, Sema4G bound to Plexin-B2, and Sema4D to Plexin-B1, -B2, and -B3.

3.3.2 Sema4C and Sema4G bind to Plexin-B2 on tissue sections

The *in vitro* binding assay showed specific ligand-receptor relations of the class 4 Semaphorins Sema4C, Sema4D, and Sema4G with the B-type Plexins. The next step was to analyze, if the binding could also be confirmed on fresh frozen tissue sections.

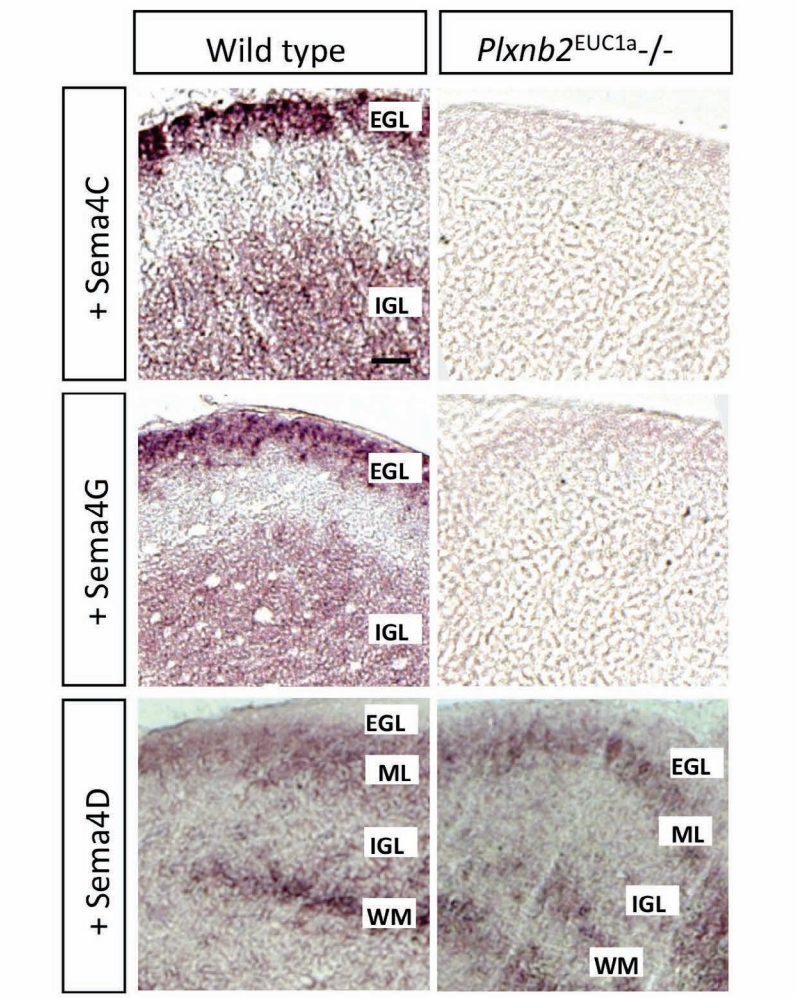

Figure 3.10 Binding of Sema4-AP proteins on cryosections of P10 cerebella of wild type and *Plxnb2*^{EUC1a} -/- mutants
Sema4C and Sema4G bound robustly to EGL and weaker to IGL on wild type sections. No binding of Sema4C-AP or Sema4G-AP was detectable on *Plxnb2*^{EUC1a}-/- mutant sections. Sema4D-AP binding was detected within the molecular layer and white matter, both on wild type and *Plxnb2*^{EUC1a} -/- mutant sections.
EGL, external granule cell layer; IGL, Internal granule cell layer; ML, molecular layer; WM, white matter. Scale bar in (D): 50µm

For this purpose, cerebellar sections from wild type and Plexin-B2 mutant mice at P10 were utilized to investigate the specificity of Sema4-AP binding to cerebellar tissue (Figure 3.10). Since the previously reported Plexin-B2 mutant allele contains an AP reporter that would obscure binding studies with AP-fusion proteins (Friedel et al., 2007), use of a different mutant allele for Plexin-B2 was required. A novel mouse mutant for Plexin-B2 that had been generated by the European Conditional Mouse Mutagenesis (EUCOMM) program was utilized (Figure 3.11).

Both Sema4C-AP and Sema4G-AP bound on wild type tissue strongly to the external granule cell layer (EGL), and with reduced intensity to the internal granule cell layer (IGL). In contrast, binding of Sema4C-AP and Sema4G-AP to sections of Plexin-B2

mutants was virtually absent. These data suggest that Sema4C and Sema4G bind in the cerebellum specifically to Plexin-B2 expressing granule cells. In contrast, Sema4D-AP protein bound both in wild type and in Plexin-B2 mutant sections to structures in the molecular layer and in the white matter, suggesting that at least in the cerebellum, Sema4D is not an *in vivo* ligand for Plexin-B2.

3.4 Analysis of Sema4 and Plexin-B mutant mice

Mouse mutant alleles

To investigate the *in vivo* function of Sema4C and Sema4G in cerebellar development, four different mutant lines were used for phenotypic analysis. The Plexin-B2 and Sema4C knock-out mutant mouse lines were generated by Dr. Roland Friedel (Helmholtz Center Munich) with the targeted trapping method. The Plexin-B2 EUCOMM mutant mouse (*Plxnb2*^{EUC1a}) was provided by the European Conditional Mouse Mutagenesis program (EUCOMM), and the Sema4G mutant mouse was provided by Dr. Hitoshi Kikutani (Osaka University, Japan).

Plexin-B2 mutation

A Plexin-B2 loss of function mutant mouse line was generated by the targeted trapping method (Friedel et al., 2005). The targeted trapping method is a strategy based on the targeting of a promoter-less gene trap cassette into a defined intron. The targeting vector was constructed by flanking the placental alkaline phosphatase (PLAP) secretory trap cassette (Leighton et al., 2001) with 5′ and 3′ homology arms of 5 kb and 3 kb size, respectively. Correct homologous recombination in mouse embryonic stem cells resulted in the insertion of the secretory trap cassette between exon 16 and 17 of the Plexin-B2 gene. The resulting bicistronic transcript encodes two proteins: first, a fusion of the N-terminal part of the endogenous protein to a transmembrane domain/ß-geo protein, which is retained in an intracellular compartment and causes therefore a functional null mutation

(Skarnes et al., 1995), and second, PLAP, which is present on the cell surface as GPI-anchored protein.

Plexin-B2 EUCOMM mutation

The Plexin-B2 EUCOMM mutant allele was generated by the European Conditional Mouse Mutagenesis program (EUCOMM). Official allele symbol is *Plxnb2*$^{tm1(EUCOMM)Wtsi}$, which is abbreviated here as *Plxnb2*^{EUC1a}. Homology arms at the 5′ and 3′ ends of the targeted trapping vector mediated gene specific targeting by homologous recombination into the intron between exon 6 and 7 of the Plexin-B2 gene. A splice acceptor–β-geo–polyadenylation signal cassette facilitated promoter-less targeting. The "critical" exons 7, 8 and 9 (whose excision creates a frame shift) are flanked by loxP sites. This cassette acts similar to a gene trap insertion and disrupts Plexin-B2 function and reports its expression.
For further analysis, it is possible to convert the EUCOMM allele into a conditional allele. For this purpose, the targeting cassette has to be removed first by FLP recombination and gene activity can then be selectively inactivated by Cre recombinase.

Sema4C mutation

The targeted trap of the mouse *Sema4c* gene was generated with a targeting construct that led to the insertion of the secretory trap vector into the intron between exons 12 and 13. This insertion creates a fusion transcript of the first 12 exons of *Sema4c* with the elements of the secretory trap vector, consisting of a transmembrane domain/ß-geo (ß-gal fused to neo) cassette, followed by an internal ribosomal entry sequence and a PLAP sequence. This insertion site is located between the Immunoglobulin (Ig) domain and the transmembrane domain of Sema4C. As described above for the Plexin-B2 mutation, the fusion protein is retained in an intracellular compartment and represents a functional null mutation.

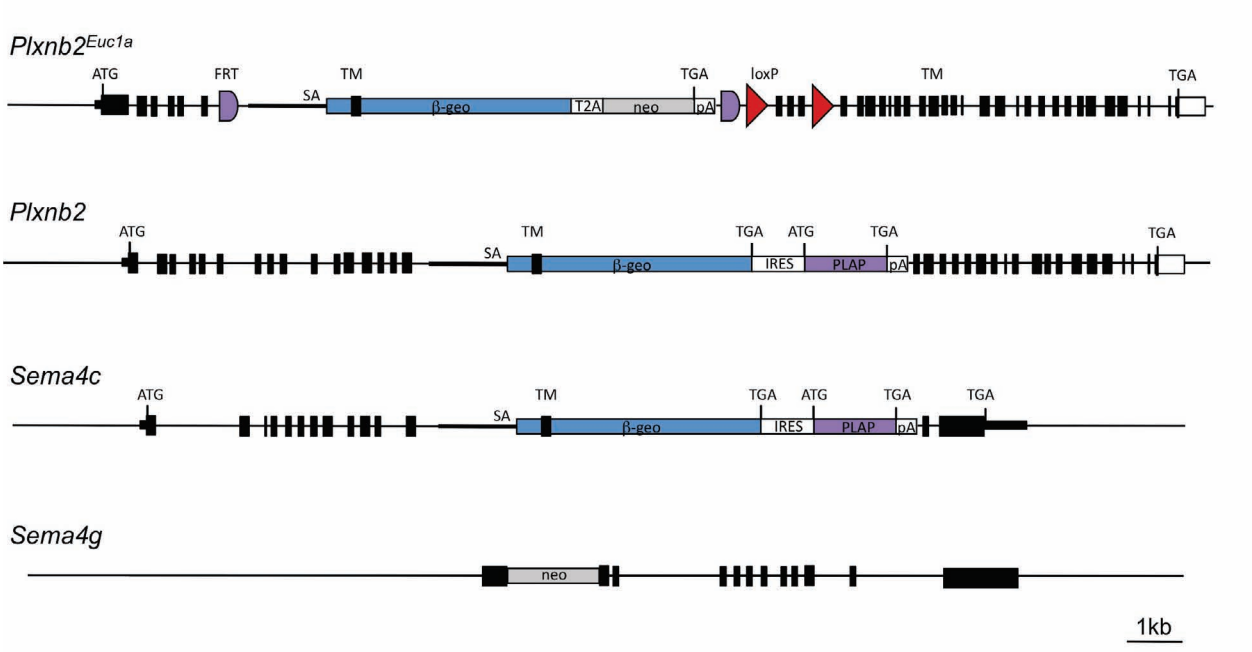

Figure 3.11 Targeted Alleles used in this study
The *Plxnb2* gene was mutated by targeted trapping. Correct homologous recombination resulted in the insertion of the secretory trap cassette between exons 16 and 17.
The Plexin-B2 EUCOMM allele was generated by the European Conditional Mouse Mutagenesis program (EUCOMM). Official allele symbol: *Plxnb2*$^{tm1(EUCOMM)Wtsi}$; abbreviated here as *Plxnb2*^{EUC1a}. The targeted trapping vector was inserted by homologous recombination into the intron between exon 6 and 7. The critical exons 7, 8 and 9 are flanked by loxP sites.
The *Sema4c* gene was mutated by targeted trapping. The insertion creates a fusion transcript of the first 12 exons of *Sema4c* with the elements of the secretory trap vector, consisting of a transmembrane domain/ß-geo (ß-gal fused to neo) cassette, followed by an internal ribosomal entry sequence and a PLAP sequence.
For the *Sema4g* mutation, a 350 bp fragment containing the first exon with the initiation codon and the second exon were replaced with a neo resistance cassette.
FRT, target site for FLP recombinase; loxP, target site for Cre recombinase; SA, splice acceptor; TM, transmembrane domain; βgal, β-galactosidase; T2A, self cleavage peptide; pA, polyadenylation sequence.

Sema4G mutation

For mutation of the Sema4G gene, a targeting vector was constructed by replacing a 350 bp fragment containing the first exon with the initiation codon and the second exon with a neomycin resistance cassette. The vector was flanked with a Herpes simplex virus thymidine kinase (HSV-*TK*) gene that was used to select against random integration.

3.5 PB2 EUCOMM

The previously reported Plexin-B2 mutant allele contains an AP reporter (Friedel et al., 2007), which would generate in binding studies on sections a background AP activity that overlaps with the signal derived from the AP-fusion proteins (3.3.2). Therefore, a novel mutant allele for Plexin-B2 without AP reporter, which had been generated by the European Conditional Mouse Mutagenesis (EUCOMM) program, was used for binding studies.

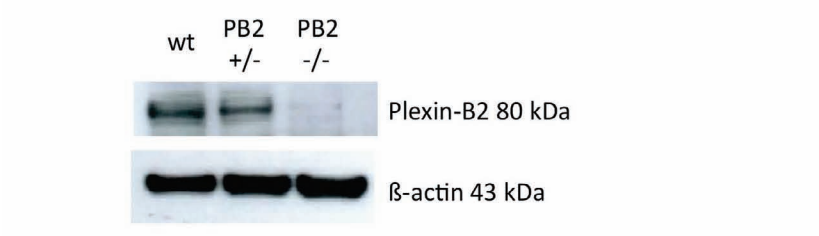

Figure 3.12 Western blot analysis of EUCOMM Plexin-B2
Western blot analysis of lysates from P5 cerebella with anti-Plexin-B2 antibody directed against a peptide downstream of the targeting site shows reduction of Plexin-B2 protein in *Plxnb2*^{EUC1a}-/- mutants to less than 5% (80 kDa band) of wild type levels. Detection of ß-actin served as loading control.

To test the mutagenesis of the Plexin-B2 EUCOMM allele, Western blot analysis of lysates from P5 cerebella with anti-Plexin-B2 antibody directed against a peptide downstream of the targeting site was performed. In wild type and *Plxnb2*+/- animals, a polypeptide of 80 kDa, corresponding to the predicted size of the protease processed Plexin-B2 C-terminal part was detected. In *Plxnb2*^{EUC1a}-/- mutants, a weak band of less than 5% of wild type levels was detected. This indicates that some splicing around the targeting cassette occurs in the Plexin-B2^{Euc1a} allele, which results in low levels of wild type protein. Detection of ß-actin served as loading control (Figure 3.12).

3.5.1 Viability and Pigmentation defect

Amongst viable newborn pups from breedings of heterozygous parents, only 8% *Plxnb2*^{EUC1a}-/- mutants were observed. For a completely viable mutation, the expected Mendelian ratio is 25%. Thus, about 66% of *Plxnb2*^{EUC1a}-/- embryos died during embryogenesis or at birth, possibly due to exencephaly, as it is the case for the targeted

trap *Plxnb2*-/- mutation, in which about 95% of mutant embryos were affected by exencephaly (Friedel et al., 2007).

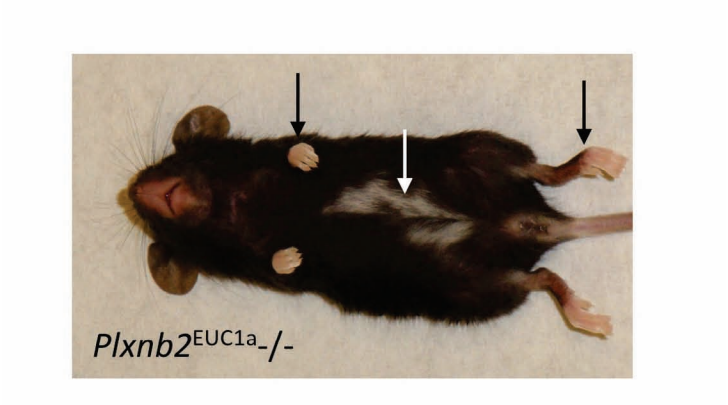

Figure 3.13 Pigmentation defects of *Plxnb2*^{EUC1a}-/- mutants
Plxnb2^{EUC1a}-/- mutants in co-isogenic C57BL/6N background show pigmentation defects at distal fore and hind limbs, and at the ventral midline.

As the Plexin-B2 protein in *Plxnb2*^{EUC1a}-/- mutants is not completely eliminated, but still present in low amounts of less than 5%, it is possible that the *Plxnb2*^{EUC1a} allele is a hypomorphic mutation, and this may be the reason why viable *Plxnb2*^{EUC1a}-/- mutants were obtained. An alternative explanation for the higher viability of Plexin-B2 EUCOMM homozygous mutants may be the fact that the Plexin-B2 EUCOMM allele was generated and bred on a pure C57BL/6 background, which is different from the targeted trap mutation, which was generated on a 129 background and then backcrossed to C57BL/6.
Interestingly, all *Plxnb2*^{EUC1a}-/- mutants displayed distinct pigmentation defects. They show white patches of fur and skin along the ventral midline, and white distal fore and hind limbs (Figure 3.13).

3.5.2 Cerebellum phenotype

The viable *Plxnb2*^{EUC1a}-/- mutants displayed a severe disruption of the cerebellar cortex, as revealed by β-galactosidase staining (Figure 3.14). The foliation defects were apparent as fusions of lobules I-III, VI-VII, and VIII and IX, and a strong disruption of the cerebellar lamination was observed. In addition, lobules I-III contained reduced numbers of granule cells. Ectopic clusters of granule cells were found at the subpial surface, mostly in caudal lobules. In comparison to the *Plxnb2*^{EUC1a}+/- animals, which appear phenotypically

normal, the cerebellum of a *Plxnb2*^{EUC1a}-/- mutant is about 40% smaller. These cerebellar defects are largely identical to defects that were described for the targeted trap mutation (Friedel et al., 2007).

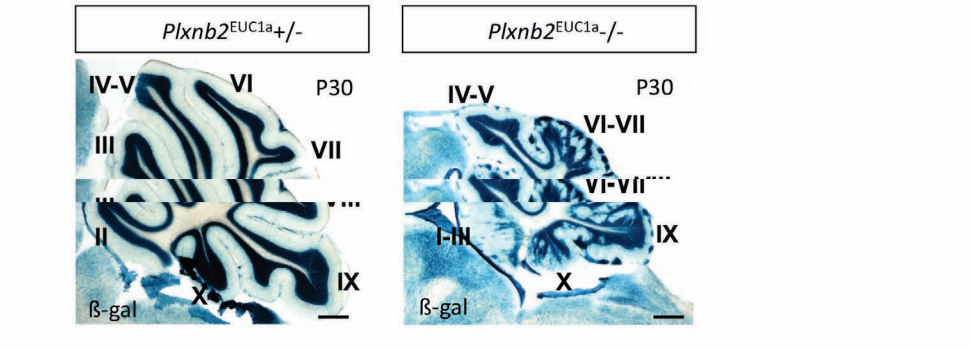

Figure 3.14 Cerebellar phenotype of *Plxnb2*^{EUC1a}+/- and *Plxnb2*^{EUC1a}-/- mutants
Sagittal cerebellum sections of *Plxnb2*^{EUC1a}+/- and *Plxnb2*^{EUC1a}-/- animals stained for β-galactosidase activity. *Plxnb2*^{EUC1a}+/- animals appear phenotypically normal. Severe cerebellar defects are found in *Plxnb2*^{EUC1a}-/- animals, largely identical to defects described in a previous loss-of-function mutation (Friedel et al., 2007). Lobules I-III, VI-VII and VIII and IX are fused and the cerebellar lamination is profoundly disturbed. Ectopic clusters of granule cells are found at the subpial surface.
Scale bar: 400µm

3.6 Defects in Sema4C mutant mice

To study the *in vivo* role of Sema4C in cerebellar development, a mutant mouse line that had been generated by the targeted trapping method was used (Friedel et al., 2005).

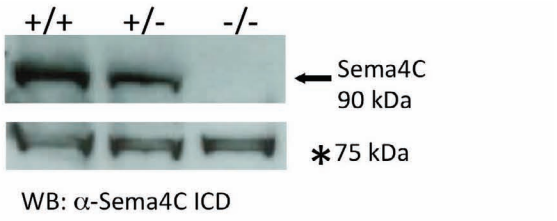

Figure 3.15 Western Blot analysis of Sema4C
By Western blot analysis of *Sema4c-/-* mutants, no wild type protein was detected. An unspecific band of 75 kDa served as loading control (asterisk).

The absence of wild type protein in *Sema4c*-/- mutants was confirmed by Western Blot analysis (Figure 3.15) of lysates from P5 cerebella with an antibody directed against the intracellular domain of Sema4C. In wild type and *Sema4c*+/- animals, a polypeptide of 90 kDa, corresponding to the predicted size of Sema4C, was detected.

This indicates that the targeted trap of *Sema4c* results in a functional null mutation. An unspecific band of 75 kDa served as loading control (Figure 3.15, asterisk).

3.6.1 Exencephaly

A screening of embryos at E15.5 for the presence of exencephaly was performed. About 40% of *Sema4c*-/- embryos on C57BL/6 genetic background developed exencephaly (Table 3.2). Exencephaly is a failure of neural tube closure in the cephalic region, resulting eventually in neonatal lethality (Figure 3.16).

This penetrance is lower than that of the Plexin-B2 mutation on the same C57BL/6 background, in which about 95% of *Plxnb2*-/- embryos were affected by exencephaly (Friedel et al., 2007). *Sema4c*-/- mutants that bypassed exencephaly developed normally and were viable and fertile, and had no obvious behavioral defects.

Figure 3.16 E15.5 *Sema4c*-/- embryo on C57BL/6 genetic background with exencephaly

Table 3.2 Exencephaly and postnatal survival of Sema4C mutants (on C57BL/6 background)

Genotype	Expected frequency	Observed frequency	Exencephaly
Embryonic stages (n=47)*			
wild type	25%	25% (12/47)	0%
Sema4c+/-	50%	45% (21/47)	0%
Sema4c-/-	25%	30% (14/47)	11% (5/47)
Postnatal animals (n=417)*			
wild type	25%	27% (113/417)	
Sema4c+/-	50%	61% (253/417)	
Sema4c-/-	25%	12% (51/417)	

* Offspring from *Sema4c*+/- x +/- matings. Embryonic stages scored at E15-E18, postnatal animals scored at P21.

3.6.2 Pigmentation defect

All *Sema4c*-/- mutants on a C57BL/6 genetic background displayed distinct pigmentation defects. They show white patches of skin and hair along the ventral midline, and white distal fore and hind limbs (Figure 3.17). Interestingly, these defects are virtually identical to the phenotype observed in viable *Plxnb2*^{EUC1a}-/- mutants (see above) (Figure 3.11). This similarity of phenotypes suggests that Sema4C and Plexin-B2 form an exclusive ligand-receptor pair during development of pigmentation.

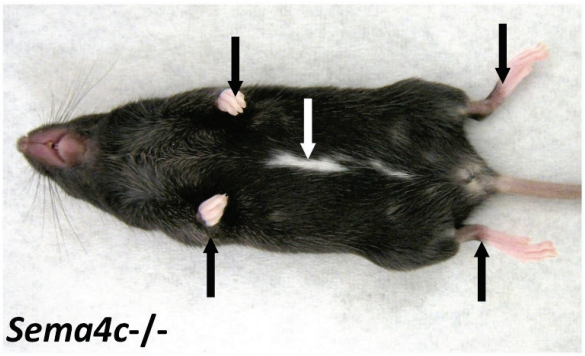

Figure 3.17 Pigmentation defects of *Sema4c*-/- mutants
Sema4c-/- mutants on congenic C57BL/6N background show pigmentation defects at distal fore- and hind limbs, and at the ventral midline.

3.6.3 Cerebellar defects

The next step was to analyze the cerebellar phenotype of *Sema4c* mutant mice. The Plexin-B2 mutation had shown different phenotypes on different genetic backgrounds (Friedel et al., 2007). Because of this observation, the Sema4C cerebellar phenotype was examined both on C57BL/6 inbred and on mixed CD-1 outbred background.

3.6.4 Cerebellar defects on C57BL/6 background

First, the consequences of ablating Sema4C for the morphogenesis of the cerebellum on C57BL/6 background were investigated. The mouse cerebellum is organized at the vermis in ten distinct lobuli, numbered I-X from rostral to caudal (Figure 3.18 A). To visualize the morphology of the cerebellar granule cell layers, the β-gal reporter that is present in the Sema4C mutant allele was utilized (Figure 3.11). The most prominent cerebellar phenotype in *Sema4c*-/- mutants and also to a lesser degree in *Sema4c*+/- mutants was a fusion that had occurred between the rostral lobules VIII and IX.

Table 3.3 Cerebellar phenotypes of Sema4C mutants on C57BL/6 background

Genotype	*n*	Normal cerebellum	Fusion of lobules VIII/IX*		Gap in IGL of lobule II	Gap in IGL of lobule X	Ectopic granule cells in molecular layer
			weak	strong			
wild type	*17*	100%	0%	0%	0%	0%	0%
Sema4c+/-	*11*	73%	18%	9%	20%	0%	10%
Sema4c-/-	*10*	20%	10%	70%	50%	0%	60%

*Fusions of lobules VIII and IX were scored as "weak" when ectopic granule cells formed a band of cells at the fusion line, and as "strong" when a continuous bridge of granule cells connected the IGL of the two lobules.

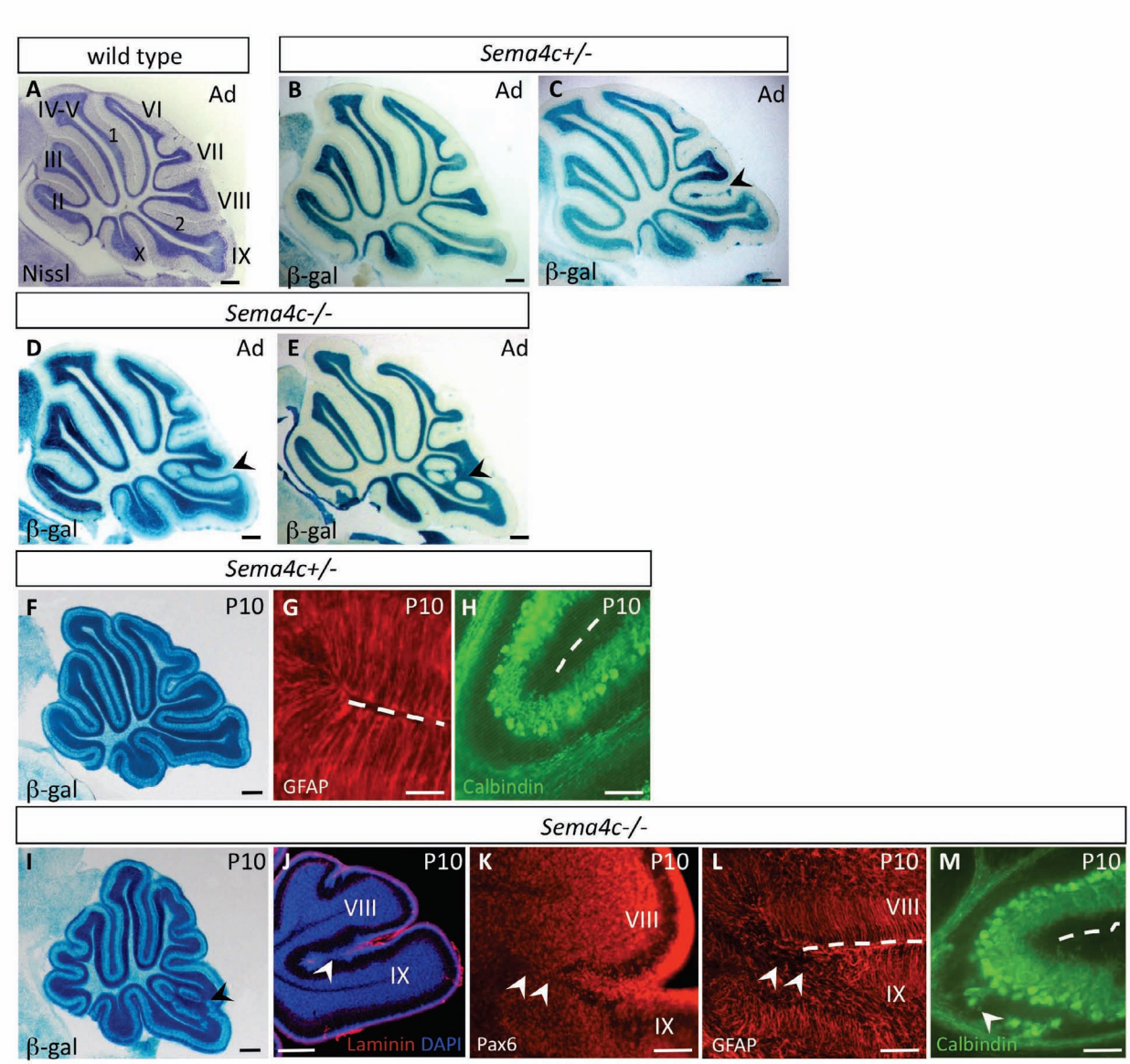

Figure 3.18 Cerebellar defects in Sema4C mutants
(A-M) Sagittal cerebellar sections of adult (Ad) or postnatal day 10 (P10) animals, stained for Nissl substance (A), β-galactosidase activity of the Sema4C mutant allele (B-F, I), or for immunoreactivity for laminin (J), Pax6 (K), glial fibrillary astrocytic protein (GFAP) (G, L), calbindin (H, M).
(A) Section of adult C57BL/6 wild type mouse. Lobules are indicated by Roman numerals. 1 primary fissure, 2 secondary fissure. (B) Normal Cerebellum of a *Sema4c*+/- mutant mouse. (C) Weak lobule VIII/IX fusion phenotype in *Sema4c*+/- cerebellum. (D, E) Cerebella of *Sema4c*-/- animals reveal weak (D) or a strong fusion (E) defects between lobules VIII and IX. (F-H) Normal Cerebellum of a *Sema4c*+/- mutant mouse at P10 with normal Bergmann glia (G) and Purkinje cells (H). (I) The lobule fusion phenotype is detectable at P10.
(J) The basal lamina between the fused lobules VIII and IX is disrupted, as shown by absence of laminin immunoreactivity. (K) Pax6 staining reveals a continuous bridge of granule cells between lobules VIII and IX.
(L) Disrupted radial Bergmann glia palisade. Dotted line indicates fissure between lobule VIII and IX.
(M) Displaced Purkinje cells.
Scale bars in (A-F, I, J): 300 µm; (G; H; K-M): 50 µm

This phenotype was present with variable intensity, ranging from a thin band of granule cells located at the fusion line between the two lobules (scored as "weak" fusion, see C and D as examples), to a continuous bridge of granule cells connecting the IGLs of the two lobules (scored as "strong" fusion, see E as example). In animals that were bred on a C57BL/6 genetic background, 18% of *Sema4c*+/- mutants and 70% of *Sema4c*-/- mutants display fusion defects between lobules VIII and IX (Table 3.3). But the majority of the *Sema4c*+/- mutants show no cerebellar phenotype (73%) (Figure 3.18 B). Fusion defects of lobules VIII/IX were already detectable during postnatal cerebellar development (Figure 3.18 I). In *Sema4c*-/- mutants, a defect basal lamina was detected at the site of lobule fusion with laminin staining (Figure 3.18 J), and fusion areas displayed defects in the architecture of all major cerebellar cortical cell types.

Immunohistochemical labeling for the granule cell marker Pax6 showed ectopic granule cells (Figure 3.18 K). Also Bergmann glia cells labeled by GFAP, and Purkinje cells marked by Calbindin are disrupted in *Sema4c*-/- mutants (Figure 3.18 L, M). In comparison, the major cerebellar cortical cell types of *Sema4c*+/- mutants developed normally (Figure 3.18 G, H).

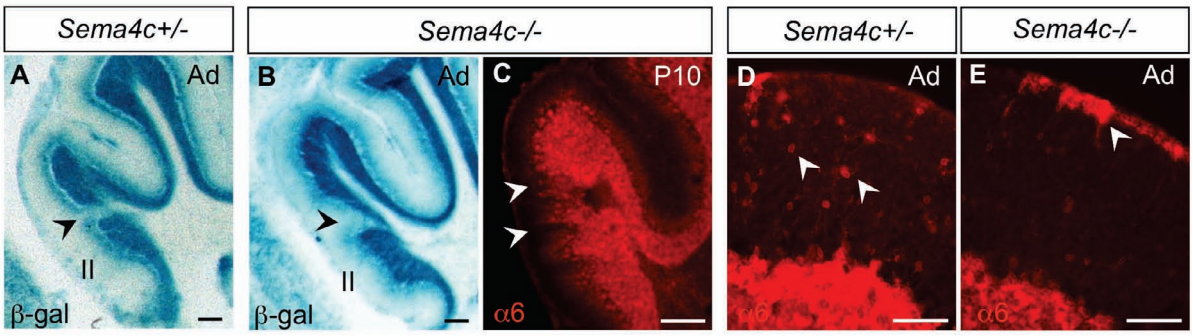

Figure 3.19 Cerebellar defects in Sema4C mutants
(A-E) Sagittal cerebellar sections of adult (Ad) or postnatal day 10 (P10) animals, stained for β-galactosidase activity of the Sema4C mutant allele (A, B), or for immunoreactivity for GABA-A receptor alpha 6 (C-E). Arrowheads in A-C indicates gaps in lobule II and arrowheads in D and E ectopic granule cells.
Scale bars in (A-E): 150µm

Sema4C homozygous mutants displayed several cerebellar malformations that are analogous to mild forms of defects seen in Plexin-B2 mutants (Friedel et al., 2007). These are disruption of the IGL of rostral lobule II by "gaps" (Figure 3.19 A-C), visualized by lacZ and alpha 6 staining, and small clusters of ectopic granule cells in the molecular layer, mainly at a subpial positions (Figure 3.19 D, E). A mild phenotype could also be observed

in *Sema4c*+/- mutants (Figure 3.19 D). The penetrance of these defects in *Sema4c*-/- mice on C57BL/6 background was 50% for gaps in lobule II, and 60% for ectopic granule cell clusters (Table 3.3). All these phenotypes occurred with lower penetrance also in *Sema4c*+/- mutants, with a frequency of 20% for gaps in lobule II, and of 10% for ectopic granule cell clusters (Table 3.3).

The fact that mild phenotypes could also be observed in heterozygous *Sema4c*+/- mutants suggests a potential haploinsufficiency effect for the *Sema4c*+/- mutation. In agreement with this notion, protein levels of Sema4C were reduced to about 50% in *Sema4c*+/- animals (Figure 3.16).

3.6.5 Cerebellar defects on mixed CD-1 background

The cerebellar phenotype of the Sema4C mutation was also analyzed on a mixed CD-1 outbred background. All phenotypes that were found on C57BL/6 could also be observed on mixed CD-1 background. However, the observed frequencies of phenotypes were significantly lower on CD-1 background (Table 3.4), suggesting that genetic modifiers present in this mixed background can to some extent attenuate the effect of the Sema4C deletion.

Table 3.4 Cerebellar phenotypes of Sema4C mutants on CD-1 background

Genotype	*n*	Normal cerebellum	Fusion of lobules VIII/IX*		Gap in IGL of lobule II	Gap in IGL of lobule X	Ectopic granule cells in molecular layer
			weak	strong			
wild type	*17*	100%	0%	0%	0%	0%	0%
Sema4c+/-	*11*	70%	10%	0%	10%	0%	10%
Sema4c-/-	*10*	20%	70%	0%	40%	0%	40%

*Fusions of lobules VIII and IX were scored as “weak” when ectopic granule cells formed a band of cells at the fusion line, and as “strong” when a continuous bridge of granule cells connected the IGL of the two lobules.

3.7 Defects in Sema4G mutant mice

3.7.1 Cerebellar phenotype

Sema4G homozygous mutants displayed normal embryonic development. Unlike Sema4C homozygous mutants, Sema4G mutants showed no exencephaly, and the ratio of live born *Sema4g*-/- mutants in litters from heterozygous parents is about 25%, close to the expected Mendelian ratio. In comparison, the observed frequency of *Sema4c*-/- mutants was 12%. Postnatal *Sema4g*-/- mutants were viable and fertile with no overt phenotypes. No cerebellar abnormalities were detected in *Sema4g*-/- mice by Nissl staining (Figure 3.20)

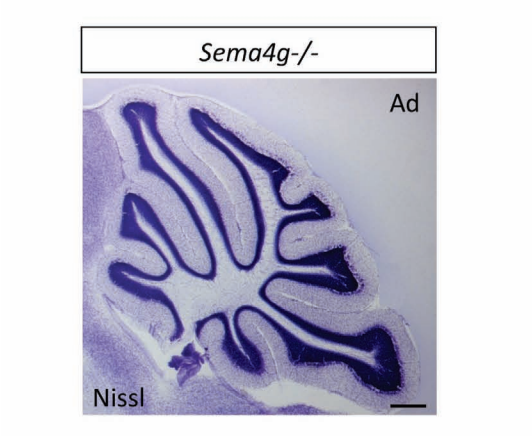

Figure 3.20 Phenotypic analysis of *Sema4g*-/- mutants
Nissl staining of Sema4G mutant section shows no cerebella phenotype.
Scale bar: 400µm.

3.8 Enhanced cerebellar defects in Sema4C/Sema4G double mutants

To investigate the possibility that Sema4C and Sema4G act in parallel as ligands for Plexin-B2, a respective double mutant mouse line was generated by interbreeding of the two mutant lines. Because the Plexin-B2 mutation and the Sema4C mutation had shown different phenotypes in dependence of the genetic background, the Sema4C/Sema4G cerebellar phenotypes were both analyzed on C57BL/6 and mixed CD-1 outbred background.

3.8.1 Cerebellar Phenotype on C57BL/6 background

The Sema4C/Sema4G cerebellar phenotype was first analyzed on C57BL/6 background. Deleting one or two copies of the *Sema4g* gene on a background of either a heterozygous or homozygous mutation of Sema4C enhanced the penetrance and the severity of the cerebellar phenotypes (Figure 3.21, Table 3.5). About half of the double heterozygous *Sema4c+/-; Sema4g+/-* mice showed weak fusion defects in lobule VIII/IX (Figure 3.21 A, Table 3.5)

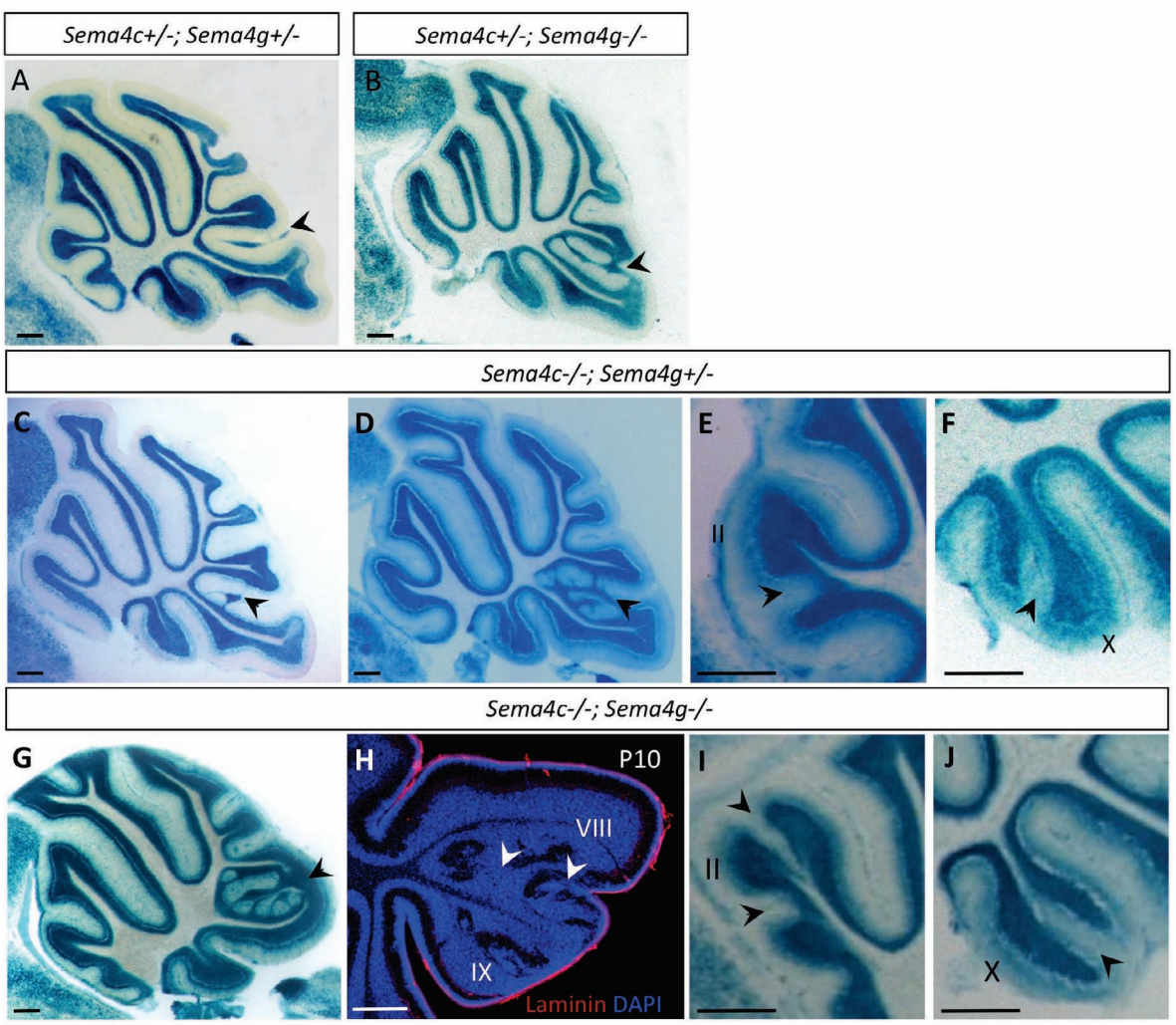

Figure 3.21 Phenotypic analysis of Sema4C/Sema4G double mutants on C57BL/6 background
(A-J) Sagittal cerebellar sections of adult animals stained for β-galactosidase activity of the Sema4C mutant allele (A-F, G, I, J), and P10 section stained for laminin immunoreactivity (F).
(A) Double heterozygous *Sema4c+/-; Sema4g+/-* mouse with weak fusion defects in lobule VIII/IX.
(B) *Sema4c+/-; Sema4g-/-* mouse with a strong fusion defect of lobules VIII and IX.
(C-F) In *Sema4c-/-; Sema4g+/-* mice, fusion defects between lobules VIII and IX occurred with weak (C) or strong (D) characteristics. In addition, gaps in the IGL of lobules II (E) and lobule X (F) occurred.
(G-J) Double homozygous *Sema4c-/-; Sema4g-/-* mutants reveal strong fusion defects between lobules VIII/IX (G, H), and gaps in the IGL of lobules II (I) and X (J). Absence of laminin staining between the lobules indicates loss of a separating basal lamina (H). Scale bars in (A-J): 300 µm.

The homozygous deletion of Sema4G increased the penetrance of strong lobule VIII/IX fusions for *Sema4c*+/- mutants from 9% to 25%, and for *Sema4c*-/- mutants from 70% to 100% (Figure 3.21 B, G, H, Table 3.5). The absence of laminin staining between the lobules indicates loss of a separating basal lamina (Figure 3.21 H), like in the Sema4C mutation alone (Figure 3.18 J).

Furthermore, deleting Sema4G increased the frequency of gaps in lobule II, for *Sema4c*+/- mutants from 20% to 50%, and for *Sema4c*-/- mutants from 50% to 67% (Figure 3.21, Table 3.5). Removing one or both copies of the *Sema4g* gene in *Sema4c*-/- mutants resulted in disruption of the IGL of lobule X (Figure 3.21 F, J), a defect that was not found in mice singly mutant for Sema4C. Also the percentage of the ectopic granule cells in the molecular layer increased from 40% in double heterozygous *Sema4c+/-; Sema4g*+/- mice to 100% in double homozygous *Sema4c-/-; Sema4g-/-* mice.

Table 3.5 Cerebellar phenotypes of Sema4C and Sema4G mutants on C57BL/6 background

Genotype	*n*	Normal cerebellum	Fusion of lobules VIII/IX*		Gap in IGL of lobule II	Gap in IGL of lobule X	Ectopic granule cells in molecular layer
			weak	strong			
wild type	*17*	100%	0%	0%	0%	0%	0%
Sema4c+/-	*11*	73%	18%	9%	20%	0%	10%
Sema4c-/-	*10*	20%	10%	70%	50%	0%	60%
Sema4c+/-; *Sema4g*+/-	*16*	31%	56%	13%	40%	0%	40%
Sema4c+/-; *Sema4g*-/-	*13*	31%	44%	25%	50%	0%	60%
Sema4c-/-; *Sema4g*+/-	*10*	0%	20%	80%	60%	60%	80%
Sema4c-/-; *Sema4g*-/-	*11*	0%	0%	100%	67%	75%	100%

*Fusions of lobules VIII and IX were scored as "weak" when ectopic granule cells formed a band of cells at the fusion line, and as "strong" when a continuous bridge of granule cells connected the IGL of the two lobules.

Thus, double mutations for Sema4C and Sema4G on C57BL/6 resulted in enhanced cerebellar phenotypes, suggesting that they act in parallel as ligands for Plexin-B2. However, since the phenotype of the combined deletion of the Sema4C and Sema4G genes

is less severe than that of the Plexin-B2 mutation (Friedel et al., 2007), it is likely that other ligands of Plexin-B2 exist in cerebellar development, which remain yet to be identified.

3.8.2 Cerebellar Phenotype on mixed CD-1 background

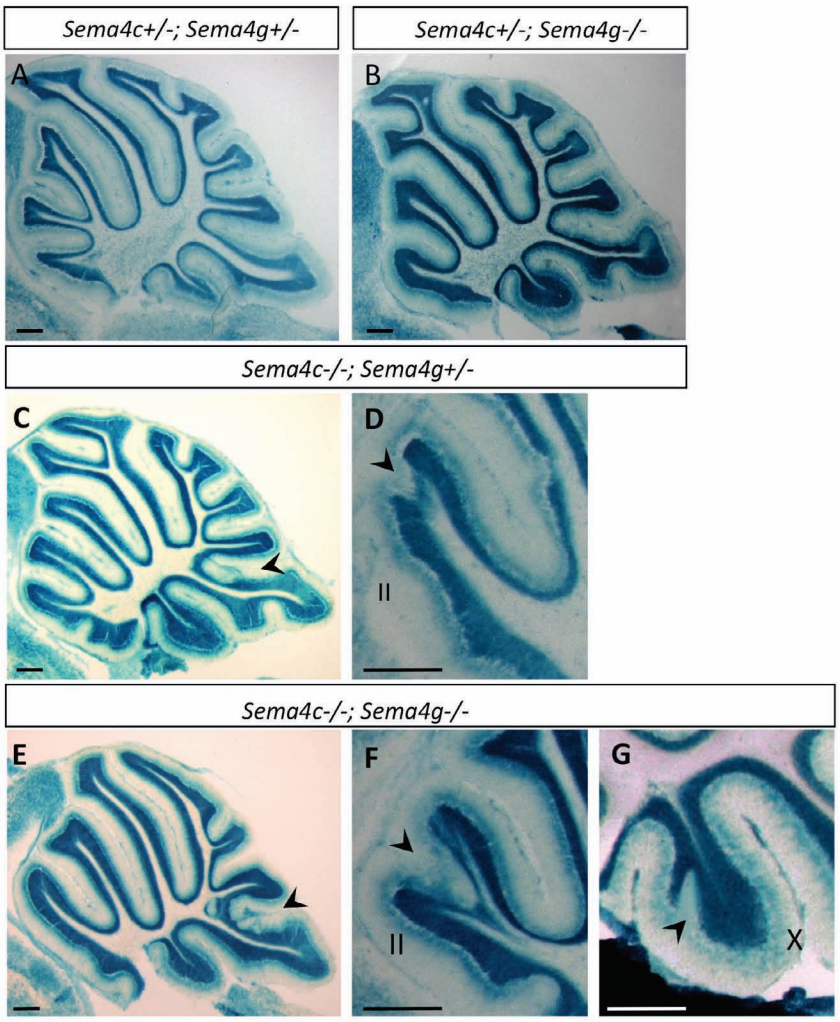

Figure 3.22 Phenotypic analysis of Sema4C/Sema4G double mutants on mixed CD-1 background
(A-J) Sagittal cerebellar sections of adult animals stained for β-galactosidase activity of the Sema4C mutant allele (A-G).
(A) Double heterozygous *Sema4c+/-; Sema4g+/-* and (B) *Sema4c+/-; Sema4g-/-* showed no phenotype.
(C, D) In *Sema4c-/-; Sema4g+/-* mice, fusion defects between lobules VIII and IX occurred with weak characteristics. In addition, gaps in the IGL of lobules II (D) occurred (arrowhead).
(E-G) Double homozygous *Sema4c-/-; Sema4g-/-* mutants reveal weak fusion defects between lobules VIII/IX (arrowhead). In addition, gaps in the IGL of lobules II (F) and lobule X (G) were observed.
Scale bars in (A-G): 300 µm.

As for the Sema4C mutant line, the cerebellar phenotype of the Sema4C/Sema4G double mutations were also analyzed on a mixed CD-1 outbred background.

The majority of the double heterozygous *Sema4c+/-; Sema4g+/-* and of *Sema4c+/-; Sema4g-/-* mice revealed no detectable phenotype. However, the mutant combination of Sema4c-/-; Sema4g+/- showed a higher frequency of cerebellar defects (Figure 3.22 C, D). For example, the frequency of weak fusion of lobule VIII and IX is 30% (Table 3.6), and of gaps in lobule II 50%.

Removing both copies of the Sema4G and Sema4C gene resulted in disruption of the IGL of lobule X (Figure 3.22 G), a defect that was not found in mice singly mutant for Sema4C or with any combination with the Sema4G gene. The double mutations for Sema4C and Sema4G resulted in enhancement of all cerebellar phenotypes,

Table 3.6 Cerebellar phenotypes of Sema4C and Sema4G mutants on mixed CD-1 background

Genotype	*n*	Normal cerebellum	Fusion of lobules VIII/IX*		Gap in IGL of lobule II	Gap in IGL of lobule X	Ectopic granule cells in molecular layer
			weak	strong			
wild type	*17*	100%	0%	0%	0%	0%	0%
Sema4c+/-	*11*	70%	10%	0%	10%	0%	10%
Sema4c-/-	*10*	20%	70%	0%	40%	0%	40%
Sema4c+/-; *Sema4g*+/-	*16*	55%	18%	0%	18%	0%	18%
Sema4c+/-; *Sema4g*-/-	*13*	40%	20%	0%	20%	0%	40%
Sema4c-/-; *Sema4g*+/-	*10*	20%	30%	0%	50%	0%	60%
Sema4c-/-; *Sema4g*-/-	*11*	0%	55%	0%	55%	55%	82%

*Fusions of lobules VIII and IX were scored as “weak” when ectopic granule cells formed a band of cells at the fusion line, and as “strong” when a continuous bridge of granule cells connected the IGL of the two lobules.

3.9 Genetic interaction of Sema4C or Sema4G and Plexin-B2

The next step was to find genetic evidence that Plexin-B2 and Sema4C act in a common pathway. Heterozygous *Plxnb2*+/- mutants are phenotypically normal, including their cerebellar morphology (Friedel et al., 2007). This heterozygous receptor mutation was utilized as a sensitized background for interaction studies with mutations of Sema4C and Sema4G on a C57BL/6 genetic background. Due to its neonatal lethality, no homozygous *Plxnb2*-/- mutations could be used for interaction studies.

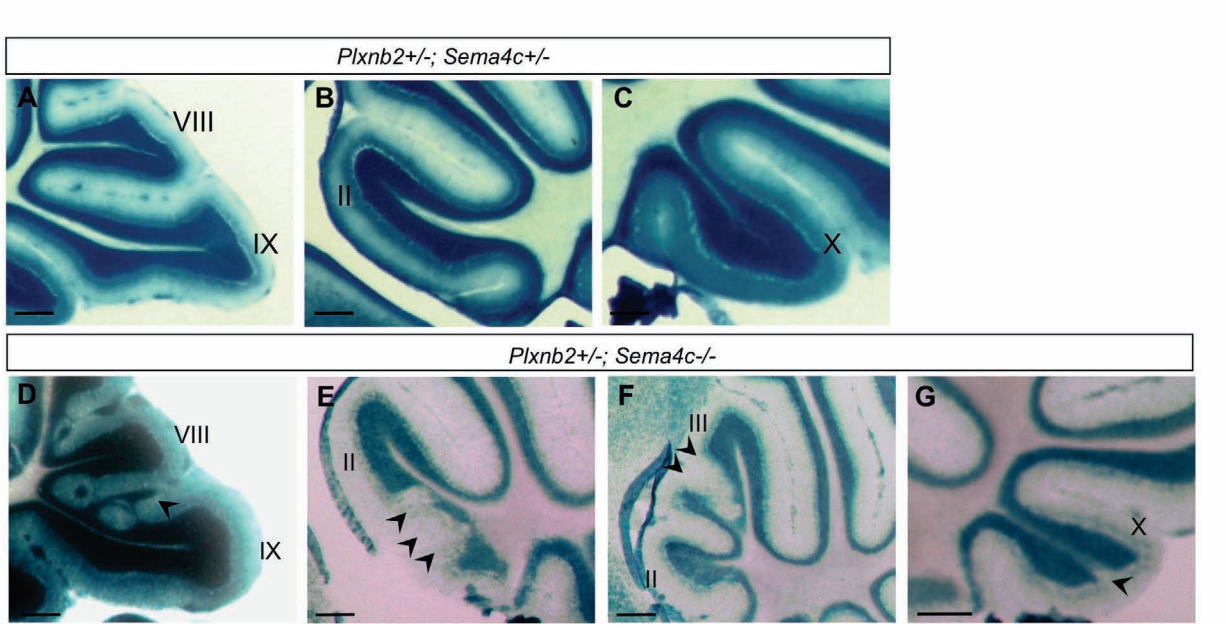

Figure 3.23 Phenotypic analysis of Plexin-B2/Sema4C mice
(A-C) *Plxnb2+/-; Sema4c+/-* double heterozygous mice show no phenotype.
(D) *Plxnb2+/-; Sema4c-/-* mutants reveal lobule VIII/IX fusion defects.
(E-G) *Plxnb2+/-; Sema4c-/-* mutants reveal severe disruptions in the IGL of rostral lobules II and III (E, F), and gaps in lobule X (G).
Scale bars in (A-G): 300 µm.

When one copy of the *Sema4c* gene on a *Plxnb2*+/- background (*Plxnb2*+/-; *Sema4c*+/-) was removed, no cerebellar abnormalities were detectable (Figure 3.23 A-C). When both copies of Sema4C on a *Plxnb2*+/- background were removed (*Plxnb2*+/-; *Sema4c*-/-), lobule VIII/IX fusion defects were detected, similar to those observed in animals completely deficient for Sema4C (Figure 3.18). Additionally, however, the IGL of lobules II and III were disrupted in a severity that could be not detected in any of the *Sema4c*-/- or *Sema4c*-/-; *Sema4g*-/- mutants (Figure 3.23 E, F). Furthermore, in *Plxnb2*+/-; *Sema4c*-/-

mutants, a gap in lobule X can also be observed (Figure 3.23 G), a defect that was absent in *Sema4c*-/- single mutants.

Thus, combining a homozygous *Sema4c*-/- mutation with a heterozygous *Plxnb2*+/- mutation resulted in cerebellar phenotypes that are stronger than the sum of the individual phenotypes, consistent with a model that Sema4 proteins and Plexin-B2 act as ligands and receptor in a common genetic pathway. In contrast, no cerebellar phenotypes in mice carrying a *Sema4g*+/- or *Sema4g*-/- mutation in combination with a *Plxnb2*+/- mutation could be observed, suggesting that Sema4C plays a more dominant role than Sema4G in mediating Plexin-B2-dependent cerebellar morphogenesis.

3.10 Migration assay

Cerebellar granule cell precursors (GCPs) deficient for Plexin-B2 show defects in their migratory behavior *in vivo* (Friedel et al., 2007). For this reason, Sema4C and Sema4G were investigated for their ability to regulate the migration of GCPs that either express or do not express the Plexin-B2 receptor. A transwell migration assay with wild type and *Plxnb2*-/- GCPs was performed (Figure 3.25).

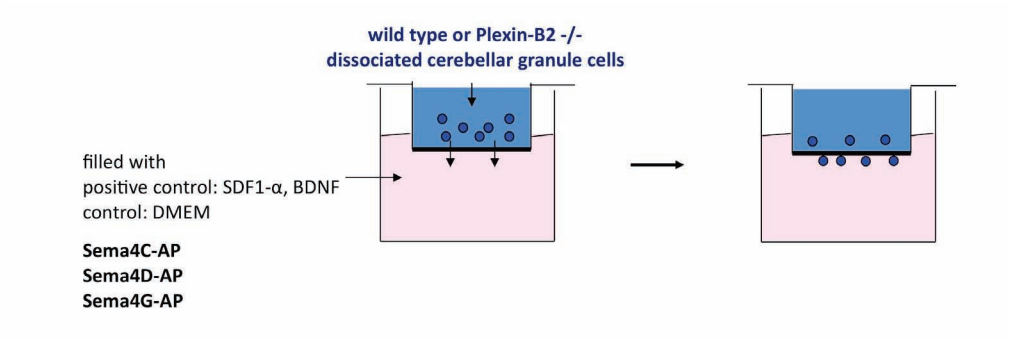

Figure 3.24 Schematic drawing of the transwell migration assay.

Cells from the EGL layer of P5 cerebella were dissociated with papain treatment and were seeded into the upper chamber of 24-well format transwell chambers. Lower chambers were filled with DMEM culture media that were conditioned either with Sema4C-AP, Sema4D-AP, or Sema4G-AP protein. As a control for the baseline migration rate, unconditioned DMEM media, and as positive controls, Stromal cell line-derived factor-1α (SDF-1α) (D'Apuzzo et al., 1997) and brain derived neurotrophic factor (BDNF) (Lindsay, 1988) were used (Figure 3.24).

After incubation over night, cells on the upper surface of the membrane were scraped off, and the granule cells that had migrated to the lower surface of the membrane were fixed and stained with DAPI. Five representative photomicrographs were taken at high magnification of each membrane and the cells were quantified. When SDF-1α or BDNF, both known promoters of GCP migration (Borghesani et al., 2002; Ma et al., 1998), were added to the lower chamber of the assay system, granule cells of both genotypes showed robustly enhanced migration through the transwell membrane when compared to unconditioned media, which served as control.

Interestingly, both SemaC and Sema4G elicited a strong migratory response of wild type GCPs. No effect, however, was seen, when these molecules were added to *Plxnb2*-/-

GCPs. In comparison, Sema4D elicited neither on wild type nor on mutant GCPs a migratory effect. Taken together, the transwell migration results indicate that Sema4C and Sema4G, but not Sema4D, act as migration stimulating factors for GCPs through the Plexin-B2 receptor.

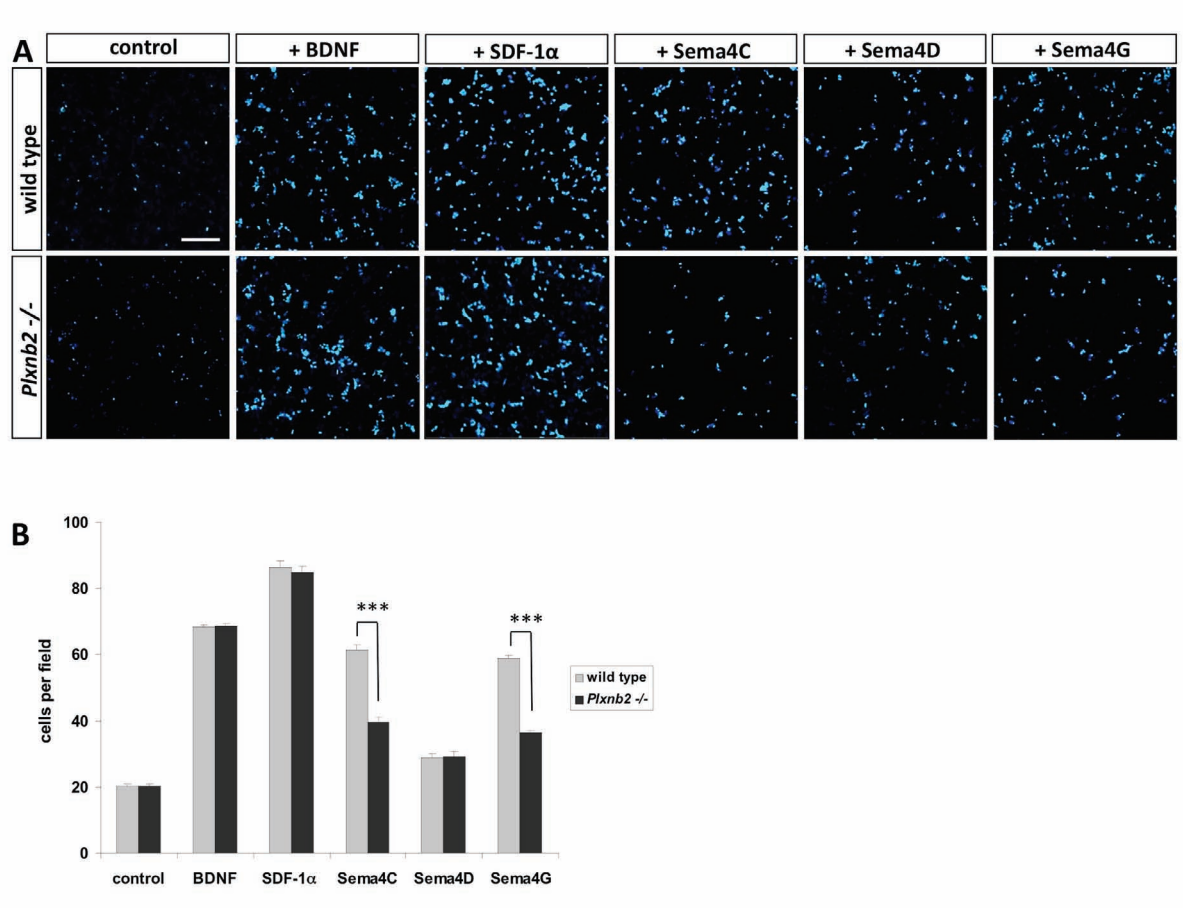

Figure 3.25 Transwell migration assay
(A) Representative photomicrographs of DAPI stained transwell membranes, revealing migration rate of GCPs. Dissociated GCPs of wild type and *Plxnb2-/-* mice were seeded on top of transwell membranes, and the lower compartment was conditioned with migration stimulating proteins (BDNF and SDF-1α), or with Sema4C-AP, Sema4D-AP, or Sema4G-AP fusion proteins. Cells that had migrated to the lower side of the membrane were stained with DAPI.
(B) Quantification of transwell migration assays. Sema4C and Sema4G promoted migration of GCPs from wild type animals, but not from *Plxnb2-/-* animals. No statistically significant effect was observed for Sema4D.
The significant difference (t-Test) is indicated by three asterisks ($p < 0.001$).
Scale bar in (A): 100µm.

3.11 EGL Explants

3.11.1 Sema4C promotes migration of cerebellar granule cell in explant cultures

To analyze the nature of the effect of Sema4 activation on GCP development in a system that closely resembles *in vivo* development, EGL microexplant cultures of the cerebellar EGL were performed. When plated on laminin, GCPs migrate outward from explants in a radial fashion for about 48 hours and begin then to form aggregates with other GCPs, thus providing an assay system that closely mimics the tangential migration of GCPs through the molecular layer to the IGL (Nagata and Nakatsuji, 1990).

For the EGL microexplants, tissue pieces of about 300 μm diameter were dissected from the EGL of P5 animals and placed on Poly-L-lysine and laminin coated cover slips. In some cases, cover slips were in addition coated with alkaline phosphatase (AP)-tagged Sema4C, Sema4D, or EGFP (as a control). After 72h, cultures were fixed and then stained with Rhodamine Phalloidin to visualize cell bodies and neurites, and with DAPI to label cell nuclei. To control if the explant is only from the EGL, the granule cells were also stained with a marker for mature granule cells, $GABA_A$ receptor $\alpha 6$ subunit. Migration rates of GCPs were determined by measuring the DAPI signal in concentric rings around the explants. The experimental series that showed the strongest migration rate was used to normalize measurements (migration rate of wild type explants on Sema4C substrate equals 100%; see Figure 3.27). Experiments were repeated four times under each condition with total explants numbers for wild type n=20, *Sema4c*+/- n= 21, and *Sema4c*-/- n=24.

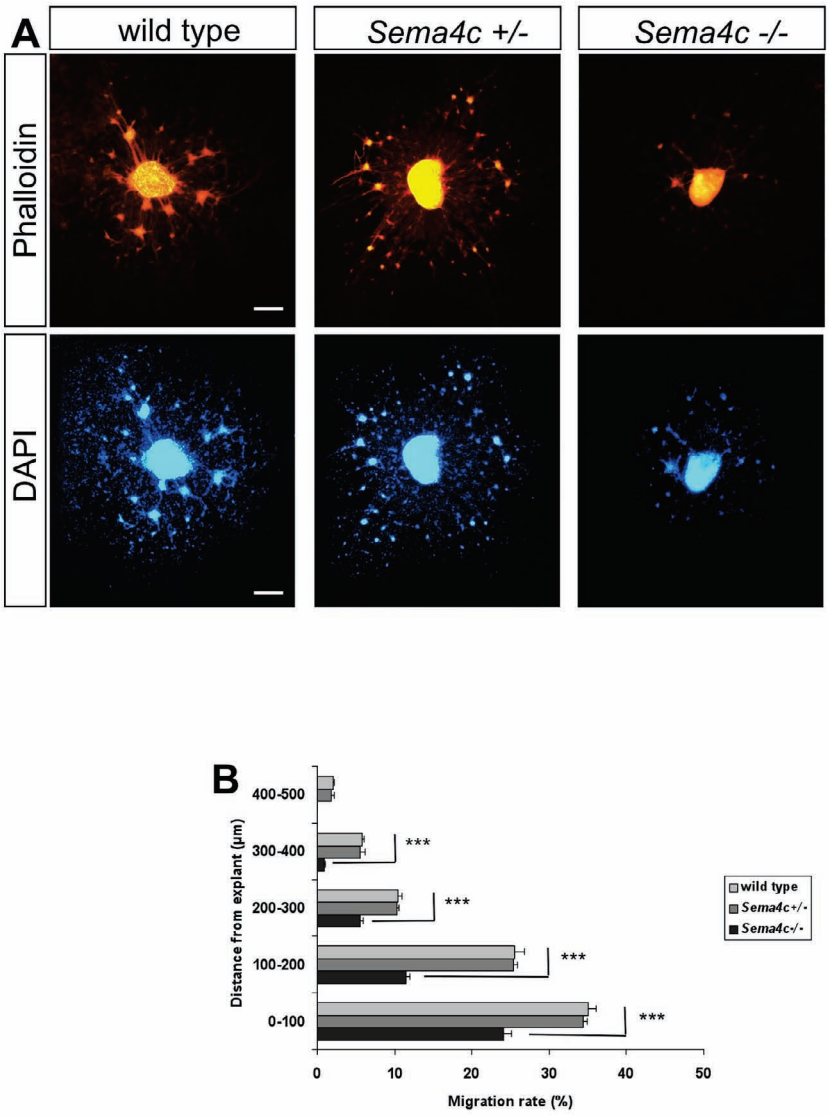

Figure 3.26 Granule cell migration of explant cultures is promoted by Sema4C
(A) EGL explants of wild type, *Sema4c*+/-, and *Sema4c*-/- animals on PLL/laminin substrate. Explants of *Sema4c*-/- mice showed reduced migration rates. (4 independent experiments; total explants numbers: wild type n=20, *Sema4c*+/- n= 21, *Sema4c*-/- n=24). EGL microexplants of wild type, *Sema4c*+/- or *Sema4c*-/- P5 mice were plated on cell culture dishes, incubated for 72h, and labeled by phalloidin and DAPI.
(B) Quantification of cell migration rates of explants cultures shown in (A). Cell nuclei were labeled by DAPI, and fluorescence signal was measured in concentric rings around the explants. Migration rates were normalized to the experimental series that showed the strongest migration rate (wild type explants on Sema4C substrate = 100%) (see Figure 3.27).
The significant differences (t-Test) are indicated by one asterisk ($p < 0.02$), two asterisks ($p < 0.002$) or three asterisks ($p < 0.001$).
Scale bar in (A): 200µm.

Since the *in vivo* mutant analysis had indicated that Sema4C plays a more prominent role than Sema4G in cerebellar morphogenesis, the focus of the explant analyses was set on Sema4C. First, the EGL explants of wild type, *Sema4c*+/-, and *Sema4c*-/- mutants were analyzed and the amount of cell migration out of the explant was quantified (Figure 3.26 B). Migration rates of *Sema4c*+/- explants were similar to those of wild type explants. However, it was observed that GCPs of *Sema4c*-/- animals migrated in significantly lower number out of the explants when compared to those from wild type or *Sema4c*+/- animals. These findings suggest that Sema4C promotes the migration of cerebellar granule cell precursors, possibly through cell-cell contacts.

Next, it was investigated if exogenous Sema4C would be able to promote granule cell migration from explants. For this purpose, culture dishes were coated with both laminin and ectodomain-AP fusion proteins of Sema4C and Sema4D. On Sema4C coated dishes, wild type explants revealed a significant increase in their migration rate, but not on control or Sema4D coated dishes (Figure 3.27 A, B).

3.11.2 Plexin-B2 promotes migration of cerebellar granule cell in explant cultures

To investigate whether Plexin-B2 is required for the migration promoting effect of Sema4C on EGL explants, explants of wild type and of *Plxnb2*-/- mutant mice were plated on dishes that were coated with either Poly-L-lysine/laminin alone, or additionally with Sema4C-AP (+Sema4C) or Sema4D-AP (+Sema4D) (Figure 3.27 A, C). Experiments were repeated four times under each condition (total explants numbers of control n=19, +Sema4C n= 20, and +Sema4D n=20).

Plxnb2-/- explants displayed a reduced migration rate of GCPs compared to wild type explants when plated on laminin alone. The migration rate of *Plxnb2*-/- explants was also not changed when either Sema4C or Sema4D protein coating was applied to the dishes. These results are consistent with a model that Plexin-B2 is the cognate receptor for Sema4C for its migration promoting effect on GCPs.

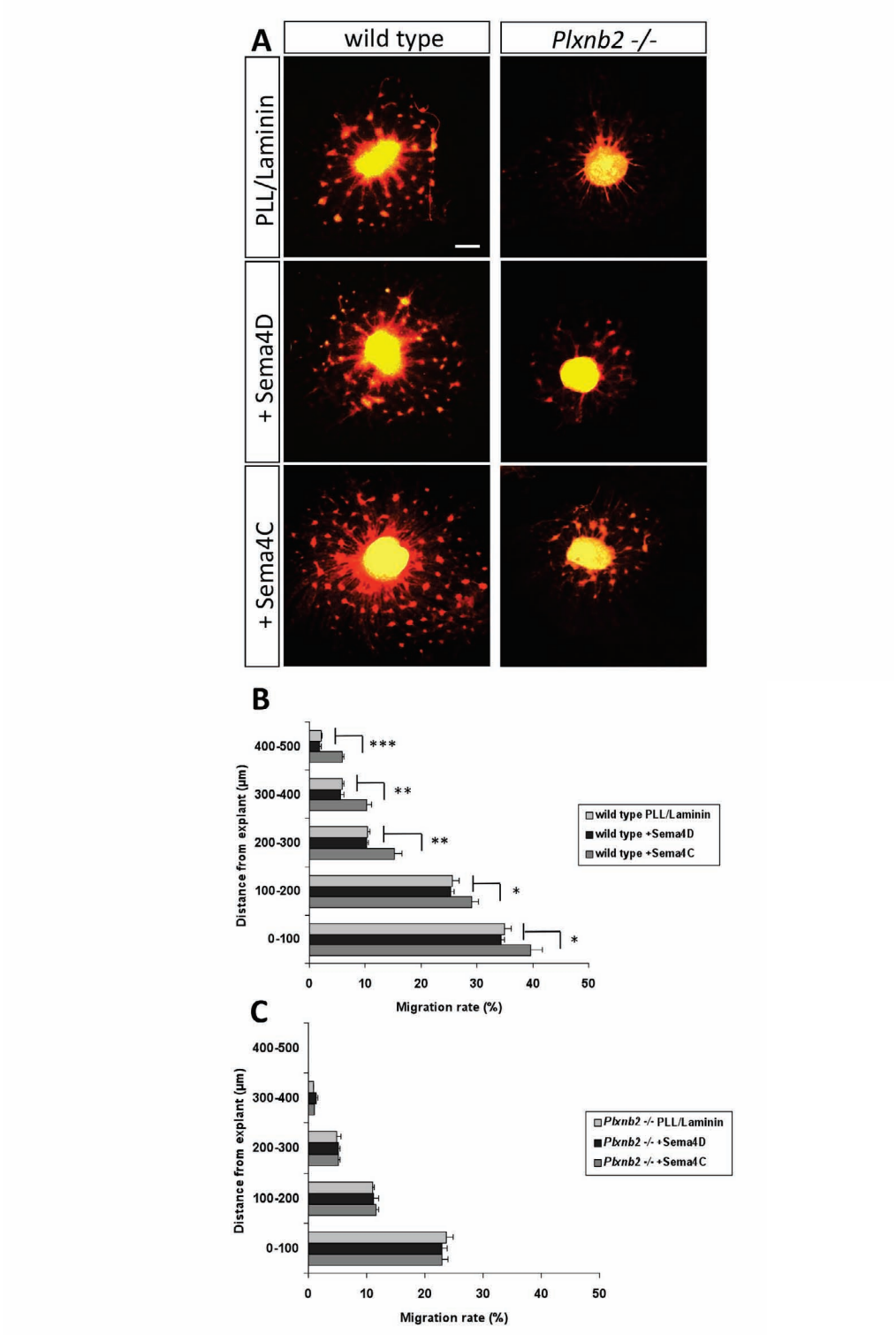

Figure 3.27 Granule cell migration of explant cultures is promoted by Sema4C
(A) EGL microexplant cultures of wild type and *Plxnb2*-/- P5 mice were plated on dishes that were coated with either only Poly-L-lysine/laminin alone, or additionally with Sema4C-AP (+Sema4C) or Sema4D-AP (+Sema4D), incubated for 72h, and labeled by rhodamine phalloidin to visualize cell bodies and neurites.
Wild type explants showed an enhanced migration rate on Sema4C coated substrate. In contrast, *Plxnb2*-/- explants showed reduced migration rates independent of substrate composition (4 independent experiments; total explants numbers: control n=19, +Sema4C n=20, +Sema4D n=20).
(B, C) Quantification of cell migration rates of explants cultures shown in (A). Cell nuclei were labeled by DAPI, and fluorescence signal was measured in concentric rings around the explants. Migration rates were

normalized to the experimental series that showed the strongest migration rate (wild type explants on + Sema4C substrate = 100%).
The significant differences (t-Test) are indicated by one asterisk ($p < 0.02$), two asterisks ($p < 0.002$) or three asterisks ($p < 0.001$).
Scale bar in (A): 200µm

4. DISCUSSION

Dissecting the Plexin-Semaphorin signaling network is important in understanding how the nervous system is built up. Most studies in the Semaphorin/Plexin field have focused on Plexin-A/Neuropilin receptors and their Sema3 ligands (Nakamura et al., 2000), but only little is known about Plexin-Bs and their *in vivo* function. The Plexin-B2 receptor is critically involved in neural tube closure and cerebellar granule cell development (Friedel et al., 2007), but its relevant *in vivo* ligands have not been identified.

In this study, *in vivo* and *in vitro* studies showed that two Semaphorin 4 family members, Sema4C and Sema4G, are potential ligands of Plexin-B2. *In situ* hybridization showed that the Sema4C and Sema4G genes are expressed in specific cell types of the developing cerebellar cortex, and binding studies demonstrated that Sema4C and Sema4G proteins bind specifically to Plexin-B2 expressing cells.

To further investigate their *in vivo* function, Sema4C and Sema4G knock-out mouse mutants were analyzed. Like *Plxnb2*-/- mutants, *Sema4c*-/- mutants reveal exencephaly with partial penetrance. Viable *Sema4c*-/- mutants display distinctive cerebellar defects, including gaps in the internal granule cell layer (IGL) of rostral lobules, fusions of caudal lobules, and ectopic granule cells in the molecular layer (ML). The Sema4G gene deletion causes no overt phenotype by itself, but Sema4C/Sema4G double mutants revealed an enhanced cerebellar phenotype. Nevertheless, the severity of the cerebellar phenotypes of Sema4C or Sema4C/Sema4G mutants is less severe than that of Plexin-B2 mutants, indicating that further ligands of Plexin-B2 exist during cerebellar development. In transwell migration assays and in explant cultures of the developing cerebellar cortex, Sema4C promoted migration of cerebellar granule cell precursors in a Plexin-B2-dependent manner.

In summary, the data presented here provides the first genetic *in vivo* evidence that Sema4C and Sema4G are ligands for Plexin-B2, and the data also indicates that Sema4C and Sema4G exert their function on cerebellar granule cell precursors through regulation of their migratory properties by binding to the Plexin-B2 receptor.

4.1 Expression and binding data identify Sema4C and Sema4G as candidate ligands of Plexin-B2

To identify candidate ligands of Plexin-B2 in neural development, a screen was performed for the mRNA expression of Sema4 genes in the developing nervous system at two different time points. At a time point when the neural tube starts to close along the dorsal midline, only expression of *Sema4c* and *Sema4g* was observed, suggesting both as candidate ligands of Plexin-B2. And at a time point during the peak period of cerebellar granule cell neurogenesis, only *Sema4c* and *Sema4g* are expressed in cerebellar neurons. *Sema4c* was detected in cerebellar granule cells of the external granule layer (EGL) and IGL, as well as in Bergmann glia, and *Sema4g* in Purkinje cells. These findings are consistent with previous findings that Sema4C and Sema4G are expressed at embryonic stages mainly in the central nervous system (Inagaki et al., 1995; Li et al., 1999).
Sema4A and Sema4B are strongly expressed in radial Bergmann glia cells. Consistent with previous reports, Sema4D, a putative ligand for Plexin-B2 (Masuda et al., 2004) is mainly expressed by oligodendrocytes in the postnatal cerebellum (Moreau-Fauvarque et al., 2003; Worzfeld et al., 2004). In agreement with previous data, Sema4F was not detected in the developing brain (Li et al., 1999), and is therefore not a potential candidate.
A survey of Plexin-B expression in the developing cerebellum revealed that Plexin-B2 is the only B-type Plexin expressed in cerebellar granule cells, while Plexin-B1 expression was found in Bergmann glia and Plexin-B3 expression in oligodendroglia.
Taken together, the expression data indicates that potential cerebellar ligands for Plexin-B2 comprise five Sema4 members (Sema4A, -B, -C, -D, and -G). Since mutant mice that are deficient for *Sema4a*, *Sema4b*, or *Sema4d* have revealed no cerebellar phenotypes (Friedel et al., 2007), the further analysis of ligand candidates was focused on Sema4C and Sema4G.

To determine whether Sema4C and Sema4G bind to Plexin-B2, *in vitro* and *in vivo* AP-binding assays were performed. In a previous study, Deng and colleagues were able to show that Sema4C binds to Plexin-B2 expressing fibroblasts with a high degree of specificity and affinity (Deng et al., 2007). In the experiments presented here, robust binding of Sema4C to Plexin-B2 was confirmed, and also a weaker binding to Plexin-B1 was revealed, but no binding to Plexin-B3 was detected. In agreement with previous

publications, Sema4D, which was utilized as control, bound robustly to both Plexin-B1 and Plexin-B2 (Masuda et al., 2004; Tamagnone et al., 1999). The fact that the binding affinity of Sema4D to Plexin-B2 is five times lower than to Plexin-B1 (Deng et al., 2007) suggest that the main receptor of Sema4D is Plexin-B1. The binding experiments in this study showed that Sema4D additionally has also a weaker binding affinity to Plexin-B3.
The binding on cerebellar tissue sections from wild type and Plexin-B2 mutant mice at P10 showed that Sema4C-AP and Sema4G-AP bound strongly to the external granule layer (EGL), and with reduced intensity also to the IGL. These data suggest that Sema4C and Sema4G bind in the cerebellum specifically to Plexin-B2 expressing granule cells. In contrast, Sema4D-AP protein bound both in wild type and Plexin-B2 mutant sections to structures in the molecular layer and in the white matter, which correlates with the expression of Plexin-B1 (Worzfeld et al., 2004). These data again suggest that at least in the cerebellum, Sema4D is not an *in vivo* ligand for Plexin-B2, but rather for Plexin-B1.

4.2 Developmental functions of Sema4C and Sema4G

The mutations of Sema4C alone or of Sema4C/Sema4G together result in neural phenotypes that are qualitatively similar, albeit less severe than those reported for Plexin-B2 mutant mice (Friedel et al., 2007). For example, exencephaly occurs in Sema4C mutants with lower frequency than in Plexin-B2 mutants, and also defects in rostral cerebellar lobulation and positioning of granule cells occur in *Sema4c*-/- mutants with less severity and lower penetrance. This indicates that further ligand(s) are required for Plexin-B2 function in neural development. These ligands may be other Sema4 members, such as Sema4A or Sema4B, which are expressed in radial Bergmann glia, and which could work with Sema4C and Sema4G in a redundant fashion. Alternatively, Plexin-B receptors may also act as homophilic ligands, as *in vitro* studies have suggested homophilic binding of Plexin receptors to each other (Hartwig et al., 2005; Ohta et al., 1995).

The Sema4C and Plexin-B2 phenotypes do not entirely overlap in regard to cerebellar topology: *Sema4c*-/- mutants show striking fusions of the caudal lobules VIII and IX, which was not a prominent defect in Plexin-B2 mutants. A possible explanation for this discrepancy may be the fact that the Plexin-B2 mutation was only studied on a CD-1

outbred background, since exencephaly had precluded postnatal analysis on C57BL/6 (Friedel et al., 2007). The C57BL/6 background may be predisposed to lobule VIII/IX fusion defects, which is indicated by the finding that weak lobule VIII/IX fusions can be found in some colonies of C57BL/6 wild type mice (Tanaka and Marunouchi, 2005). In agreement with this notion, more severe lobule fusion defects of Sema4C and Sema4C/Sema4G mutants on C57BL/6 than on CD-1 outbred background were observed in this study.

The influence of the genetic background on the severity of the Sema4C and Plexin-B2 phenotypes is not completely surprising. A dramatic case for a background dependent cerebellar phenotype is, for example, the Engrailed-1 (En-1) mutation (Bilovocky et al., 2003). In 129/Sv background, the En-1 mutation leads to perinatal lethality accompanied by near-total absence of the cerebellum. These phenotypes are almost completely suppressed on a C57BL/6J genetic background and the cerebellum appears similar to wild type animals.

It is not known why certain lobules of the cerebellum are more sensitive to genetic disruptions than others, and the precise cellular defects that cause cerebellar lobule fusions have not been described. *In situ* expression data for Sema4C or Plexin-B2 does not reveal a localized expression in certain lobules and cannot explain the lobule-specific defects. Rather, the specific localization of phenotypes may be a result of the complex dynamics of EGL growth and lobule folding (Sillitoe and Joyner, 2007), which may put some cerebellar regions under higher constraints regarding cell motility. During cerebellar development, the process of foliation begins with the formation of four principal fissures, dividing the developing cerebellum in five cardinal lobes, anterobasal (I-III), anterodorsal (IV, V), central (VI-VIII), posterior (IX), and inferior (X) (Sillitoe and Joyner, 2007). Data on lobule fusions in rat and mouse wild type strains that appear similar to the Sema4C fusion defects suggest that the lobules begin to fuse only after the formation of the initial fissures has occurred (Necchi and Scherini, 2002; Tanaka and Marunouchi, 2005). An alternative explanation for the lobule specific Sema4C/Sema4G phenotypes may be based on the fact that the cerebellum is subdivided in regions of distinctive molecular coding, as has been shown by recent studies on four functional domains of engrailed proteins in the cerebellum (Sgaier et al., 2007), and these regions may display different requirements for Sema4 and Plexin-B function.

The Sema4G mutation by itself did not cause a detectable cerebellar phenotype. However, loss of Sema4G gene function enhanced the phenotype of the Sema4C mutation, and Sema4G promoted the migration of GCPs in a transwell migration assay, indicating that both Sema4C and Sema4G act redundantly as ligands for Plexin-B2 on GCPs, with Sema4C playing a more dominant role. Sema4G is expressed by Purkinje cells, and therefore may promote migration of GCPs by its localization on Purkinje cell dendritic arbors.

As an alternative to an activity as transmembrane ligands, Sema4C and Sema4G may potentially also act as secreted proteins. Such a mechanism has been demonstrated for the extracellular domain of Sema4D, which is shed by proteolytic cleavage from the surface of lymphocytes (Elhabazi et al., 2001; Wang et al., 2001). In analogy, Sema4C and Sema4G may also promote migration of GCPs in form of secreted ligands. It is interesting to note in this context that Sema4C has been recently reported to be a substrate for the protease BACE1 (Hemming et al., 2009). However, no evidence exists so far for the *in vivo* shedding of Sema4C or Sema4G, and this model will require future experimental examination.

Both Sema4C and Plexin-B2 homozygous mutants develop exencephaly, which leads to neonatal lethality. The frequency of exencephaly of *Sema4c*-/- E15.5 embryos is with about 40% lower than that of the Plexin-B2 mutation on the same C57BL/6 background, in which about 95% of embryos were affected (Friedel et al., 2007). The lower frequency of exencephaly in Sema4C mutants is comparable to the phenotypes in cerebellar topology, in which the Sema4C mutation caused a weaker phenotype than the mutation of Plexin-B2. These data suggest that Sema4C, in analogy to the model of its function in cerebellar development, is not the only ligand of Plexin-B2 during neural tube closure, and further Plexin-B2 ligands are likely to exist for this process.

Semaphorins and Plexins are known to regulate the actin cytoskeleton of axonal growth cones (Kruger et al., 2005; Liu and Strittmatter, 2001), and several genes that are involved in actin regulation have also been implicated in neural tube closure (Juriloff and Harris, 2000). Thus, it seems likely that the functional involvement of Sema4C and Plexin-B2 in neural tube closure involves actin re-organization in neuroepithelial cells of the closing neural tube. Until now, there are only few reports implicating Semaphorins or Plexins in neural tube development. Interestingly, Sema6D has been reported to regulate neural tube

closing (Toyofuku et al., 2004a), which suggests that a Sema6-Plexin-A signaling may act in parallel to Sema4-Plexin-B signaling in the regulation of the folding of the neural plate.

In respect to the pigmentation defects of forelimbs, hindlimbs, and ventral midline seen in Sema4C and Plexin-B2 homozygous mutants, it is tempting to speculate that these might be caused by disturbances in the development of melanocytes. Melanocyte precursors, called melanoblasts, are generated from the neural crest during embryonic development, and migrate along a dorsal-lateral pathway beneath the ectoderm. After extensive migration and proliferation, melanoblasts differentiate into melanocytes and begin production of melanin pigment (Baxter et al., 2004). To date several genes have been identified that are associated with white-spotting phenotypes in mouse and some are also associated with neural crest and melanocyte disorders in humans (Osawa, 2008). One example is the *splotch* heterozygous mutation (a deletion within the paired homeodomain of *Pax-3*), which exhibits a characteristic white belly spot (Epstein et al., 1991; Potterf et al., 2000). Like the Plexin-B2 homozygous mutants, the *splotch* homozygous mutants develop a neural tube closure defect. Other examples are the transcription factor Sox10, which is expressed in early emigrating neural crest cells (Pingault et al., 1998; Potterf et al., 2001) and mutation in the *Kit* (c-Kit tyrosine kinase receptor) and *Kitl* (Kit ligand) genes with characteristic head and belly spots (Baxter et al., 2004). A recent study on β-catenin signaling on pigmentation has identified Sema4C as potential mediator of β-catenin effects (Zhang et al., 2008). Future studies will shed light on how Sema4C and Plexin-B2 interact with the above listed pigmentation genes, and they will reveal how the Sema4C Plexin-B2 ligand-receptor interaction is involved in one of the steps of melanocyte development, such as proliferation, migration, or differentiation, which are critical for melanocyte development (Barsh, 1996).

4.3 Migration promoting effect of Sema4C and Sema4G on granule cell precursors

An important aspect of this thesis is the analysis of the functional roles of Sema4 and Plexin-B2 in neuronal migration, which were addressed by *in vitro* assays. Several studies have described stimulatory as well as inhibitory modulation of cell migration by Sema4s *in*

vitro (Kruger et al., 2005). For example, Sema4D was shown to inhibit cell migration of PC12 cells (rat tumor cells of the adrenal medulla) by suppressing β1-integrin function (Oinuma et al., 2006). However, Sema4D was also reported to have stimulatory effects on cell migration and invasion of head and neck squamous cell carcinoma cells (Basile et al., 2006).

The *in vitro* transwell migration assay used in this study indicated that Sema4C and Sema4G act through the Plexin-B2 receptor, and that this interaction promotes the migration of cerebellar granule cell precursors (GCPs). To mimic more closely the *in vivo* situation, microexplant cultures of cerebellar EGL were performed. In EGL microexplant cultures, GCPs differentiate synchronously, and migrate radially from the explant in a manner that parallels their *in vivo* tangential migration in the lower EGL (Kawaji et al., 2004; Nagata and Nakatsuji, 1990). *Sema4c*-/- explants showed a significantly reduced number of GCPs outside of explants when compared to *Sema4c*+/- or wild type explants, supporting the model of Sema4C as a migration-promoting factor. Glial cells do not migrate out of EGL explants (Nagata and Nakatsuji, 1990), and a GCP-glial interaction is therefore not likely to be involved in the regulation of GCP migration in microexplant cultures. The fact that cells migrating out of explants are almost exclusively GCPs that are in extensive cell-cell contact with each other (Kawaji et al., 2004) suggests that Sema4C acts possibly as paracrine factor from granule cell to granule cell to promote migration.
Furthermore, the *Plxnb2*-/- explants displayed a reduced GCP migration rate compared to wild type explants when plated on laminin alone. When Sema4C protein was additionally presented as a substrate, the reduced migration rate of *Plxnb2*-/- explants was not altered, indicating that Plexin-B2 is a receptor for the migration promoting effect of Sema4C. In summary, these findings suggest that Sema4C and Plexin-B2 may function as a ligand-receptor pair in the EGL, and that Sema4C stimulates migration of GCPs through binding to Plexin-B2.
A considerably reduced number of migrating granule cells in EGL explant cultures has also been reported for homozygous mutants of Sema6A and of its receptor Plexin-A2 (Kerjan et al., 2005; Renaud et al., 2008). However, the phenotypes of Sema6A and Plexin-A2 mutants, in which dispersed ectopic granule cells are found in the molecular layer of all lobules, suggest that these molecules regulate an aspect of GCP migration that is functionally different from Sema4/Plexin-B signaling (see discussion below).

4.4 How do the cerebellar phenotypes in Sema4C/Sema4G mutants relate to known functions of Sema4 genes?

In this study, the first description of the *in vivo* function of the Sema4C and Sema4G genes was provided. The findings are in agreement with several *in vitro* studies that describe a cell-migration promoting effect for the Sema4D/Plexin-B1 pathway, such as for the migration of endothelial cells (Basile et al., 2007) or for liver epithelial cells (Giordano et al., 2002). In addition, it has also been shown that Sema4D promotes the migration of cortical precursor cells through the Plexin-B2 receptor (Hirschberg et al., 2010). However, Sema4D can also inhibit cell migration, as has been shown for a breast carcinoma cell line (Swiercz et al., 2008). Additionally, Sema4D inhibits branching morphogenesis during early stages of development of the ureteric collecting duct system in the kidney (Korostylev et al., 2008). It was also shown that activation of Plexin-B1 via Sema4D leads to an acute collapse of axonal growth cones in hippocampal and retinal neurons during early stages of neurite outgrowth, and promotes dendritic branching in hippocampal neurons (Vodrazka et al., 2009). Sema4D also stimulate axonal branching and growth in developing sensory neurons (Fujioka et al., 2003; Masuda et al., 2004) and reduce dendritic outgrowth (Saito et al., 2009).

These seemingly opposing activities of Sema4s, acting in some contexts as positive and in others as negative regulators of cell migration highlight the diverse roles of Sema4s in different biological systems, and may be explained by different components of co-receptors in different cell lines that dictate the outcome of Plexin-B activation (Swiercz et al., 2008).

Sema4C and Sema4G, which are widely expressed in the developing nervous system, but also in other developing organs such as kidney and lung (Inagaki et al., 1995; Li et al., 1999), may have other morphogenetic functions beyond the promotion of GCP migration. For example, Sema4C was identified as potential mediators of the effects of β-catenin signaling on pigmentation and innervation (Zhang et al., 2008). Interestingly, the Sema4C protein has been also detected in zones of adult neurogenesis, where it is upregulated during recovery from ischemic stroke (Wu et al., 2009a). The further elucidation of the functions of Sema4C/Sema4G proteins will require a more detailed understanding of the cellular and molecular responses upon Plexin activation.

4.5 How do Semaphorins orchestrate the development of cerebellar granule cells?

Lobule fusion defects that are similar to the lobule VIII/IX defects of Sema4C mutants have been described for FGF9, integrin-β1, and integrin-linked kinase mutants (Belvindrah et al., 2006; Blaess et al., 2004; Lin et al., 2009; Mills et al., 2006). The FGF9 and integrin phenotypes are, however, different from the Sema4C mutants in that they affect the entire cerebellum instead of specific lobules. It has been suggested that the phenotypes of these mutants are caused by a primary defect in radial Bergmann glia development, which then leads to a breakdown of the basal lamina between lobules and subsequent fusions of granule cell layers (Belvindrah et al., 2006; Lin et al., 2009). In Sema4C-/- mutants, a disruption of the basal lamina between lobules VIII and IX was shown by the absence of laminin staining. Although it cannot be ruled out that some aspects of the Sema4C/Sema4G phenotypes may be caused by Bergmann glia defects, our data supports a model that the Sema4C/Sema4G phenotypes are mainly a consequence of primary defects in cerebellar granule cell migration.

Besides the Sema4/Plexin-B pathway, also the Sema6/Plexin-A pathway is involved in cerebellar development. In particular, Sema6A and Plexin-A2 act as a ligand-receptor pair that regulates the migration of postmitotic GCPs that have left the proliferative zone of the upper EGL and migrate tangentially in the lower EGL (Kerjan et al., 2005; Renaud et al., 2008). Sema6A function in granule cells is non-autonomous, indicating that Sema6A functions as a ligand, and not as a receptor (Kerjan et al. 2005). Two mechanisms may account for Sema6A function in granule cell migration. Sema6A expressed in the deeper EGL may be involved in contact-mediated repulsion, guiding the nuclear/soma migration of granule cells away from the EGL. Alternatively, Sema6A may serve as a deadhesion molecule, facilitating granule cell radial migration by preventing cellular attachments among granule cells (Renaud et al., 2008). Interestingly, Plexin-B2 is highly expressed in the upper EGL, while Sema6A and Plexin-A2 are expressed in the lower EGL. Thus, it has been suggested that Plexin-As regulate cell migration of postmitotic GCPs in the lower EGL, while Plexin-B2 acts mainly on the migration of proliferating GCPs in the upper EGL (Chedotal, 2010).

In addition, the Sema3/Neuropilin system may also be involved in cerebellar development by guiding axonal growth of cerebellar neurons. For example, both Sema3A and Sema3F are expressed in rat cerebellum during development. It was shown that Sema3F can act through a Plexin-A/Npn-2 receptor complex as a chemoattractant for axons of cultured cerebellar granule cells (Ding et al., 2007).

4.6 Model

In summary, the results of this thesis suggest the following model for Sema4C/Sema4G function during cerebellar development. In the early development, granule cell precursors (GCPs) are initially born in the upper rhombic lip and then migrate rostrally over the cerebellar anlage from approximately embryonic day E13 on to form the external granule layer (EGL), which give rise to the entire population of cerebellar granule cells (Figure 4.1 A). In contrast the ventricular progenitor zone gives rise to Purkinje neurons, local interneurons, neurons of deep cerebellar nuclei, and Bergmann glia. Plexin-B2 and Sema4C are expressed by the GCPs and interact as receptor and ligand pair to promote their migration. Defects in the early rostral GCP migration may account for the gaps in rostral lobules in the mature cerebellum.

Sema4C/Sema4G may also promote the migration of postmitotic granule cells from the EGL to the IGL during formation of the cerebellar cortex, where Sema4C is present as a ligand on GCPs and on Bergmann glial cells, and Sema4G on Purkinje cell dendrites (Figure 4.1 B). Defects in this migration process may account for the presence of ectopic granule cells in the molecular layer of the mature cerebellum. Future functional studies with purified cerebellar granule neurons cultured with or without cerebellar Bergmann glia will help to address the question whether Sema4C/Sema4G signaling occurs mainly from granule cell to granule cell, or from radial glia to granule cell.

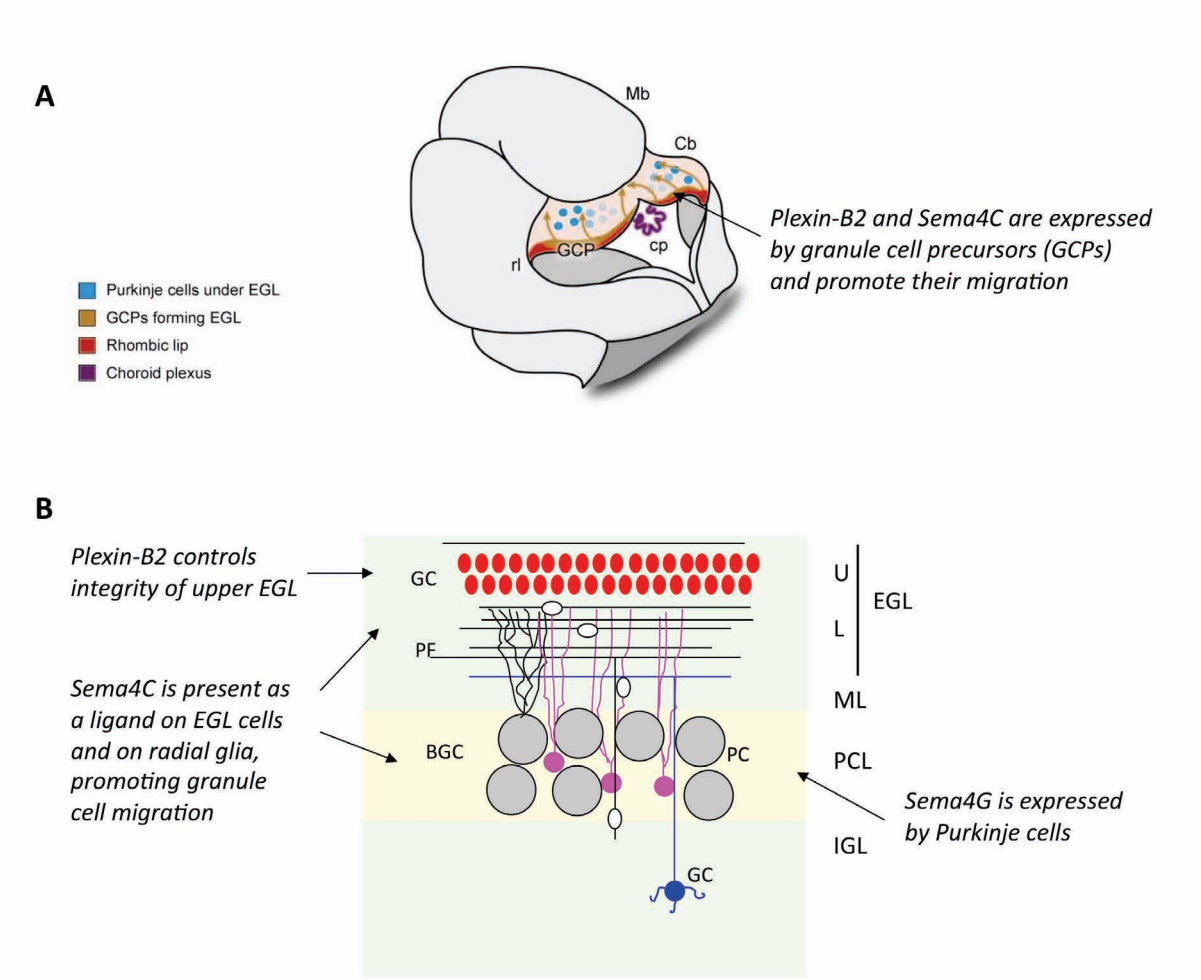

Figure 4.1 Model for Sema4C/Sema4G function during cerebellar development
(A) In early cerebellar development, at E13, granule cell precursors (GCPs), which express Plexin-B2 and Sema4C migrate from the rhombic lip (rl) over the surface of the cerebellum.
Mb, midbrain; Cb, cerebellum; cp, choroid plexus
(B) In the developing postnatal cerebellar cortex, granule cell progenitors (in red), which express Plexin-B2 and Sema4C, proliferate exclusively in the upper EGL (U). Postmitotic granule cells (GC) start differentiating and migrate in the lower EGL (L) before migrating radially along the Bergmann glia cells (BGC) through the molecular layer (ML) and the Purkinje cell layer (PCL) to the IGL. Sema4C is presented on Bergmann glia fibers and Sema4G on Purkinje cells, which project dendrites through the ML.
At this developmental stage, Purkinje cells (in gray) are still distributed in multiple layers. Note: the Purkinje cell dendritic tree is shown here only for a single cell.
Figure (A) modified after (Sillitoe and Joyner, 2007)

The experiments in this thesis support the model that Sema4C and Sema4G are *in vivo* ligands of Plexin-B2, with a more dominant function of Sema4C. However, the mild phenotypes of Sema4C and Sema4G mutants suggest that further ligand(s) for Plexin-B2 exist during neural development. These possible ligands may be other Sema4 members, such as Sema4A or Sema4B, which are expressed in radial Bergmann glia, and which could work with Sema4C and Sema4G in a redundant fashion.

The proposed model thus helps to explain why defects that are associated with deficiencies of granule cells, such as gaps in the IGL, occur mainly in rostral lobules and defects

associated with excess of granule cells, such as subpial ectopic clusters, occur in caudal lobules. Other mechanisms, though, are needed to explain other neural defects, including the fusions of caudal lobules, the disruption of lobule X, and the neural tube closure defects. Further studies will help to explain the full range of defects seen in the mutants, and will also help to identify downstream effectors of Plexin-B2 to elucidate how the Semaphorin/Plexin network regulates neural development.

5. MATERIAL AND METHODS

5.1 Reagents

5.1.1 Common solutions

1x PBS

171 mM NaCl
3.4 mM KCl
10 mM Na2HPO4
1.8 mM KH2PO4
pH 7.4

paraformaldehyde solution

4% PFA w/v in PBS

20x SSC (saline sodium citrate)

3 M NaCl
0.3 M sodium citrate
pH 7.0

sucrose solution (20%)

20% sucrose w/v in PBS

10x TAE

0.4 M Tris base
0.1 M acetate
0.01 M EDTA

10x TBS

0.25 M Tris-HCl pH 7.6
1.37 M NaCl

TE (Tris-EDTA)

10 mM Tris-HCl pH 7.4
1 mM EDTA

1x TBS-T

1 x TBS
0.05% Tween 20

Tris-HCl

1 M Tris base, pH 7.5

5.1.2 Working Solutions

Solution for work with bacteria

LB agar

98.5% LB-Media
1.5% Bacto agar

Ampicillin selection with LB agar with 100 µg/ml ampicillin
Kanamycin selection with LB agar with 50 µg/ml kanamycin

LB Media (Luria-Bertani-Media)
10 g Trypton
5 g yeast extract
10 g NaCl
ad 1 l H_2O, pH 7.0

Ampicillin selection with LB media with 100 µg/ml ampicillin
Kanamycin selection with LB media with 50 µg/ml kanamycin

Solution for Western Blot

Lysis Buffer
50 mM HEPES, pH 7.5
150 mM NaCl
1% Triton X-100
10% Glycerol
1 tablet Proteinase inhibitors
(Complete mini, Roche,
add fresh to 10 ml lysis buffer)

Laemmli buffer (5x)
313 mM Tris-HCl, pH 6.8
50% glycerol
10% SDS
0.05% bromphenol blue
5% ß-mercaptoethanol

10x NuPAGE MES Running Buffer
500 mM MES (2-(N-morpholino) ethane sulfonic acid)
500 mM Tris
1% SDS
10 mM EDTA
pH 7.2

10x TBS-T
200 mM Tris-HCl, pH 7.5
1.5 M NaCl
0.5% Tween20

10x NuPAGE transfer buffer
250 mM bicine (N,N-Bis(2-hydroxyethyl) glycine)
250 mM bis-tris
10 mM EDTA
0.05 mM chlorobutanol

1x NuPAGE transfer buffer
10% 10x transfer buffer
10% Methanol

Blocking solution
4% skim milk powder in TBS-T

Solutions for DIG labeled mRNA *in situ* hybridization

0.1M Phosphate buffered saline, pH 7.2
1.59 g $NaH_2PO_4 \cdot H_2O$
5.47 g Na_2HPO_4
9.0 g NaCl
ad 500 ml H_2O

Cryoprotection Solution (200 ml)
0.1 M Phosphate buffered saline, pH 7.2
30% Ethylene glycol
30% Sucrose
1% Polyvinylpyrrolidone (PVP-40)
ad 200 ml DEPC-treated H_2O

RIPA buffer
150 mM NaCl
1% NP-40
50 mM Tris-HCl pH 8.0
0.5% sodium desoxycholate
1 mM EDTA
0.1% SDS

Prehybridization solution
50% Formamide
5x SSC, pH 4.5
1% SDS
50 µg/ml yeast tRNA
50 µg/ml heparin

Solution I for post-hybridization wash (50 ml)
50% Formamide
5x SSC, pH 4.5
1% SDS

Solution III for post-hybridization wash (50 ml)
50% Formamide
2x SSC, pH 4.5
0.1% Tween 20

10x TBS (1000 ml)
80 g NaCl
2 g KCl
0.25 M Tris-HCl, pH 7.5

NTMT (10 ml)
0.1 M Tris-HCl, pH9.5
0.1 M NaCl
50 mM $MgCl_2$
1% Tween-20

20x SSC
3 M NaCl
0.3 M NaCitrat

Staining solutions

X-Gal staining buffer
0.1 M Phosphate buffer pH7.3 (see below)
with
2 mM $MgCl_2$ (0.2 g for 500ml)
5 mM potassium ferrocyanide ($K_4Fe(CN)_6$)
5 mM potassium ferricyanide ($K_3Fe(CN)_6$)
Add fresh before use: 1 mg/ml X-Gal (from 20mg/ml stock solution in dimethyl formamide)

0.1 M phosphate buffer pH7.3:
Dissolve 11.92 g Na_2HPO_4 and 2.5 g $NaH_2PO4.2H_2O$ in 1 liter H_2O

Cresyl violet staining solution (Nissl staining)
0.5% cresyl violet acetate
2.5 mM sodium acetate
0.31% acetic acid
ad 500 ml H_2O
filter before use

Stain	Working dilution	Company and Order number
Phalloidin	1:40	Invitrogen, R415
DAPI	1:100,000	Invitrogen, D1306

Solutions for Alkaline Phosphatase Fusion Protein Binding Assay

Binding Buffer
250 ml Hank`s Salt Solution
0.1% NaN_3
5 mM $CaCl_2$
1 mM $MgCl_2$
20 mM HEPES pH 7.2
0.2% BSA

HBS
150 mM NaCl
20 mM HEPES pH 7.0

AP Staining Buffer for cells

100 mM	Tris, pH 9.5
100 mM	NaCl
50 mM	$MgCl_2$

AP Staining Buffer for sections

100 mM	Tris, pH 9.0
100 mM	NaCl
5 mM	$MgCl_2$

Fixative for cells

4%	PFA/PBS

Fixative for sections

60%	acetone
15%	formaldehyde
40 mM	HEPES pH 7.0

5.1.3 Antibodies

Antibody for DIG labeled mRNA *in situ* hybridization

Antibody	Organism and type	Working dilution	Company and Order number
Anti- Digoxigenin Fab fragments, AP conjugated	sheep monoclonal	1:2000	Roche, 11093274910

Antibodies for Western Blot

Antibodies	Organism and type	Working dilution	Company and Order number
Anti-β-Actin,	mouse monoclonal	1:100,000	Abcam, ab 8226
Anti-PLAP	rabbit polyclonal	1:200	Santa Cruz Biotechnology, Inc., sc-28904
Anti-Plexin-B2	rabbit polyclonal	1:200	Santa Cruz Biotechnology, Inc., sc-67034
Anti-S4C	mouse monoclonal	1:500	BD Transduction Laboratories, 612486
Anti-VSV	mouse monoclonal	1:150,000	Sigma, V 5507

Antibodies for Immunohistochemistry

Antibodies	Organism and type	Working dilution	Company and Order number
Anti-$GABA_A$ receptor α6 subunit	rabbit, polyclonal	1:250	Chemicon, AB5610
Anti-Calbindin	rabbit polyclonal	1:500	Chemicon, AB 1778
Anti-GFAP	rabbit polyclonal	1:80	Sigma, G4546
Anti-Laminin	rabbit polyclonal	1:60	Sigma, L9393
Anti-Olig2	rabbit polyclonal	1:100	Chemicon, AB9610
Anti-S100β	rabbit polyclonal	1:250	Abcam, ab 868
Anti-Pax6	rabbit polyclonal	1:1000	Developmental studies Hybridoma Bank
Anti-4D7/TAG1	mouse monoclonal	1:600	Developmental studies Hybridoma Bank

Secondary Antibodies

Antibodies	Organism and type	Working dilution	Company and Order number
Anti-mouse, peroxidase conjugated	goat, polyclonal	1:10,000	Jackson ImmunoResearch, 115-035-174
Anti-rabbit, peroxidase conjugated	goat, polyclonal	1:10,000	Jackson ImmunoResearch, 211-032-171
Anti-mouse IgG, Cy2 conjugated	goat, polyclonal	1:200	Dianova, 115-225-146
Anti-rabbit IgG, Cy3 conjugated	goat, polyclonal	1:200	Dianova, 111-165-144

5.1.4 Enzymes

DNase I (RNase-free)	Roche
Klenow fragment of DNA Polymerase I	NEB
proteinase K	Roche
restriction enzymes	Roche, NEB
RNA polymerases (T7, SP6)	Roche
RNase A	Serva
RNase inhibitor	Roche
Shrimp alkaline phosphatase (SAP)	Roche
Reverse Transcriptase, SuperScriptII	Invitrogen
T4 DNA ligase	NEB

5.1.5 Plasmids

Name	Type of plasmid	Provider
ph-PB1-VSV	Expression plasmid for human Plexin-B1 with a N-terminal VSV peptide tag	Dr. Luca Tamagnone, Università di Torino
pm-PB2-VSV	Expression plasmid for murine Plexin-B2 with a N-terminal VSV peptide tag	Dr. Roland Friedel, Helmholtz Zentrum München
pcDNA1-S4C-hPLAP-Str	Expression plasmid for ectodomain of murine Sema4C, C-terminally fused to human PLAP	Dr. S. M. Strittmatter, Department of Neurology, Yale (USA)
pAPtag5	Cloning plasmid for expression of AP tagged plasmids	Genehunter, Nashville (USA)
pS4D-AP 5	Expression plasmid for murine Sema4D with a C-terminal AP peptide tag	Dr. Roland Friedel, Helmholtz Zentrum München
pCRII-TOPO	General cloning plasmid	Invitrogen

5.1.6 Oligonucleotides

All Oligonucleotides were ordered from Sigma and designed by usage of the software VectorNTI (Invitrogen).

Oligonucleotides for genotyping

Name	Sequence
Sema4B (RST235)	
R235 (S4B)-F	5´-TAAATCTGGATCAGTGGACAGCAG-3´
R235 (S4B)-R	5´-GCAGGAGGCAGAGGCATTGACT-3´
RO3b	5´-TTGTCATGGAGGAGAAAGGGCAGA-3´

works as multiplex PCR, use 3 fold amount of R235 (S4B)-F
Size of product:
Wild type band 390bp
Mutant band 800bp

Sema4C	
S4C-F	5´-TGGTGTGGCTTACCCTGTGCTTTG-3´
S4C-R	5´-AGAAAGGAGCCAGGTTGTTCTGCA-3´
RO1b	5´-ACTTCCGGAGCGGATCTCAAACTC-3´

works as multiplex PCR, use 3 fold amount of S4C-R
Size of product:
Wild type band 620bp
Mutant band 430bp

Sema4G	
S4G-F	5´-ATCACACCCTGGACTTTGAACCC-3´
S4G-R	5´-TTTCCCTTTCTGATGACACTTGC-3´
Neo-out-r	5´-CAATCCATCTTGTTCAATGGCCGA-3´

works as multiplex PCR, use 3 fold amount of S4G-F
Size of product:
Wild type band 450bp
Mutant band 304bp

Plexin-B2

PB2-SS	5´-GCCATTGAGAACTTTGTCAGGTG-3´
PB2-AA	5´-GCAAACTTCTGGATGAGGCTGAAG-3´
RO1b	5´-ACTTCCGGAGCGGATCTCAAATC-3´

works as multiplex PCR, use 3 fold amount of PB2-AA
Size of product:
Wild type band 390bp
Mutant band 280bp

Plexin-B2^{Euc1a}	5´-TACTAGGATCAGAGGTCATCG-3´
Plxnb2^{Euc1a}-5´arm	5´-GCTTTGGTGTCAACTCCCAAG-3´
Plxnb2^{Euc1a}-3´arm	5´-CACAACGGGTTCTTCTGTTAGTCC-3´

LAR3
works as multiplex PCR, use 3 fold amount of *Plxnb2*^{Euc1a}-5´arm
Size of product:
Wild type band 723bp
Mutant band 526bp

Oligonucleotides for cloning of expression plasmids

For cloning of a Plexin-B3 expression plasmid, with a VSV tag and cloning of a Sema4G expression plasmid with AP, the following oligonucleotides were used.

Name	Sequence	Restriction site, integration in Primer sequence
hPLAP-F	5´-TCTAGAATCATCCCAGTTGAGGAGGAGAAC-3´	*Xba*I
hPLAP-R2	5´-CTCGAGACCCGGGTGCGCGGCGTCGGTGGTG-3´	*Xho*I
PB3-S1-F	5´-AGTCGACGGTCCATCGCTTCTCTGTACCAA-3´	*Sal*I
PB3-N1-R	5´-AGCGGCCGCGCAGGTCTCAGGTAATCACTGTGG-3´	*Not*I
S4G-HindIII-F2	5´-AAGCTTGGAAGATGTGGGGGAGGCTCTGGCCCCTCCTCT-3´	*Hind*III

S4G-XbaI-R	5′-TCTAGAGAACATCCTCATGTCATGTGCCAG-3′	*Xba*I

Oligonucleotides for cloning of ISH probes

The following oligonucleotides were used for cloning of ISH probes of approximately 2 kb length.

Gene	Name	Sequence
Sema4a	S4A-ISH-F	5′-TCCCTGGGCCAGGACTCATGGAGT-3′
	S4A-ISH-R	5′-AGAGTGAGCACTCCCAGGAGCACG-3′
Sema4b	S4B-ISH-F	5′-GCGCTGCTGCTGCTGCTGCTACTG-3′
	S4B-ISH-R	5′-TGCACTCACTCGTGATGTGTTGAT-3′
Sema4c	S4C-ISH-F	5′-ATGGCCCCACACTGGGCTGTCTGG-3′
	S4C-ISH-R	5′-ACAGCAACAAGGTAGCTTTCTGCA-3′
Sema4d	S4D-ISH-F	5′-ATGAGGATGTGTGCCCCCGTTAGG-3′
	S4D-ISH-R	5′-CCATCTTTGGTTCACAGGATGTGC-3′
Sema4f	S4F-ISH-F3	5′-CGTACAATTACTCTGCTCTCCTGG-3′
	S4F-ISH-R2	5′-TTCCTGGCTTTAGATAGACGTCTC-3′
Sema4g	S4G-ISH-F	5′-ATGTGGGGGAGGCTCTGGCCCCTC-3′
	S4G-ISH-R	5′-GCTACCACATAGAACATCCTCATG-3′
Plxnb1	PB1-ISH2000-F	5′-GAGTCACCTCTTCATGAGAAGC-3′
	PB1-ISH2000-R	5′-GGGCTCACAGTACAGGTGGTTC-3′
Plxnb2	PB2-ISH2000-F	5′-GCCATCACTGATGCCTTTCCAC-3′
	PB2-ISH2000-R	5′-GTAGGTTGTGTGCCGTGTCTCG-3′
Plxnb3	PB3-ISH2000-F	5′-AATCCTCCAGGCTCAGATCATG-3′
	PB3-ISH2000-R	5′-GGTGGACATCATGGACTCTGCT-3′

5.1.7 Cell culture

Solution for cell culture

GIBCO DMEM Media (Invitrogen, 21969)
Contains
4.5 g/l Glucose
0.11 g/l Sodium Pyruvate
no L-Glutamin
1% PSG (penicillin, streptomycin, glutamin) and 10% FCS (Hyclone) were added before first use of the media.

GIBCO OPTI-MEM Media (Invitrogen, 51985)
Contains Glutamax

Media for cerebellar explants
Neurobasal media (Invitrogen, 21103-049)
N2 Supplement (Invitrogen)
1 mg/ml BSA (fraction V, Invitrogen)
1% PSG (penicillin, streptomycin, glutamin)

Solution for Transwell migration assay

Neurobasal mix (20ml)
19 ml Neurobasal media (Invitrogen)
200 µl Sodium pyruvate 100x
400 µl PSG 100x
400 µl B27 supplement 50x
20 µl N-acetyl cysteine (60mg/ml)

Ovo solution (trypsin inhibitor)
2.5 ml DPBS-BSA
0.5 ml Trypsin Inhibitor (TI) stock
60 µl DNaseI (10 mg/ml)

Solution for 1 papain tube
2 ml DPBS-BSA
50 µl papain (20U, Sigma)
40 µl DNaseI (10mg/ml)
activation with L-cysteine

5.2 Methods

All techniques on DNA, RNA, or Protein level were performed according to standard protocols (Sambrook, 1989).

5.2.1 Cloning and work with plasmid DNA

Preparation of plasmid DNA

To extract plasmid DNA the following Qiagen kits were used: DNA Maxi Prep Kit and DNA Mini Prep Kit (Invitrogen). For mini-prep production, one colony was inoculated in 2 ml LB media containing an appropriate antibiotic and incubated over night. 1.5 ml of the culture was used for preparation following the manufacturer's instructions.
In case of maxi-prep production, colonies were picked and cultivated in 2 ml selective LB media for several hours at 37°C in the incubator. This preculture was poured into 100 ml of LB media with antibiotic and incubated over night. The whole culture was used for preparation following the manufacturer's instructions.
DNA concentration was determined with Nanodrop ND-1000 Spectrophotometer (peQLab Biotechnologie GmbH).

Polymerase Chain Reaction (PCR)

The PCR technique amplifies a DNA fragment definded by the oligonucleotide primers used in the reaction, flanking the fragment of interest. The DNA strands are denatured at 95°C and then cooled down to 65°C for the primers to anneal. Elongation of the DNA fragment takes place at 72°C. Those three steps are repeated for 15-35 cycles.

Cloning of Sema4G

Since hPLAP does not have a 3' end restriction site in the pcDNA1-S4C-hPLAP-Str construct, PCR was performed to extract the hPLAP fragment from the vector and providing it with an *Xho*I restriction site by primer design. The DNA polymerase of

Thermus aquaticus (Taq) does not have a proof reading function, so to reduce mutations the number of cycles was kept at 15-20.

PCR Reaction Mix:

3,0 µl	pcDNA1-S4C-AP-Str (ca. 90 ng)
2,5 µl	10x buffer
0,5 µl	dNTPS
0,5 µl	hPLAP Primer F (10µM)
0,5 µl	hPLAP Primer R (10µM)
18,0 µl	H_2O
0,2 µl	Taq
25,0 µl	Final volume

Program:

95°C	3 min	
95°C	15 s	15 cycles
65°C	30 s	
72°C	30 s	

Cloning of Plexin-B3

After cDNA was generated from embryonic mouse RNA, PCR was performed to amplify Plexin-B3 cDNA from the total mRNA. Two restriction sites (*Sal*I and *Not*I) were added to the oligonucleotide primers for Plexin-B3 cDNA, so that the fragment could be easily inserted in the VSV vector via restriction digest and ligation. AccuPrime High fidelity Taq DNA polymerase (Invitrogen) was used to reduce mutations and was added to the reaction mix when it had reached its peak temperature of 95°C (hot start).

2.0 µl	PB3 mouse embryonic cDNA
5.0 µl	10x AccuPrime PCR buffer I (containing dNTPs)
1.0 µl	Primer PB3-F (10µM)
0.5 µl	Primer PB3-R (10µM)
41.0 µl	H_2O
0.2 µl	AccuPrime Taq High Fidelity, add by hot start
50 µl	Final volume

Program:

95°C	2:30 min	
add 0.2 µl Taq manually (hot start)		
95°C	15 s	30 cycles
65°C	30 s	
68°C	7 min	

Restriction digest of plasmid DNA

The amount of restriction enzyme was determined in relation to the amount of plasmid DNA used. For one µg of supercoiled DNA, two units (U) of enzyme were used. The reaction conditions were adjusted to the manufacturer's instructions and requirements of the used enzyme(s). The restriction digest was incubated at least for one hour at the appropriate temperature of each enzyme used. If blunt ends were required, 5 U of large (Klenow) fragment of *E.coli* DNA polymeraseI and 25 nm dNTPs were added to the sample after the restriction digest and incubated at room temperature (RT) for 20 min. Klenow was inactivated by incubation for 15 min at 75°C.

To minimize the religation of an opened vector it is useful to remove the terminal phosphates of the DNA, which prevents DNA ligase from joining these ends. This dephosphorylation is performed by 1 µl CIP (Alkaline Phosphatase, Calf Intestinal). For sticky vector ends, the sample was incubated for 15 min, blunt vector ends were dephosphorylated for 60 min. CIP was inactivated by incubation for 10 min at 75°C.

Isolation of DNA fragments

For cloning, the vector fragments were separated using gel electrophoresis. In general 1% Agarose gels were used, containing ethidium bromide to visualize the DNA using ultraviolet light. The gels were run using 1x TAE buffer. The complete restriction digest was loaded with 5x loading buffer and as a length standard the 1kb ladder was used. After separation in the gel, the needed fragments were cut out with a clean scalpel. The DNA fragments were isolated from the Agarose using the Qiagen Gel Extraction Kit (Invitrogen) following manufacturer's instructions. The concentration of the DNA fragments was measured with Nanodrop ND-1000 Spectrophotometer (peQLab Biotechnologie GmbH).

Ligation of DNA fragments

For ligation, linearized vector and insert DNA fragment were combined in a molar ratio of approximately 1:3. They were mixed and T4 DNA ligase buffer was added to the sample. The reaction was performed at RT with 600 U T4 DNA ligase in a total volume of 15 µl. For cloning of PCR fragments, the TOPO TA Cloning Kit (Invitrogen) was used. This kit contained a linearized vector conjugated with TopoisomeraseI, which allowed subcloning without ligase. The reaction was done following manufacturer's instructions.

Ligation of DNA and pCRII TOPO vector (Invitrogen):
4 µl DNA
1 µl Salt Solution
1 µl pCRII Topo vector

Ligation of DNA and other vectors
3 µl vector
7 µl insert
10 µl 2x buffer
1 µl Ligase

Transformation of competent bacteria

For one transformation, a 50 µl aliquot of competent bacteria (DH5α, Gibco or TOP10, Invitrogen) was slowly thawed on ice and 2 µl of ligation product (approx. 25 ng of plasmid DNA) was added to the bacterial suspension. The sample was mixed gently and incubated on ice for at least 30 min. The following heat shock for 40 sec at 42°C allows the DNA to enter the bacteria. 250 µl of LB media was added and the sample was incubated at 37°C for 60 min. During this time the transformed bacteria express the plasmid based antibiotic resistance genes, used for selection. Afterwards the bacteria were plated on LB agar plates containing the appropriate antibiotic and incubated over night at 37°C. In general, Ampicillin (100 µg/ml) or Kanamycin (50 µg/ml) was used for selection.

For Retransformation already prepared circular plasmids was used.
2 µl plasmid DNA in 1:100 dilution were added to 50 µl TOP10 or TOP10/P3 bacteria (Invitrogen). They were kept on ice for 5 min and then exposed to a heat shock at 42°C for 40 sec. After addition of 200 µl LB media, the bacteria were incubated for 10 min in the

incubator shaker and subsequently spread on LB agar plates. The plates were incubated at 37°C over night.

DNA Sequencing

The sequences of cloned vectors or amplified DNA fragments were verified by DNA sequencing with the Sanger method with fluorescently labeled dideoxynucleotides. 5 pmol of a specific primer were mixed with DNA and a reaction mix containing Big dye (Applied Biosystems) to a total volume of 5 µl. After initial denaturation of the template DNA at 95°C, the reaction was performed for 25 cycles each consisting of the following steps: 30 sec at 95°C, 15 sec of annealing at a primer specific temperature, 4 min of primer elongation at 60°C. To purify the fragments, the DNA was precipitated with 100% ethanol and resuspended in pure water. The samples were loaded to a 96-well sequencer plate and analyzed with an ABI sequencer. Analysis of sequence reads was performed with Vector NTI software.

5.2.2 Polymerase chain reaction (PCR) for Genotyping of mouse lines

For Genotyping, a small mouse tail tip (approximately 1mm) was used for DNA preparation. The tail tip was incubated in 100 µl of 50 mM NaOH and heated for 99°C for 20 min (embryos) or 30 min (adult). To neutralize 30 µl of 1M Tris-HCl, pH7.0 were added and 0.5 µl of the DNA preparation was used as PCR-template.

Reaction:

10x Qiagen PCR buffer	1.25 µl
dNTP (10mM)	0.25 µl
Primer1 (10µM)	0.25 µl
Primer2 (10µM)	0.75 µl
Primer3 (10µM)	0.25 µl
H_2O	9.25 µl
DNA prep	0.5 µl
	--
	12.5 µl

The Taq enzyme was added on ice (0.1 µl/rxn).

PCR-Program:

95°C	3 min	
95°C	15 s	34 cycles
65°C	30 s	
72°C	30 s	

5.2.3 Histology

LacZ staining of mouse tissues

Mouse brains were fixed in 4% paraformaldehyde in PBS (4% PFA/PBS) for about 4-5 h (longer fixation will decrease X-Gal staining), washed 60 min in PBS and stored in PBS at 4°C.

Tissue was embedded in 4% Agarose/PBS and the histochemical stainings for the β-galactosidase reporter were performed on 100 µm vibratome sections as described previously (Leighton et al., 2001). The sections were stained with X-Gal (1 mg/ml) in X-Gal staining buffer at RT for homozygous mutants and at 37°C for heterozygous mutants, for 1h up to 2 days. Staining reaction was monitored every hour. The reaction can be slowed down by incubation at 4°C and stopped by transferring to PBS. After postfixation for 10 min in 4% PFA/PBS, the section were mounted with Aquapoly/Mount.

Nissl staining (cresyl violet)

The histochemical stainings for Cresyl violet were also performed on 100 µm vibratome sections. First, the sections were rinsed in distilled water and acetate buffer and then stained in cresyl violet solution for 2-10 min. After a quick wash step in distilled water, the sections were dehydrated in 50% ethanol for 2 min, in 70% ethanol for 2 min, in 95% ethanol for 2x 2 min and in 100% ethanol for 2 min. The sections were cleared in xylene for 2x 5 min and mounted with DPX (Fluka).

Immunohistochemistry

For immunohistochemistry, brains were perfused and postfixed over night with 4% paraformaldehyde in 0.1 M phosphate buffer. Immunohistochemistry was performed on sections either cut with vibratome (100 µm, free floating) or microtome (40 µm).
The sections were washed with 0.1 M TBS 3 times for 15 min each and blocked with 3% normal serum in TBS with 0.25% Triton-X (TBST) for at least 60 min.
Sections were then incubated with different primary antibodies in TBST for 24 hours at 4°C. After washing in TBS, the sections were incubated in TBST once for 30 min, followed by species-specific secondary antibodies (Dianova) in TBST for 120 min at RT on a shaker.
After four washing steps with TBS at RT, sections were counterstained with DAPI and mounted with Aquapoly/Mount (Polyscienes).
For a colorigenic substrate staining with DAB (3,3 Diaminobenzidine), a peroxidase conjugated secondary antibody was used. After washing in TBS, TBST and 0.1 M Tris-HCl, the sections were stained for 20 min with 1% DAB in 0.1 M Tris-HCl and 3% H_2O_2. The staining reaction was stopped with PBS.

DIG labeled mRNA *in situ* hybridization

The sensitivity of the already existing *in situ* probes of 700bp length was not sufficient for non radioactive ISH. To increase the sensitivity of the *in situ* hybridization signal, a second set of longer probes about 2kb was cloned.

Slice preparation

The brains were dissected in PBS and fixed in freshly prepared (or thawed from frozen aliquot) 4% PFA/PBS at 4°C over night. After washing with PBS for 5 min, 10 min and 45 min to remove the fixative, the brains were embedded in 4% Agarose/PBS. The analyses were performed on adjacent sagittal vibratom sections with a thickness of 70 µm with digoxigenin-labeled riboprobes as described (Dolan et al., 2007).
In case the sections were to be stored, PBS was replaced with cryoprotection solution and transferred to -20°C. The cryoprotection solution was replaced with PBS before starting hybridization.

Probe labeling

The cDNA fragments were used for synthesizes for RNA ISH probes. Corresponding primer pairs and cDNA of E11.5 embryos were used. After cloning into the TOPO TA cloning vector (pCRII-TOPO), they were sequenced with SP6 and T7 primers. Before the ISH probes were synthesized, the vector was linearized with different restriction enzymes on the end of the cDNA insert (Table 5.1).

Table 5.1 Restriction enzymes and RNA polymerase for antisense and sense ISH probes

Plasmid name	Gene	Antisense probe		Sense probe	
		Cut with	RNA polymerase	Cut with	RNA polymerase
pCRII-Sema4A-ISH2000	*Sema4a*	*EcoR*V	Sp6	*Spe*I	T7
pCRII-Sema4B-ISH2000	*Sema4b*	*Spe*I	T7	*EcoR*V	Sp6
pCRII-Sema4C-ISH2000	*Sema4c*	*Spe*I	T7	*EcoR*V	Sp6
pCRII-Sema4D-ISH2000	*Sema4d*	*EcoR*V	Sp6	*Spe*I	T7
pCRII-Sema4F-ISH2000	*Sema4f*	*Spe*I	T7	*EcoR*V	Sp6
pCRII-Sema4G-ISH2000	*Sema4g*	*Not*I	Sp6	*Hind*III	T7
pCRII-PlexinB1-ISH2000	*Plexinb1*	*EcoR*V	Sp6	*Spe*I	T7
pCRII-PlexinB2-ISH2000	*Plexinb2*	*EcoR*V	Sp6	*Spe*I	T7
pCRII-PlexinB3-ISH2000	*Plexinb3*	*EcoR*V	Sp6	*Spe*I	T7

The riboprobes were synthesized by *in vitro* Transcription with T7 RNA polymerase or Sp6 RNA polymerase (Table 2.1)

Reverse Transcription PCR:

1 µg	linear DNA
2 µl	10x Transcription buffer (Roche)
2 µl	10x DIG labeling Mix (Roche)
0.5 µl	RNase Inhibitor (Roche)
2µl	T7 or Sp6 Polymerase
12.5	H_2O (RNase free)
20µl	

After 2h incubation at 37°C, 2 µl DNaseI RNase free (Roche) were added and incubated for additional 15 min. After this, the probes were cleaned up with RNeasy kit (Qiagen) and analyzed on a 1% TAE-Gel.

Hybridization

On the first day of the experiment Prehybridization steps were performed and Hybridization was started.
The sections were washed twice in PBT (PBS + 0.1% Tween-20) for 5 min each and then dehydrated in a 25%, 50%, 75% methanol/PBT and 100% methanol series for 5 min each. After rehydration in a 75%, 50% and 25% methanol/PBT series, the sections were washed twice with PBT for 5 min each. After permeabilization with RIPA buffer (3x 30 min) and postfixation with 4% PFA with 0.2% glutaraldehyde in PBT for 40 min, the brain sections were washed with PBT. Half of the volume of PBT was replaced with prehybridization solution, and incubated for 10 min and then incubated for at least 1 h at 65°C.
Hybridization was performed in a humified environment over night at 65°C with 1 µg/ml labeled probe in hybridization buffer.
Posthybridization washes were performed at 65°C using solution I (50% formamide, 5x SSC pH4.5, 1% SDS) and solution III (50% formamide, 2x SSC pH4.5, 0.1% Tween-20) and at RT using TBST (TBS containing 1% Tween-20). Brain sections were blocked with blocking buffer (TBST containing 10% heat-inactivated sheep serum) for 1h and the Immunodetection was carried out in blocking buffer at 4°C over night using a phosphatase conjugated anti-digoxigenin antibody (Roche) at a 1:2000 dilution.

After three washing steps for 15 min at RT with TBST, sections were equilibrated in NTMT (100 mM Tris-HCl pH 9.5, 100 mM NaCl, 50 mM MgCl2, 1% Tween-20) prior to

colorimetric detection using 20 µl/ml NBT/BCIP (Roche, 11 681 451 001) in NTMT. Sections were mounted with Aquapoly/Mount and analyzed by light microscopy.
Hybridization with sense probes was included in all experiments to control for nonspecific background signals.

5.2.4 Western blot analysis

Tissues and protein samples were kept on ice during all steps of preparation. Tissue parts of the cerebellum cortex from P3-P5 mice of about 3 diameter in size were homogenized in 100 µl lysis buffer containing a protease inhibitor cocktail (Complete mini, Roche) in a dounce homogenizer. The cell debris and nuclei in the homogenate were pelleted by centrifugation for 10 min at 4°C (13,000 rpm in a table top centrifuge). The supernatant containing the protein lysate was stored at -80°C.

SDS Polyacrylamide Gel Electrophoresis (SDS-PAGE)

Proteins were separated according to their size with SDS-PAGE (Laemmli, 1970).
A NuPAGE Bis-Tris gel (Invitrogen) was placed into the XCell SureLoc Mini-Cell (Invitrogen) and covered with MES (2-(N-morpholino) ethane sulfonic acid) running buffer. To each 15 µl sample, 5 µl Laemmli loading buffer were added and the samples were denatured for 3 min at 90°C. Then, they were briefly cooled on ice and then loaded into gel pockets. As size standard, 10 µl protein standard (HiMark Pre-Stained High Molecular Weight Protein Standard, Invitrogen) were loaded. The gel running apparatus was then filled with 1x NuPage MES running buffer and the samples were separated at 200 V for 1-1.5 h (resulting in a current 140 mA).

Western Blot Transfer

The gel was placed onto a gel-sized whatman paper wet with transfer buffer and put into the blotting chamber on top of two blotting pads, which were also soaked in transfer buffer. The PVDF (polyvinylidene difluoride) membrane (BioTrace, Pall corporation) was bathed in 100% methanol for 1 min and then moved into transfer buffer. Then, the

membrane was fitted onto the gel in the blotting chamber. Three wet whatman paper were put atop the membrane. The cell was next filled with blotting pads that were soaked with transfer buffer. The blotting chamber was closed and placed inside the Mini-Cell apparatus. The blotting chamber was covered with transfer buffer, and the outer compartments were filled with Millipore filtered water for cooling purposes. The samples were blotted for 1 h at 30 V.

Protein detection

After Western blot transfer, the membrane was blocked with 4% skim milk, and then incubated in TBST for 1 hour at RT, and over night at 4°C with the primary antibody in TBST. The membrane was washed three times with TBST. Then the secondary horseradish-peroxidase-conjugated antibody was applied and incubated for 1 h, and washed three times with TBST. The membrane bound proteins were detected with ECL detection reagent (Amersham) by incubating for 1 min, and the membrane was exposed to an X-ray film (Hyperfilm ECL, GE Health Care 28-9068-37) for 10 sec to several min, depending on the signal intensity.

5.2.5 Cell Culture

COS and HEK293 fibroblast cells were incubated in DMEM media with 10% fetal calf serum at 37°C and 5% CO_2. The COS cells were split 1:10 every 2-3 days, and the HEK293 cells were split 1:20 every 3-5 days. To split cells that had reached subconfluency, cells were washed with PBS and then detached by Trypsin-EDTA (Invitrogen) incubation for 4 min at 37°C. The Trypsin was neutralized by addition of DMEM media and the cells were dissociated by pipetting up and down before they were transferred to a fresh dish.

Transfection

One day before the transfection, the cells were splitted 1:4. On the next day, the cells were transfected with either 2 µg (6-well plate) or 10 µg plasmid DNA (10 cm plate). 6 µl Fugene transfection reagent (Roche) for a 6-well plate or 30 µl Fugene transfection reagent for a 10 cm plate were mixed with 100 µl OPTI-MEM media (Invitrogen) for a 6-well plate or 500 µl OPTI-MEM media for a 10 cm plate and incubated at RT for 5 min. The DNA was added and incubated for 20 min at RT. The transfection solution was dropped onto the cell culture dishes and mixed by gentle shaking. The cells were incubated over night, and media was changed on the next morning. For Western blot analysis, transfected cells were typically lysed 2 days after transfection. For the collection of conditioned cell culture supernatant, the media was changed on day 3 after transfection to OPTI-MEM media, which contained also freshly added 1x Pen-Strep-glutamate (Invitrogen). After two days, the conditioned cell media was collected and poured into a syringe provided with a filter tip. The filtered media was stored at 4°C.

Cell Lysis

For cell lysis, the cell culture dishes were washed with PBS and put on ice. They were then lysed with 500 µl lysis buffer for a 6-well plate or 1 ml lysis buffer for a 10 cm plate. Cells were scraped off the plate and kept on ice for 30 min. The lysate was centrifuged at maximal velocity for 30 min in a table top cooling centrifuge at 4°C. The supernatant was transferred to a fresh eppendorf tube and stored at -20°C.

Protein concentration with Centriprep Ultracel

The Centriprep Ultracell (Centriprep YM-50, nominal molecular weight limit of 50 kD, Millipore) was used to obtain higher Sema4 protein concentrations of the conditioned cell media. A maximum of 15 ml was loaded in each Centriprep Sample Container and the Filtrate Collector was gently pushed down to displace the solution to the sides of the Sample Container. The Centriprep was centrifuged for 10 min, 5 min and 5 min at 1500 g. After each centrifugation step, the filtrate was disposed by removing the Air Seal Cap and pouring the solution into a beaker. After the last centrifugation step, the Filtrate Collector

was removed and the concentrated sample collected from the Sample Container. The concentrated samples were stored at 4°C

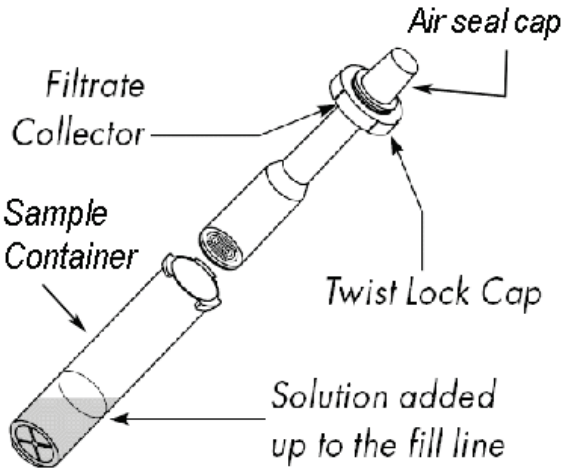

Figure 5.1 Assembly of the Centriprep Ultracell device

Alkaline Phosphatase staining of conditioned cell media

To test the AP activity of the cell media conditioned with Sema4-AP proteins, aliquots of the supernatant were stained for AP activity:

100 µl AP buffer for PLAP staining
10 µl NBT/BCIP (Roche, 11 681 451 001)
10 µl sterile cell supernatant containing Sema4-AP protein

The samples were incubated at 37°C for several hours or over night until the solution changed from yellow to a bluish-purple color.

5.2.6 Alkaline Phosphatase Fusion Protein Binding Assay

Alkaline Phosphatase Fusion Protein Binding Assay on cells

The alkaline phosphatase fusion protein binding assay was performed to determine ligand receptor pairing of class 4 Semaphorins and B-type Plexins. Cells transfected with Plexin expression plasmids were incubated with Semaphorin-AP conditioned cell media, and bound Semaphorins were visualized by alkaline phosphatase staining reaction. Binding and detection were performed as described (Flanagan et al., 2000).
On the first day, COS cells were split 1:4 from a 10 cm dish to a 6-well plate (both Nunc). Then, the cells were transfected with Fugene (Roche) as described under 5.2.5 with phPlexin-B1-VSV, pmPlexin-B2-VSV, pmPlexin-B3-VSV or pEGFP-F as a control. One day before the assay was started, the media was replaced to ensure optimal growth of the cells. On the day of the binding assay, the cells were washed with binding buffer for 1min. Then, 400 µl binding buffer were mixed with 400 µl of conditioned cell media (Sema4C-AP, Sema4D-AP and Sema4G-AP) and given onto the cells and incubated for 90 min at RT. The cells were washed three times with binding buffer and then fixed in 3.7% formaldehyde (Sigma) in PBS for 12 min at RT. Then, the cells were washed with HBS three times. To inactivate endogenous alkaline phosphatase activity, cells were incubated in a 65°C water bath covered with 2 ml HBS per well for 15 min.
The cells were washed with AP buffer for PLAP staining for 3-5 min, before applying the staining solution with 1x NBT/BCIP solution (Roche). After incubation at 37°C over night or up to several days, the staining reaction was stopped with 4% PFA in PBS.

Alkaline Phosphatase Fusion Protein Binding Assay on sections

Binding of Sema4-AP proteins on sections was performed with fresh frozen sections as described (Renaud et al., 2008). Briefly, fresh-frozen cryoststat sections (18 µm) of P10 mouse cerebella were fixed in cooled methanol for 5 min. After three washing steps in PBS with 4 mM $MgCl_2$ for 5 min, the sections were blocked with 10% fetal bovine serum in PBS with 4 mM $MgCl_2$, for 1 h. Then, the sections were incubated with supernatant from Sema4C-AP, Sema4D-AP and Sema4G-AP transfected COS cells for 2 h. The sections were washed in PBS with 4 mM $MgCl_2$ while gently shaking (50 rpm), and then

fixed in 60% acetone, 15% formaldehyde and 20 mM HEPES pH 7.0 for 2 min. The endogenous phosphatase was inactivated at 65°C for 2 h in PBS and the sections were washed briefly in TBS. Ligands bound to sections were revealed by staining with NBT/BCIP color substrate in 100 mM Tris pH 9.0, 100 mM NaCl, 5 mM $MgCl_2$ over night in a wet chamber. To stop color development, the sections were fixed in 60% acetone with 15% formaldehyde and 40 mM HEPES pH 7.0 for 30 min. Sections were then mounted with Aquapoly/Mount mounting media.

5.2.7 Transwell migration assay

Coating of transwell inserts

One day before the assay, transwell inserts for 24-well plates (Greiner ThinCert; #662630; pore size 3.0 µm; transparent PET membrane) were coated with Poly-L-lysine solution (20 µg/ml) and incubated over night at 4°C. Before the assay, the inserts were washed three times with PBS and incubated with laminin (5 µg/ml) in PBS for 2 h at 37°C.

Preparation of dissociated granule cells

Primary granule cells were purified from mouse cerebella at postnatal day 5 as described (Wechsler-Reya and Scott, 1999). Cerebella were dissected into small pieces and incubated with papain (20U, Sigma, P3125) and DNaseI (10 mg/ml, Sigma) in PBS for 30 min at 37°C. Prior to the incubation, papain was activated with L-cysteine crystals at 37°C for 10 min. A buffer containing 1 mg/ml BSA, 0.5 units/ml Trypsin Inhibitor, and 10 mg/ml DNaseI in PBS ("ovo solution") were added to the papain tube, and tissue was triturated using Pasteur pipettes of decreasing bore size to obtain a single-cell suspension. The cells were triturated by gently pipetting up and down 5 times. The tissue pieces were let to deposit for 1 minute and the topmost 1 ml of cell suspension were transferred to the "cells tube". Then, 1 ml ovo solution was added to the papain tube and the cells were again triturated with a Pasteur pipet. This procedure was repeated two more times. The cell suspension was further triturated with a P1000 pipet and then for the final trituration with a P200 pipet. The cell suspension was passed through a cell strainer to remove debris and

then centrifuged for 10 min at RT at 1000 rpm in a table top centrifuge. Next, the cells were resuspended in Neurobasal media supplemented with sodium pyruvate (1x), L-glutamine (2 mM), and penicillin/streptomycin, N-acetyl cysteine (60 μg/ml), and B27 supplement (1x, Invitrogen) at a concentration of 1x 10^6 cells/ml and used for the Transwell migration assay.

Transwell migration assay

To investigate the *in vitro* migration of granule cells, Poly-L-lysine and laminin coated transwell inserts with a membrane of 3 μm pore size (Greiner) in a 24-well plate were used. Lower chambers were filled with 500 μl culture supernatant containing secreted Sema4C-AP, Sema4D-AP, or Sema4G-AP in DMEM or SDF1-alpha (100 ng/ml, PeproTech) or BDNF (100 ng/ml, PeproTech) as positive controls. As controls media alone or media conditioned by EGFP transfected cells were used. 0.25 x 10^6 granule cells in 250 μl of Neurobasal media supplemented with sodium pyruvate, B27, and N-acetyl cysteine were added to the upper chambers. To control the growth of the granule cells, cells were also plated on wells without insert. Plates were incubated over night at 37°C in 5% CO_2 for 22 h, to allow sufficient time for the migration of cells.

After over night incubation, cells on the upper surface of the membrane were scraped off with cotton swabs, and the granule cells that had migrated to the lower surface of the membrane were fixed with 4% PFA in PBS for 10 min. The cells were washed with 0.1% PBT and stained with DAPI (0.1 μg/ml) for 20 min. Five representative photomicrographs were taken at high magnification of each membrane and the cells were counted. Experiments were repeated at least five times under each condition.

5.2.8 Cerebellar EGL Explants

Preparing and coating of cover slips

Round cover slips of 15 mm diameter were treated with 65% nitric acid for 24 h and washed extensively with water (> 2 days). After drying on filter paper, the cover slips were baked at 175°C. The cover slips were coated in 4-well plates with Poly-L-lysine solution (20 µg/ml) by over night incubation at 4°C, washed twice with water, and dried for 1 h in a cell culture hood. On the experimental day, the cover slips were coated with laminin (5 µg/ml) in PBS for 1 hour at 37°C and washed with PBS 2x. In some cases, the cover slips were also coated with different Sema-AP supernatants over night at 37°C.

Preparing EGL Explants

After decapitation of P5 mice, cerebellum was dissected out and freed from meninges in cold 0.5 mg/ml glucose in PBS. Cerebellar parasagittal slices (300 µm thick) were cut with a tissue chopper and separated by needles. Under a dissection microscope, EGL explants were cut with needles (approximately 300 µm x 300 µm) and explants were cultured on coated cover slips in 4-well plates in 200 µl of Neurobasal media containing N2 Supplement (Invitrogen) and BSA. Explants were incubated at 37°C and 5% CO_2 for 48 h and then fixed with 4% PFA/0.33 M sucrose in PBS for 20 min.

Staining of explants

After fixation, explants were washed twice with PBS and blocked in blocking buffer (TBST containing 3% normal serum) for 30 min. Then, the explants were stained with Rhodamin-coupled Phalloidin (1:40 in TBST, Invitrogen), which is a fungal protein with high binding affinity to filamentous actin, for 30 min at 4°C. To visualize cell nuclei, explants were then washed and stained with DAPI (0.1 µg/ml).

Migration and outgrowth analysis

Quantitative analysis of neuronal migration was performed with ImageJ software. To measure the migration of the granule cells, concentric areas of 100 µm width were defined around the explant. The number of DAPI stained pixels in each area was counted. To normalize the values of migration rates, 100% migration rate was defined as the pixel value of the class of explants with the highest pixel values, which were wild type explants on Sema4C substrate. To calculate the migration rates of other explant types, their pixel values were related to this value.

5.2.9 Mouse husbandry

Mice were bred at the Helmholtz Zentrum Munich in accordance with national and institutional guidelines. Mice were group housed with maximal five animals per cage, and were kept in open cages at a light/dark cycle of 12 hours. Food and water were provided *ad libitum*. For breeding one male was paired with one or two females, and pups were weaned at 21 days of age. Mice were then seperated according to their gender and received earmarks for identification. Genomic DNA was extracted from tail clips.

The Plexin-B2, Sema4C, and Sema4G knock-out mutants that were used for experimental studies on C57BL/6 background had been backcrossed for at least 5 generations to C57BL/6N wild type mice (Charles River, Germany). The Plexin-B2 EUCOMM mutation was maintained as coisogenic line by backcrossing to C57BL/6N wild type mice. For mutant analysis on mixed CD-1 outbred background, mice were outcrossed to CD-1 mice (Charles River, Germany).

6. LITERATURE

Adams, R.H., Betz, H., and Puschel, A.W. (1996). A novel class of murine semaphorins with homology to thrombospondin is differentially expressed during early embryogenesis. Mech Dev *57*, 33-45.

Adams, R.H., Lohrum, M., Klostermann, A., Betz, H., and Puschel, A.W. (1997). The chemorepulsive activity of secreted semaphorins is regulated by furin-dependent proteolytic processing. EMBO J *16*, 6077-6086.

Apps, R., and Garwicz, M. (2005). Anatomical and physiological foundations of cerebellar information processing. Nat Rev Neurosci *6*, 297-311.

Argast, G.M., Croy, C.H., Couts, K.L., Zhang, Z., Litman, E., Chan, D.C., and Ahn, N.G. (2009). Plexin B1 is repressed by oncogenic B-Raf signaling and functions as a tumor suppressor in melanoma cells. Oncogene *28*, 2697-2709.

Artigiani, S., Conrotto, P., Fazzari, P., Gilestro, G.F., Barberis, D., Giordano, S., Comoglio, P.M., and Tamagnone, L. (2004). Plexin-B3 is a functional receptor for semaphorin 5A. EMBO Rep *5*, 710-714.

Bagnard, D., Lohrum, M., Uziel, D., Puschel, A.W., and Bolz, J. (1998). Semaphorins act as attractive and repulsive guidance signals during the development of cortical projections. Development *125*, 5043-5053.

Barsh, G.S. (1996). The genetics of pigmentation: from fancy genes to complex traits. Trends Genet *12*, 299-305.

Basile, J.R., Castilho, R.M., Williams, V.P., and Gutkind, J.S. (2006). Semaphorin 4D provides a link between axon guidance processes and tumor-induced angiogenesis. Proc Natl Acad Sci U S A *103*, 9017-9022.

Basile, J.R., Gavard, J., and Gutkind, J.S. (2007). Plexin-B1 utilizes RhoA and Rho kinase to promote the integrin-dependent activation of Akt and ERK and endothelial cell motility. The Journal of biological chemistry *282*, 34888-34895.

Baxter, L.L., Hou, L., Loftus, S.K., and Pavan, W.J. (2004). Spotlight on spotted mice: a review of white spotting mouse mutants and associated human pigmentation disorders. Pigment Cell Res *17*, 215-224.

Behar, O., Golden, J.A., Mashimo, H., Schoen, F.J., and Fishman, M.C. (1996). Semaphorin III is needed for normal patterning and growth of nerves, bones and heart. Nature *383*, 525-528.

Belvindrah, R., Nalbant, P., Ding, S., Wu, C., Bokoch, G.M., and Muller, U. (2006). Integrin-linked kinase regulates Bergmann glial differentiation during cerebellar development. Molecular and cellular neurosciences *33*, 109-125.

Bielenberg, D.R., Hida, Y., Shimizu, A., Kaipainen, A., Kreuter, M., Kim, C.C., and Klagsbrun, M. (2004). Semaphorin 3F, a chemorepulsant for endothelial cells, induces a poorly vascularized, encapsulated, nonmetastatic tumor phenotype. J Clin Invest *114*, 1260-1271.

Bilovocky, N.A., Romito-DiGiacomo, R.R., Murcia, C.L., Maricich, S.M., and Herrup, K. (2003). Factors in the genetic background suppress the engrailed-1 cerebellar phenotype. J Neurosci *23*, 5105-5112.

Blaess, S., Graus-Porta, D., Belvindrah, R., Radakovits, R., Pons, S., Littlewood-Evans, A., Senften, M., Guo, H., Li, Y., Miner, J.H.*, et al.* (2004). Beta1-integrins are critical for cerebellar granule cell precursor proliferation. J Neurosci *24*, 3402-3412.

Borghesani, P.R., Peyrin, J.M., Klein, R., Rubin, J., Carter, A.R., Schwartz, P.M., Luster, A., Corfas, G., and Segal, R.A. (2002). BDNF stimulates migration of cerebellar granule cells. Development *129*, 1435-1442.

Bougeret, C., Mansur, I.G., Dastot, H., Schmid, M., Mahouy, G., Bensussan, A., and Boumsell, L. (1992). Increased surface expression of a newly identified 150-kDa dimer early after human T lymphocyte activation. J Immunol *148*, 318-323.

Cajal, S.R.Y. (1911). Histologie Système Nerveux de l`Homme et des Vertébrés. A. Maloine.

Castro-Rivera, E., Ran, S., Thorpe, P., and Minna, J.D. (2004). Semaphorin 3B (SEMA3B) induces apoptosis in lung and breast cancer, whereas VEGF165 antagonizes this effect. Proc Natl Acad Sci U S A *101*, 11432-11437.

Chedotal, A. (2010). Should I stay or should I go? Becoming a granule cell. Trends in neurosciences *33*, 163-172.

Committee, S.N. (1999). Unified nomenclature for the semaphorins/collapsins. Semaphorin Nomenclature Committee. Cell *97*, 551-552.

Conrotto, P., Valdembri, D., Corso, S., Serini, G., Tamagnone, L., Comoglio, P.M., Bussolino, F., and Giordano, S. (2005). Sema4D induces angiogenesis through Met recruitment by Plexin B1. Blood *105*, 4321-4329.

D'Apuzzo, M., Rolink, A., Loetscher, M., Hoxie, J.A., Clark-Lewis, I., Melchers, F., Baggiolini, M., and Moser, B. (1997). The chemokine SDF-1, stromal cell-derived factor 1, attracts early stage B cell precursors via the chemokine receptor CXCR4. Eur J Immunol *27*, 1788-1793.

Delaire, S., Billard, C., Tordjman, R., Chedotal, A., Elhabazi, A., Bensussan, A., and Boumsell, L. (2001). Biological activity of soluble CD100. II. Soluble CD100, similarly to H-SemaIII, inhibits immune cell migration. J Immunol *166*, 4348-4354.

Delaire, S., Elhabazi, A., Bensussan, A., and Boumsell, L. (1998). CD100 is a leukocyte semaphorin. Cell Mol Life Sci *54*, 1265-1276.

Deng, S., Hirschberg, A., Worzfeld, T., Penachioni, J.Y., Korostylev, A., Swiercz, J.M., Vodrazka, P., Mauti, O., Stoeckli, E.T., Tamagnone, L.*, et al.* (2007). Plexin-B2, but not

Plexin-B1, critically modulates neuronal migration and patterning of the developing nervous system in vivo. J Neurosci *27*, 6333-6347.

Ding, S., Luo, J.H., and Yuan, X.B. (2007). Semaphorin-3F attracts the growth cone of cerebellar granule cells through cGMP signaling pathway. Biochem Biophys Res Commun *356*, 857-863.

Dolan, J., Walshe, K., Alsbury, S., Hokamp, K., O'Keeffe, S., Okafuji, T., Miller, S.F., Tear, G., and Mitchell, K.J. (2007). The extracellular leucine-rich repeat superfamily; a comparative survey and analysis of evolutionary relationships and expression patterns. BMC Genomics *8*, 320.

Elhabazi, A., Delaire, S., Bensussan, A., Boumsell, L., and Bismuth, G. (2001). Biological activity of soluble CD100. I. The extracellular region of CD100 is released from the surface of T lymphocytes by regulated proteolysis. J Immunol *166*, 4341-4347.

Epstein, D.J., Vekemans, M., and Gros, P. (1991). Splotch (Sp2H), a mutation affecting development of the mouse neural tube, shows a deletion within the paired homeodomain of Pax-3. Cell *67*, 767-774.

Fazzari, P., Penachioni, J., Gianola, S., Rossi, F., Eickholt, B.J., Maina, F., Alexopoulou, L., Sottile, A., Comoglio, P.M., Flavell, R.A., and Tamagnone, L. (2007). Plexin-B1 plays a redundant role during mouse development and in tumour angiogenesis. BMC Dev Biol *7*, 55.

Feiner, L., Webber, A.L., Brown, C.B., Lu, M.M., Jia, L., Feinstein, P., Mombaerts, P., Epstein, J.A., and Raper, J.A. (2001). Targeted disruption of semaphorin 3C leads to persistent truncus arteriosus and aortic arch interruption. Development *128*, 3061-3070.

Flanagan, J.G., Cheng, H.J., Feldheim, D.A., Hattori, M., Lu, Q., and Vanderhaeghen, P. (2000). Alkaline phosphatase fusions of ligands or receptors as in situ probes for staining of cells, tissues, and embryos. Methods in enzymology *327*, 19-35.

Friedel, R.H., Kerjan, G., Rayburn, H., Schuller, U., Sotelo, C., Tessier-Lavigne, M., and Chedotal, A. (2007). Plexin-B2 controls the development of cerebellar granule cells. J Neurosci *27*, 3921-3932.

Friedel, R.H., Plump, A., Lu, X., Spilker, K., Jolicoeur, C., Wong, K., Venkatesh, T.R., Yaron, A., Hynes, M., Chen, B.*, et al.* (2005). Gene targeting using a promoterless gene trap vector ("targeted trapping") is an efficient method to mutate a large fraction of genes. Proc Natl Acad Sci U S A *102*, 13188-13193.

Fujioka, S., Masuda, K., Toguchi, M., Ohoka, Y., Sakai, T., Furuyama, T., and Inagaki, S. (2003). Neurotrophic effect of Semaphorin 4D in PC12 cells. Biochem Biophys Res Commun *301*, 304-310.

Gherardi, E., Love, C.A., Esnouf, R.M., and Jones, E.Y. (2004). The sema domain. Curr Opin Struct Biol *14*, 669-678.

Giacobini, P., Messina, A., Morello, F., Ferraris, N., Corso, S., Penachioni, J., Giordano, S., Tamagnone, L., and Fasolo, A. (2008). Semaphorin 4D regulates gonadotropin

hormone-releasing hormone-1 neuronal migration through PlexinB1-Met complex. J Cell Biol *183*, 555-566.

Giordano, S., Corso, S., Conrotto, P., Artigiani, S., Gilestro, G., Barberis, D., Tamagnone, L., and Comoglio, P.M. (2002). The semaphorin 4D receptor controls invasive growth by coupling with Met. Nature cell biology *4*, 720-724.

Goldowitz, D., and Hamre, K. (1998). The cells and molecules that make a cerebellum. Trends Neurosci *21*, 375-382.

Gómez Román, J.J., Garay, G.O., Saenz, P., Escuredo, K., Sanz Ibayondo, C., Gutkind, S., Junquera, C., Simon, L., Martinez, A., Fernandez Luna, J.L., and Val-Bernal, J.F. (2008). Plexin B1 is downregulated in renal cell carcinomas and modulates cell growth. Transl Res *151*, 134-140.

Gu, C., Yoshida, Y., Livet, J., Reimert, D.V., Mann, F., Merte, J., Henderson, C.E., Jessell, T.M., Kolodkin, A.L., and Ginty, D.D. (2005). Semaphorin 3E and plexin-D1 control vascular pattern independently of neuropilins. Science *307*, 265-268.

Hall, K.T., Boumsell, L., Schultze, J.L., Boussiotis, V.A., Dorfman, D.M., Cardoso, A.A., Bensussan, A., Nadler, L.M., and Freeman, G.J. (1996). Human CD100, a novel leukocyte semaphorin that promotes B-cell aggregation and differentiation. Proc Natl Acad Sci U S A *93*, 11780-11785.

Hartwig, C., Veske, A., Krejcova, S., Rosenberger, G., and Finckh, U. (2005). Plexin B3 promotes neurite outgrowth, interacts homophilically, and interacts with Rin. BMC Neurosci *6*, 53.

Hatten, M.E., and Heintz, N. (1995). Mechanisms of neural patterning and specification in the developing cerebellum. Annu Rev Neurosci *18*, 385-408.

Hatten, M.E., and Mason, C.A. (1990). Mechanisms of glial-guided neuronal migration in vitro and in vivo. Experientia *46*, 907-916.

Hemming, M.L., Elias, J.E., Gygi, S.P., and Selkoe, D.J. (2009). Identification of beta-secretase (BACE1) substrates using quantitative proteomics. PloS one *4*, e8477.

Hirotani, M., Ohoka, Y., Yamamoto, T., Nirasawa, H., Furuyama, T., Kogo, M., Matsuya, T., and Inagaki, S. (2002). Interaction of plexin-B1 with PDZ domain-containing Rho guanine nucleotide exchange factors. Biochem Biophys Res Commun *297*, 32-37.

Hirschberg, A., Deng, S., Korostylev, A., Paldy, E., Costa, M.R., Worzfeld, T., Vodrazka, P., Wizenmann, A., Gotz, M., Offermanns, S., and Kuner, R. (2010). Gene deletion mutants reveal a role for semaphorin receptors of the plexin-B family in mechanisms underlying corticogenesis. Molecular and cellular biology *30*, 764-780.

Hoshino, M., Nakamura, S., Mori, K., Kawauchi, T., Terao, M., Nishimura, Y.V., Fukuda, A., Fuse, T., Matsuo, N., Sone, M.*, et al.* (2005). Ptf1a, a bHLH transcriptional gene, defines GABAergic neuronal fates in cerebellum. Neuron *47*, 201-213.

Huang, C.M., Wang, L., and Huang, R.H. (2006). Cerebellar granule cell: ascending axon and parallel fiber. Eur J Neurosci *23*, 1731-1737.

Huber, A.B., Kania, A., Tran, T.S., Gu, C., De Marco Garcia, N., Lieberam, I., Johnson, D., Jessell, T.M., Ginty, D.D., and Kolodkin, A.L. (2005). Distinct roles for secreted semaphorin signaling in spinal motor axon guidance. Neuron *48*, 949-964.

Inagaki, S., Furuyama, T., and Iwahashi, Y. (1995). Identification of a member of mouse semaphorin family. FEBS Lett *370*, 269-272.

Inagaki, S., Ohoka, Y., Sugimoto, H., Fujioka, S., Amazaki, M., Kurinami, H., Miyazaki, N., Tohyama, M., and Furuyama, T. (2001). Sema4c, a transmembrane semaphorin, interacts with a post-synaptic density protein, PSD-95. J Biol Chem *276*, 9174-9181.

Janssen, B.J., Robinson, R.A., Perez-Branguli, F., Bell, C.H., Mitchell, K.J., Siebold, C., and Jones, E.Y. (2010). Structural basis of semaphorin-plexin signalling. Nature *467*, 1118-1122.

Juriloff, D.M., and Harris, M.J. (2000). Mouse models for neural tube closure defects. Hum Mol Genet *9*, 993-1000.

Kahle, W., Leonhardt, H., and Platzer, W. (1993). Nervous System and Sensory Organs. Thieme; Color Atlas and Textbook of Human Anatomy *3*.

Kantor, D.B., Chivatakarn, O., Peer, K.L., Oster, S.F., Inatani, M., Hansen, M.J., Flanagan, J.G., Yamaguchi, Y., Sretavan, D.W., Giger, R.J., and Kolodkin, A.L. (2004). Semaphorin 5A is a bifunctional axon guidance cue regulated by heparan and chondroitin sulfate proteoglycans. Neuron *44*, 961-975.

Kawaji, K., Umeshima, H., Eiraku, M., Hirano, T., and Kengaku, M. (2004). Dual phases of migration of cerebellar granule cells guided by axonal and dendritic leading processes. Mol Cell Neurosci *25*, 228-240.

Kawasaki, H., Nakayama, S., and Kretsinger, R.H. (1998). Classification and evolution of EF-hand proteins. Biometals *11*, 277-295.

Kerjan, G., Dolan, J., Haumaitre, C., Schneider-Maunoury, S., Fujisawa, H., Mitchell, K.J., and Chedotal, A. (2005). The transmembrane semaphorin Sema6A controls cerebellar granule cell migration. Nature neuroscience *8*, 1516-1524.

Kigel, B., Varshavsky, A., Kessler, O., and Neufeld, G. (2008). Successful inhibition of tumor development by specific class-3 semaphorins is associated with expression of appropriate semaphorin receptors by tumor cells. PLoS One *3*, e3287.

Kitsukawa, T., Shimizu, M., Sanbo, M., Hirata, T., Taniguchi, M., Bekku, Y., Yagi, T., and Fujisawa, H. (1997). Neuropilin-semaphorin III/D-mediated chemorepulsive signals play a crucial role in peripheral nerve projection in mice. Neuron *19*, 995-1005.

Ko, J.A., Gondo, T., Inagaki, S., and Inui, M. (2005). Requirement of the transmembrane semaphorin Sema4C for myogenic differentiation. FEBS Lett *579*, 2236-2242.

Kolodkin, A.L., and Ginty, D.D. (1997). Steering clear of semaphorins: neuropilins sound the retreat. Neuron *19*, 1159-1162.

Kolodkin, A.L., Matthes, D.J., and Goodman, C.S. (1993). The semaphorin genes encode a family of transmembrane and secreted growth cone guidance molecules. Cell *75*, 1389-1399.

Komuro, H., and Yacubova, E. (2003). Recent advances in cerebellar granule cell migration. Cell Mol Life Sci *60*, 1084-1098.

Komuro, H., Yacubova, E., and Rakic, P. (2001). Mode and tempo of tangential cell migration in the cerebellar external granular layer. J Neurosci *21*, 527-540.

Korostylev, A., Worzfeld, T., Deng, S., Friedel, R.H., Swiercz, J.M., Vodrazka, P., Maier, V., Hirschberg, A., Ohoka, Y., Inagaki, S.*, et al.* (2008). A functional role for semaphorin 4D/plexin B1 interactions in epithelial branching morphogenesis during organogenesis. Development *135*, 3333-3343.

Kruger, R.P., Aurandt, J., and Guan, K.L. (2005). Semaphorins command cells to move. Nat Rev Mol Cell Biol *6*, 789-800.

Kumanogoh, A., Marukawa, S., Suzuki, K., Takegahara, N., Watanabe, C., Ch'ng, E., Ishida, I., Fujimura, H., Sakoda, S., Yoshida, K., and Kikutani, H. (2002). Class IV semaphorin Sema4A enhances T-cell activation and interacts with Tim-2. Nature *419*, 629-633.

Kumanogoh, A., Watanabe, C., Lee, I., Wang, X., Shi, W., Araki, H., Hirata, H., Iwahori, K., Uchida, J., Yasui, T.*, et al.* (2000). Identification of CD72 as a lymphocyte receptor for the class IV semaphorin CD100: a novel mechanism for regulating B cell signaling. Immunity *13*, 621-631.

Laemmli, U.K. (1970). Cleavage of structural proteins during the assembly of the head of bacteriophage T4. Nature *227*, 680-685.

Lau, A.O., Sacci, J.B., Jr., and Azad, A.F. (2001). Host responses to Plasmodium yoelii hepatic stages: a paradigm in host-parasite interaction. J Immunol *166*, 1945-1950.

Leighton, P.A., Mitchell, K.J., Goodrich, L.V., Lu, X., Pinson, K., Scherz, P., Skarnes, W.C., and Tessier-Lavigne, M. (2001). Defining brain wiring patterns and mechanisms through gene trapping in mice. Nature *410*, 174-179.

Li, H., Wu, D.K., and Sullivan, S.L. (1999). Characterization and expression of sema4g, a novel member of the semaphorin gene family. Mech Dev *87*, 169-173.

Liesi, P., Dahl, D., and Vaheri, A. (1983). Laminin is produced by early rat astrocytes in primary culture. J Cell Biol *96*, 920-924.

Lin, Y., Chen, L., Lin, C., Luo, Y., Tsai, R.Y., and Wang, F. (2009). Neuron-derived FGF9 is essential for scaffold formation of Bergmann radial fibers and migration of granule neurons in the cerebellum. Developmental biology *329*, 44-54.

Lindsay, R.M. (1988). Nerve growth factors (NGF, BDNF) enhance axonal regeneration but are not required for survival of adult sensory neurons. J Neurosci *8*, 2394-2405.

Liu, B.P., and Strittmatter, S.M. (2001). Semaphorin-mediated axonal guidance via Rho-related G proteins. Curr Opin Cell Biol *13*, 619-626.

Liu, H., Juo, Z.S., Shim, A.H., Focia, P.J., Chen, X., Garcia, K.C., and He, X. (2010). Structural basis of semaphorin-plexin recognition and viral mimicry from Sema7A and A39R complexes with PlexinC1. Cell *142*, 749-761.

Luo, Y., Raible, D., and Raper, J.A. (1993). Collapsin: a protein in brain that induces the collapse and paralysis of neuronal growth cones. Cell *75*, 217-227.

Ma, Q., Jones, D., Borghesani, P.R., Segal, R.A., Nagasawa, T., Kishimoto, T., Bronson, R.T., and Springer, T.A. (1998). Impaired B-lymphopoiesis, myelopoiesis, and derailed cerebellar neuron migration in CXCR4- and SDF-1-deficient mice. Proc Natl Acad Sci U S A *95*, 9448-9453.

Marie, Y., Sanson, M., Mokhtari, K., Leuraud, P., Kujas, M., Delattre, J.Y., Poirier, J., Zalc, B., and Hoang-Xuan, K. (2001). OLIG2 as a specific marker of oligodendroglial tumour cells. Lancet *358*, 298-300.

Masuda, K., Furuyama, T., Takahara, M., Fujioka, S., Kurinami, H., and Inagaki, S. (2004). Sema4D stimulates axonal outgrowth of embryonic DRG sensory neurones. Genes Cells *9*, 821-829.

Millen, K.J., and Gleeson, J.G. (2008). Cerebellar development and disease. Curr Opin Neurobiol *18*, 12-19.

Mills, J., Niewmierzycka, A., Oloumi, A., Rico, B., St-Arnaud, R., Mackenzie, I.R., Mawji, N.M., Wilson, J., Reichardt, L.F., and Dedhar, S. (2006). Critical role of integrin-linked kinase in granule cell precursor proliferation and cerebellar development. J Neurosci *26*, 830-840.

Moreau-Fauvarque, C., Kumanogoh, A., Camand, E., Jaillard, C., Barbin, G., Boquet, I., Love, C., Jones, E.Y., Kikutani, H., Lubetzki, C.*, et al.* (2003). The transmembrane semaphorin Sema4D/CD100, an inhibitor of axonal growth, is expressed on oligodendrocytes and upregulated after CNS lesion. J Neurosci *23*, 9229-9239.

Nagata, I., and Nakatsuji, N. (1990). Granule cell behavior on laminin in cerebellar microexplant cultures. Brain Res Dev Brain Res *52*, 63-73.

Nakamura, F., Kalb, R.G., and Strittmatter, S.M. (2000). Molecular basis of semaphorin-mediated axon guidance. J Neurobiol *44*, 219-229.

Necchi, D., and Scherini, E. (2002). The malformation of the cerebellar fissura prima: a tool for studying histogenetic processes. Cerebellum *1*, 137-142.

Neufeld, G., Shraga-Heled, N., Lange, T., Guttmann-Raviv, N., Herzog, Y., and Kessler, O. (2005). Semaphorins in cancer. Front Biosci *10*, 751-760.

Nogi, T., Yasui, N., Mihara, E., Matsunaga, Y., Noda, M., Yamashita, N., Toyofuku, T., Uchiyama, S., Goshima, Y., Kumanogoh, A., and Takagi, J. (2010). Structural basis for semaphorin signalling through the plexin receptor. Nature *467*, 1123-1127.

Ohoka, Y., Hirotani, M., Sugimoto, H., Fujioka, S., Furuyama, T., and Inagaki, S. (2001). Semaphorin 4C, a transmembrane semaphorin, [corrected] associates with a neurite-outgrowth-related protein, SFAP75. Biochem Biophys Res Commun *280*, 237-243.

Ohta, K., Mizutani, A., Kawakami, A., Murakami, Y., Kasuya, Y., Takagi, S., Tanaka, H., and Fujisawa, H. (1995). Plexin: a novel neuronal cell surface molecule that mediates cell adhesion via a homophilic binding mechanism in the presence of calcium ions. Neuron *14*, 1189-1199.

Oinuma, I., Katoh, H., and Negishi, M. (2006). Semaphorin 4D/Plexin-B1-mediated R-Ras GAP activity inhibits cell migration by regulating beta(1) integrin activity. J Cell Biol *173*, 601-613.

Osawa, M. (2008). Melanocyte stem cells.

Pasterkamp, R.J., Peschon, J.J., Spriggs, M.K., and Kolodkin, A.L. (2003). Semaphorin 7A promotes axon outgrowth through integrins and MAPKs. Nature *424*, 398-405.

Perälä, N., Jakobson, M., Ola, R., Fazzari, P., Penachioni, J.Y., Nymark, M., Tanninen, T., Immonen, T., Tamagnone, L., and Sariola, H. (2010). Sema4C-Plexin B2 signalling modulates ureteric branching in developing kidney. Differentiation.

Perälä, N.M., Immonen, T., and Sariola, H. (2005). The expression of plexins during mouse embryogenesis. Gene Expr Patterns *5*, 355-362.

Pingault, V., Bondurand, N., Kuhlbrodt, K., Goerich, D.E., Prehu, M.O., Puliti, A., Herbarth, B., Hermans-Borgmeyer, I., Legius, E., Matthijs, G.*, et al.* (1998). SOX10 mutations in patients with Waardenburg-Hirschsprung disease. Nat Genet *18*, 171-173.

Plachez, C., and Richards, L.J. (2005). Mechanisms of axon guidance in the developing nervous system. Curr Top Dev Biol *69*, 267-346.

Potterf, S.B., Furumura, M., Dunn, K.J., Arnheiter, H., and Pavan, W.J. (2000). Transcription factor hierarchy in Waardenburg syndrome: regulation of MITF expression by SOX10 and PAX3. Hum Genet *107*, 1-6.

Potterf, S.B., Mollaaghababa, R., Hou, L., Southard-Smith, E.M., Hornyak, T.J., Arnheiter, H., and Pavan, W.J. (2001). Analysis of SOX10 function in neural crest-derived melanocyte development: SOX10-dependent transcriptional control of dopachrome tautomerase. Dev Biol *237*, 245-257.

Rakic, P., Cameron, R.S., and Komuro, H. (1994). Recognition, adhesion, transmembrane signaling and cell motility in guided neuronal migration. Curr Opin Neurobiol *4*, 63-69.

Reidy, K.J., Villegas, G., Teichman, J., Veron, D., Shen, W., Jimenez, J., Thomas, D., and Tufro, A. (2009). Semaphorin3a regulates endothelial cell number and podocyte differentiation during glomerular development. Development *136*, 3979-3989.

Renaud, J., Kerjan, G., Sumita, I., Zagar, Y., Georget, V., Kim, D., Fouquet, C., Suda, K., Sanbo, M., Suto, F.*, et al.* (2008). Plexin-A2 and its ligand, Sema6A, control nucleus-centrosome coupling in migrating granule cells. Nature neuroscience *11*, 440-449.

Rody, A., Holtrich, U., Gaetje, R., Gehrmann, M., Engels, K., von Minckwitz, G., Loibl, S., Diallo-Danebrock, R., Ruckhaberle, E., Metzler, D.*, et al.* (2007). Poor outcome in estrogen receptor-positive breast cancers predicted by loss of plexin B1. Clin Cancer Res *13*, 1115-1122.

Saito, Y., Oinuma, I., Fujimoto, S., and Negishi, M. (2009). Plexin-B1 is a GTPase activating protein for M-Ras, remodelling dendrite morphology. EMBO Rep *10*, 614-621.

Sambrook, J., Fritsch, E.F., Maniatis, T. (1989). Molecular Cloning: A Laboratory Manual. Cold Spring Harbor Lab. Press, Plainview, NY, 2nd Ed.

Schmahmann, J.D., Rosene, D.L., and Pandya, D.N. (2004). Ataxia after pontine stroke: insights from pontocerebellar fibers in monkey. Ann Neurol *55*, 585-589.

Sgaier, S.K., Lao, Z., Villanueva, M.P., Berenshteyn, F., Stephen, D., Turnbull, R.K., and Joyner, A.L. (2007). Genetic subdivision of the tectum and cerebellum into functionally related regions based on differential sensitivity to engrailed proteins. Development *134*, 2325-2335.

Shifman, M.I., and Selzer, M.E. (2006). Semaphorins and their receptors in lamprey CNS: Cloning, phylogenetic analysis, and developmental changes during metamorphosis. J Comp Neurol *497*, 115-132.

Sillitoe, R.V., and Joyner, A.L. (2007). Morphology, molecular codes, and circuitry produce the three-dimensional complexity of the cerebellum. Annu Rev Cell Dev Biol *23*, 549-577.

Skarnes, W.C., Moss, J.E., Hurtley, S.M., and Beddington, R.S. (1995). Capturing genes encoding membrane and secreted proteins important for mouse development. Proc Natl Acad Sci U S A *92*, 6592-6596.

Song, H., and Poo, M. (2001). The cell biology of neuronal navigation. Nat Cell Biol *3*, E81-88.

Suzuki, K., Kumanogoh, A., and Kikutani, H. (2008). Semaphorins and their receptors in immune cell interactions. Nat Immunol *9*, 17-23.

Suzuki, K., Okuno, T., Yamamoto, M., Pasterkamp, R.J., Takegahara, N., Takamatsu, H., Kitao, T., Takagi, J., Rennert, P.D., Kolodkin, A.L.*, et al.* (2007). Semaphorin 7A initiates T-cell-mediated inflammatory responses through alpha1beta1 integrin. Nature *446*, 680-684.

Swiercz, J.M., Worzfeld, T., and Offermanns, S. (2008). ErbB-2 and met reciprocally regulate cellular signaling via plexin-B1. The Journal of biological chemistry *283*, 1893-1901.

Tamagnone, L., Artigiani, S., Chen, H., He, Z., Ming, G.I., Song, H., Chedotal, A., Winberg, M.L., Goodman, C.S., Poo, M.*, et al.* (1999). Plexins are a large family of receptors for transmembrane, secreted, and GPI-anchored semaphorins in vertebrates. Cell *99*, 71-80.

Tanaka, M., and Marunouchi, T. (2005). Abnormality in the cerebellar folial pattern of C57BL/6J mice. Neurosci Lett *390*, 182-186.

Taniguchi, M., Yuasa, S., Fujisawa, H., Naruse, I., Saga, S., Mishina, M., and Yagi, T. (1997). Disruption of semaphorin III/D gene causes severe abnormality in peripheral nerve projection. Neuron *19*, 519-530.

Tomizawa, Y., Sekido, Y., Kondo, M., Gao, B., Yokota, J., Roche, J., Drabkin, H., Lerman, M.I., Gazdar, A.F., and Minna, J.D. (2001). Inhibition of lung cancer cell growth and induction of apoptosis after reexpression of 3p21.3 candidate tumor suppressor gene SEMA3B. Proc Natl Acad Sci U S A *98*, 13954-13959.

Tong, Y., and Buck, M. (2005). 1H, 15N and 13C Resonance assignments and secondary structure determination reveal that the minimal Rac1 GTPase binding domain of plexin-B1 has a ubiquitin fold. J Biomol NMR *31*, 369-370.

Toyofuku, T., Zhang, H., Kumanogoh, A., Takegahara, N., Suto, F., Kamei, J., Aoki, K., Yabuki, M., Hori, M., Fujisawa, H., and Kikutani, H. (2004a). Dual roles of Sema6D in cardiac morphogenesis through region-specific association of its receptor, Plexin-A1, with off-track and vascular endothelial growth factor receptor type 2. Genes Dev *18*, 435-447.

Toyofuku, T., Zhang, H., Kumanogoh, A., Takegahara, N., Yabuki, M., Harada, K., Hori, M., and Kikutani, H. (2004b). Guidance of myocardial patterning in cardiac development by Sema6D reverse signalling. Nat Cell Biol *6*, 1204-1211.

Tse, C., Xiang, R.H., Bracht, T., and Naylor, S.L. (2002). Human Semaphorin 3B (SEMA3B) located at chromosome 3p21.3 suppresses tumor formation in an adenocarcinoma cell line. Cancer Res *62*, 542-546.

Van Eldik, L.J., Ehrenfried, B., and Jensen, R.A. (1984). Production and characterization of monoclonal antibodies with specificity for the S100 beta polypeptide of brain S100 fractions. Proc Natl Acad Sci U S A *81*, 6034-6038.

Vodrazka, P., Korostylev, A., Hirschberg, A., Swiercz, J.M., Worzfeld, T., Deng, S., Fazzari, P., Tamagnone, L., Offermanns, S., and Kuner, R. (2009). The semaphorin 4D-plexin-B signalling complex regulates dendritic and axonal complexity in developing neurons via diverse pathways. Eur J Neurosci *30*, 1193-1208.

Walther, C., Guenet, J.L., Simon, D., Deutsch, U., Jostes, B., Goulding, M.D., Plachov, D., Balling, R., and Gruss, P. (1991). Pax: a murine multigene family of paired box-containing genes. Genomics *11*, 424-434.

Wang, X., Kumanogoh, A., Watanabe, C., Shi, W., Yoshida, K., and Kikutani, H. (2001). Functional soluble CD100/Sema4D released from activated lymphocytes: possible role in normal and pathologic immune responses. Blood *97*, 3498-3504.

Wechsler-Reya, R.J., and Scott, M.P. (1999). Control of neuronal precursor proliferation in the cerebellum by Sonic Hedgehog. Neuron *22*, 103-114.

Wong, O.G., Nitkunan, T., Oinuma, I., Zhou, C., Blanc, V., Brown, R.S., Bott, S.R., Nariculam, J., Box, G., Munson, P.*, et al.* (2007). Plexin-B1 mutations in prostate cancer. Proc Natl Acad Sci U S A *104*, 19040-19045.

Worzfeld, T., Puschel, A.W., Offermanns, S., and Kuner, R. (2004). Plexin-B family members demonstrate non-redundant expression patterns in the developing mouse nervous system: an anatomical basis for morphogenetic effects of Sema4D during development. Eur J Neurosci *19*, 2622-2632.

Worzfeld, T., Rauch, P., Karram, K., Trotter, J., Kuner, R., and Offermanns, S. (2009). Mice lacking Plexin-B3 display normal CNS morphology and behaviour. Mol Cell Neurosci *42*, 372-381.

Wu, H., Fan, J., Zhu, L., Liu, S., Wu, Y., Zhao, T., Wu, Y., Ding, X., Fan, W., and Fan, M. (2009a). Sema4C Expression in Neural Stem/Progenitor Cells and in Adult Neurogenesis Induced by Cerebral Ischemia. J Mol Neurosci.

Wu, H., Fan, J., Zhu, L., Liu, S., Wu, Y., Zhao, T., Wu, Y., Ding, X., Fan, W., and Fan, M. (2009b). Sema4C expression in neural stem/progenitor cells and in adult neurogenesis induced by cerebral ischemia. J Mol Neurosci *39*, 27-39.

Wu, H., Wang, X., Liu, S., Wu, Y., Zhao, T., Chen, X., Zhu, L., Wu, Y., Ding, X., Peng, X.*, et al.* (2007). Sema4C participates in myogenic differentiation in vivo and in vitro through the p38 MAPK pathway. Eur J Cell Biol *86*, 331-344.

Xiang, R.H., Hensel, C.H., Garcia, D.K., Carlson, H.C., Kok, K., Daly, M.C., Kerbacher, K., van den Berg, A., Veldhuis, P., Buys, C.H., and Naylor, S.L. (1996). Isolation of the human semaphorin III/F gene (SEMA3F) at chromosome 3p21, a region deleted in lung cancer. Genomics *32*, 39-48.

Yamada, K., and Watanabe, M. (2002). Cytodifferentiation of Bergmann glia and its relationship with Purkinje cells. Anat Sci Int *77*, 94-108.

Ye, S., Hao, X., Zhou, T., Wu, M., Wei, J., Wang, Y., Zhou, L., Jiang, X., Ji, L., Chen, Y.*, et al.* (2010). Plexin-B1 silencing inhibits ovarian cancer cell migration and invasion. BMC Cancer *10*, 611.

Zabarovsky, E.R., Lerman, M.I., and Minna, J.D. (2002). Tumor suppressor genes on chromosome 3p involved in the pathogenesis of lung and other cancers. Oncogene *21*, 6915-6935.

Zhang, Y., Andl, T., Yang, S.H., Teta, M., Liu, F., Seykora, J.T., Tobias, J.W., Piccolo, S., Schmidt-Ullrich, R., Nagy, A.*, et al.* (2008). Activation of beta-catenin signaling programs embryonic epidermis to hair follicle fate. Development *135*, 2161-2172.

Zhou, Y., Gunput, R.A., and Pasterkamp, R.J. (2008). Semaphorin signaling: progress made and promises ahead. Trends Biochem Sci *33*, 161-170.

7. APPENDIX

7.1 Abbreviation

A	purine base adenine
α	anti
AP	alkaline Phosphatase
ATP	adenosine triphosphate
BCIP	5-Bromo-4-Chloro-3-Indolylphosphate
Bis	Bis-hydroxymethyl-aminomethan
bp	base pair
BSA	bovine serum albumine
°C	degree Celsius
C	pyrimidine base cytosine
$CaCl_2$	calcium chloride
cDNA	copy Deoxyribonucleic Acid
CIP	Calf Intestinal Phosphatase
CO_2	Carbon dioxide
CNS	central nervous system
DAB	3,3'-diaminobenzidine
DIG	Digoxigenin
DMEM	Dulbecco's Modified Eagle's Medium
DNA	deoxyribonucleic acid
dNTP(s)	desoxyribonucleotide triphosphate
DPBS	Dulbecco's Phosphate Buffered Saline
E	embryonic day
E. coli	Escherichia coli
ECL	electrogenerated Chemiluminescence
EDTA	ethylendiamintetraacetate
EGFP	enhanced green fluorescent protein
EGL	external granule layer
EtOH	ethanol

FCS	fetal calf serum
g	gram
G	purinbase guanine
GFP	green fluorescent protein
h	hour(s)
HBS	HEPES Buffer Saline
HCl	Hydrogen Chloride
HEK	Human epithelial kidney
HEPES	4-(2-hydroxyethyl)-1-piperazineethanesulfonic acid
HRPO	Horseradish Peroxidase
IgG	Immunoglobulin G
IGL	internal granule layer
ISH	in situ hybridization
kb	kilo bases
kd	kilo dalton
l	liter
LB Medium	Luria-Bertani-Medium
MEM	Modified Eagle's Medium
MES	2-(N-morpholino)ethanesulfonic acid
M	molar (mol/l)
m	milli
$MgCl_2$	magnesium chloride
min	minute(s)
ML	molecular layer
mm	millimeter
mRNA	messenger ribonucleic acid
n	nano
n	sample size
NaCl	sodium chloride
neo	neomycin
NP-40	Nonidet P-40
p	p-value for statistical analysis
P	postnatal day
PBS	phosphate buffered saline
PCR	polymerase chain reaction

PFA	paraformaldehyde
RIPA	protein lysis buffer
RNA	ribonucleic acid
rpm	rounds per minute
RT	room temperature
SDS	sodium dodecyl sulfate
sec	second
SSC	sodium saline citrate
T	pyrimidine base thymine
TAE	tris acetate with EDTA
TBS	tris buffered saline
TE	tris-EDTA
Tris	trishydroxymethyl-aminoethane
U	unit(s)
V	Volt
wt	wild type
µ	micro

7.2 Index of figures and tables

Figures

Tables

7.3 Danksagung

An dieser Stelle möchte ich mich ganz herzlich bei allen bedanken, die mich während meiner Zeit als Doktorandin unterstützt haben.

Zuerst möchte ich mich ganz herzlich bei Herrn Prof. Dr. Wolfgang Wurst dafür bedanken, dass er mir die Möglichkeit gegeben hat, meine Promotionsarbeit an seinem Institut durchzuführen. Sein Ideenreichtum und seine konstruktive Kritik in zahlreichen Diskussionen haben mich unterstützt als Wissenschaftlerin zu wachsen.

Meinem direkten Betreuer Herr Dr. Roland Friedel möchte ich ganz besonders danken für seine große Unterstützung, seine Motivationsfähigkeit und seine immer vorhandene Verfügbarkeit auch über diese weite Entfernung. Mit seinem fundierten Wissen und seiner Bereitschaft für zahlreiche Diskussionen schärfte er mein wissenschaftliches Denken und Verständnis maßgeblich.

Mein Dank geht auch an Frau Prof. Dr. Magdalena Götz und Herrn Prof. Dr. Sigfried Scherer für ihre Bereitschaft, meine Dissertation zu beurteilen und die Promotionsprüfung durchzuführen.
Dr. Andrea Huber-Brösamle und Dr. Reinhard Köstner möchte ich danken, dass sie als Teil meines Thesis Committees mir mit Rat und Tat zur Seite gestanden sind.

Meinen Arbeitskollegen von EUCOMM, vorallem Sarah Weber, Dorota German, Susi Pfeiffer, Flavia Volner, und Denise Herold möchte ich für die freundschaftliche und angenehme Arbeitsatmosphäre danken. Auch bei meiner Diplomandin Anna-Lena Marwedel möchte ich mich für ihre tatkräftige Unterstützung bedanken.

Dr. Anja Harmeier bin ich zusätzlich zu großem Dank verpflichtet für ihr gewissenhaftes und kritisches Korrekturlesen des Manuskripts.

Zu guter Letzt möchte ich meiner Familie, vorallem meiner Mama für ihre selbstlose Unterstützung, gute Ratschläge und unermüdliches Verständnis danken.

7.4 Lebenslauf

Dipl. Biol., Viola Maier

Adresse:	Falkenauerstr.17 85435 Erding
Geburtsdatum/-ort:	18.09.1979 in Erding
Nationalität:	deutsch
E-Mail:	violamaier@googlemail.com

Seit 12/2010	**Prof.Dr. W. Wurst / Dr.Andreas Hörlein** Verteilungszentrum EUCOMM
Seit 10/2006	**Doktorarbeit: Prof. Dr. W. Wurst / Dr. Roland Friedel** **Institut für Entwicklungsgenetik,** **Helmholtz Zentrum München, Neuherberg** Thema: "Charakterisierung von Semaphorin 4C and Semaphorin 4G als potentielle Liganden von Plexin-B2."

Schul- und Hochschulausbildung

10/2009	**Prof. Dr. Marry Hatten,** **Laboratory of Developmental Neurobiology** **The Rockefeller University, New York, NY** Erlernen von Kokulturen
06/2006-08/2006	Auslandsaufenthalt in New York
12/2005	Auslandaufenthalt in Amsterdam
11/2004 – 08/2005	**Diplomarbeit: Dr. Klaus-Peter Janssen,** **KFG „Molekulare Tumorbiologie", Chirurgische Klinik, Klinikum rechts der Isar, TU München** Thema: „Das potenzielle Tumorsuppressorgen SASH1: Analyse der intrazellulären Verteilung anhand von Deletionskonstrukten und GFP-Fusionsproteinen."
03/2002 - 08/2005	**Hauptstudium der Biologie an der Technischen Universität München** Schwerpunkt: Humangenetik, Genetik, Mikrobiologie, Immunologie Abschluss Diplom (1,6)

11/1999 – 03/2002	**Grundstudium der Biologie an der Technischen Universität München** Abschluss: Vordiplom
09/1990 – 06/1999	**Gymnasium Erding, Erding** Abschluss: Allgemeine Hochschulreife (2,9)

Veröffentlichungen:

Publikationen:

Korostylev A., Worzfeld T., Friedel RH., Swiercz JM., Vodrazka P., **Maier V.**, Hirschberg A., Ohoka Y., Inagaki S., Offermanns S., Kuner R. "A functional role for semaphorin 4D/plexin B1 interactions in epithelial branching morphogenesis during organogenesis.", Development (2008)

Maier V., Jolicoeur C., Rayburn H., Takegahara N., Kumanogoh A., Kikutani H., Tessier-Lavigne M., Wurst W., Friedel RH. "Semaphorin 4C and S4G are Plexin-B2 ligands required for cerebellar development."
Molecular and cellular Neuroscience (2011)

Konferenzbeiträge:

23.-25. Januar 2008 First International conference on functional Annotation of the mammalian genome Conference Center Rottach, Egern Germany

Maier V., Wurst W., Friedel RH.;"Characterization of Semaphorin-4C and -4G as candidate ligands of Plexin-B2."
Neuroscience 2009 SfN 39th Annual Meeting in Chicago, USA; 17.-21. Oktober 2009; (Poster)

Maier, V., Wurst, W., Friedel RH.;"Characterization of Semaphorin-4C and Semaphorin-4G as candidate ligands of Plexin-B2." Munich interact, 7. Dezember 2007 (Poster)

Organisation von munich interact 2009 (PhD symposium)

Maier, V., Wurst, W., Friedel RH.;"Characterization of Semaphorin-4C and Semaphorin-4G as candidate ligands of Plexin-B2." Munich interact, 23. März 2010 (Poster)

Zusatzqualifikationen:

2007	Protection and Commercialization of Intellectual Property (Ascenion GmbH)
2008	Project management for young scientists (Golin Wissenschaftsmanagement)
2009	English for Science and the Laboratory

EDV-Kenntnisse und Sprachen:

EDV:	Microsoft Office, Adobe Creative Suite 3 (Photoshop, InDesign, Illustrator), EndNote,, ImageJ, GraphPad Prism	
Sprache:	Deutsch:	Muttersprache
	Englisch:	verhandlungsicher
	Italienisch:	Grundkenntnisse

Viola Maier